



TITLE:

Biochemical and molecular biological studies on enzymatic synthesis of vitamin B6 derivatives and optically active carboxylic acids(Dissertation_全文)

AUTHOR(S):

Yamamura, Ei-tora

CITATION:

Yamamura, Ei-tora. Biochemical and molecular biological studies on enzymatic synthesis of vitamin B6 derivatives and optically active carboxylic acids. 京都大学, 2020, 博士(農学)

ISSUE DATE:

2020-01-23

URL:

<https://doi.org/10.14989/doctor.r13305>

RIGHT:

**Biochemical and molecular biological studies on
enzymatic synthesis of vitamin B₆ derivatives and
optically active carboxylic acids**

Ei-Tora Yamamura

2020

CONTENTS

ABBREVIATIONS

GENERAL INTRODUCTION	1
REFERENCES	6
CHAPTER I Molecular biological studies on novel expression system using <i>Rhodococcus</i> sp.	13
SECTION 1 Isolation of two plasmids, pRET1100 and pRET1200, from <i>Rhodococcus erythropolis</i> IAM1400 and construction of a <i>Rhodococcus–Escherichia coli</i> shuttle vector	13
REFERENCES	27
SUMMARY	29
SECTION 2 Construction of <i>Rhodococcus</i> expression vectors and expression of the aminoalcohol dehydrogenase gene in <i>Rhodococcus erythropolis</i>	30
REFERENCES	42
SUMMARY	44

CHAPTER II	Biochemical and molecular biological studies on enzymatic synthesis of vitamin B ₆ derivatives and optically active carboxylic acids	45
SECTION 1	Bioconversion of pyridoxine to pyridoxamine through pyridoxal using a <i>Rhodococcus</i> expression system	45
REFERENCES		60
SUMMARY		62
SECTION 2	A novel method of producing the pharmaceutical intermediate (<i>R</i>)-2-chloromandelic acid by bioconversion	63
REFERENCES		81
SUMMARY		84
SECTION 3	A novel method of producing the key intermediate ASI-2 of ranirestat using a porcine liver esterase (PLE) substitute enzyme	85
REFERENCES		107
SUMMARY		111
CONCLUSIONS		112
ACKNOWLEDGEMENTS		114
LIST OF PUBLICATIONS		115

ABBREVIATIONS

16s rRNA	16s ribosomal RNA
LB broth	Luria-Bertani broth
SD	standard deviation
SDS-PAGE	sodium dodecyl sulfate-polyacrylamide gel electrophoresis
NADP ⁺	nicotinamide adenine dinucleotide phosphate
NADPH	reduced nicotinamide adenine dinucleotide phosphate
FAD	flavin adenine dinucleotide
Km	kanamycin
Ap	ampicillin
Cm	chloramphenicol
<i>km^r</i>	kanamycin resistance gene
<i>ap^r</i>	ampicillin resistance gene
<i>cm^r</i>	chloramphenicol resistance gene
Ap ^r	ampicillin resistance
Km ^r	kanamycin resistance
Cm ^r	chloramphenicol resistance
<i>Ori</i>	ColE1 ori involved in plasmid replication in <i>Escherichia coli</i>

<i>repT</i>	replication protein gene involved in plasmid replication <i>Rhodococcus erythropolis</i>
<i>P_{TRR}</i>	<i>TRR</i> promoter
<i>P₁₂₀₀</i>	<i>1200rep</i> promoter
<i>P_{hsp}</i>	<i>hsp</i> promoter
<i>P_{T5}</i>	<i>T5</i> promoter
U	μmol/min

GENERAL INTRODUCTION

In the manufacturing industries, environmental aspects are emphasized in addition to production costs. Many production processes using bioconversion reactions occur at ambient temperature and pressure (1–4), and are good for environmental conservation.

Many *Rhodococcus* strains contain diverse enzymes that are beneficial for manufacturing industries. In particular, *Rhodococcus erythropolis* tolerates organic solvents (5) and is utilized in the industrial production of chiral building blocks, pharmaceuticals (6, 7), and chemicals (4). However, genetic tools are needed to further analyze and utilize *Rhodococcus* in manufacturing industries.

Plasmids capable of replicating in *R. erythropolis*, including pRC4 (8), pAL5000 (9), pRE2895 (10), and pRE8424 (11), have been reported by some researchers. In addition, using plasmids isolated from Actinomycetes, *R. erythropolis*–*Escherichia coli* shuttle vectors have been constructed. However, there have been few studies concerned with identifying a compatible expression vector other than pRE8424 (11). Therefore, I constructed a novel *Rhodococcus* expression system.

Using the novel *Rhodococcus* expression system and an *E. coli* expression system, three types of pharmaceutical intermediates were produced in this study. First, pyridoxamine (PM) was produced by bioconversion using the *Rhodococcus* expression system. PM, a type of vitamin B₆, interferes with the formation of advanced lipoxidation end-products (ALEs) and advanced glycation end-products (AGEs) (12, 13). ALEs and AGEs are the major pathogenic factors in diabetic complications (14). For this reason, PM is a promising candidate for a prophylactic and/or remedy for diabetic complications.

PM is chemically synthesized using an oxidative method in manufacturing. The oxidative method changes pyridoxine (PN) to pyridoxal (PL), and then PL to PM through

pyridoxaloxime, which is reduced with a Pd/C catalyst to PM (15). Bioconversion is generally preferable in the context of environmental and energetic aspects (16). As far as I know, no bioconversion of PM production from PN, which is a readily and economically available starting material, has been reported.

Mesorhizobium loti contains the degradation pathway of vitamin B₆ (17). In this study, two enzymes, pyridoxine 4-oxidase (PNO) and pyridoxamine-pyruvate aminotransferase (PPAT), were derived from *M. loti* and used for bioconversion. PNO, which is encoded by the *pno* gene (also known as *mll6785*), catalyzes the FAD (flavin adenine dinucleotide)-dependent oxidation of PN to PL (18). It is expressed in *Escherichia coli* and recombinant PNO has been purified and characterized (17). However, the expression of *pno* in *E. coli* (17) has the disadvantage that it needs coexpression of the chaperonins, GroEL and GroES. Therefore, the present study investigates the bioconversion of PN to PM through PL, using the *Rhodococcus* expression system without chaperonins.

Second, (*R*)-2-Chloromandelic acid (*R*-CM), an intermediate used in the pharmaceutical industry, was produced by bioconversion. *R*-CM is valuable for the industrial synthesis of clopidogrel (methyl (*S*)-2-(2-chlorophenyl)-2-(4,5,6,7-tetrahydrothieno[3,2-*c*]-5-pyridyl)acetate) (19–22), which is highly useful as an antithrombotic agent and is commercialized under the brand name Plavix® (23). Various methods of producing *R*-CM have been reported by some researchers and a patent has been applied for.

As the method for producing *R*-CM by using a resolving agent for optical resolution, Bálint et al. (24) have described the method of optical resolution of racemic 2-chloromandelic acid by using optically active *threo*-1-(*p*-nitrophenyl)-2-amino-1,3-propanediol or optically active lysine, in which a diastereomeric salt thereof is prepared.

However, this method has the drawback of requiring an expensive reagent as a resolving agent for the optical resolution.

Nitrilases, which catalyze the hydrolysis of nitriles to carboxylic acids and ammonia (25), are beneficial for some manufacturing industries. Methods of performing asymmetric hydrolysis of cyanohydrin (2-chloromandelonitrile) with nitrilase to obtain optically active 2-chloromandelic acid have been reported by Wang et al. (23). This method has the drawback that these reactions are dangerous to handle, as hydrogen cyanide is formed from 2-chloromandelonitrile through a nonenzymatic reaction.

Reductases catalyze reduction reactions, and most of them require coenzymes (26). Methods for obtaining an optically active mandelic acid derivative using a microorganism harboring asymmetric reductase that reduces the α -carbonyl group of a phenylglyoxylic acid derivative have been described by Kimoto and Yamamoto (27). However, the α -keto acid (phenylglyoxylic acid derivative) used as the starting material is expensive, and a regeneration system of coenzymes is also required in this method. Therefore, these methods suffer from the drawback of high production cost. In this study, I described a novel method of producing *R*-CM from racemic 2-chloromandelic acid methyl ester (CMM), which is a readily and economically available starting material, by a bioconversion using recombinant cells harboring a novel esterase EstE.

Third, ASI-2 [(*R*)-2-amino-2-ethoxycarbonylsuccinimide], which is a key intermediate used in the pharmaceutical industry, was produced by a method in which bioconversion and chemical synthesis are combined. ASI-2 is valuable for the industrial synthesis of ranirestat ((*R*)-(-)-2-(4-bromo-2-fluorobenzyl)-1,2,3,4-tetrahydropyrrolo[1,2-*a*]pyrazine-4-spiro-3'-pyrrolidine-1,2',3,5'-tetrone) (28). Ranirestat is a potent aldose reductase inhibitor that was initially developed as a therapeutic agent for diabetic complications (28). Aldose reductase is the rate-limiting

enzyme of the polyol pathway and catalyzes the reduction reaction from glucose to sorbitol. Increases in aldose reductase activity and accumulation of sorbitol in diabetic patients have been reported (29). Toyoda et al. (30) have described that ranirestat reduced the area of stained glial fibrillary acidic protein and retinal thickness in Spontaneously Diabetic Torii (SDT) rats.

Several methods for synthesizing the key intermediate of ranirestat, ASI-2, using the optical resolution method have been reported (28,31–34). These methods have the drawback that recovery and racemization of enantiomer are needed after optical resolution. Kasai et al. (35) have described a method of synthesizing ASI-2 without optical resolution. The method includes a hydrolysis step of a prochiral ester derivative to an optically active carboxylic acid derivative using a porcine liver esterase (PLE). There is an advantage that optically active carboxylic acid derivatives can be obtained with a theoretical yield of 100%; however, this method has the drawback of using PLE.

PLE, which is a type of the valuable esterases (36,37–39) used in manufacturing industries, is one of the most useful esterases for process chemistry and organic synthesis. Numerous reports (33, 35, 40–44) have highlighted various methods producing a wide range of optically active molecules using commercial PLE. However, commercial PLE has the drawback of being derived from porcine liver tissue extracts, which are obtained from an animal organ. In addition, commercial PLE has the drawback that its activity differs between various batches, since commercial PLE extracted from porcine liver tissue has different ratios of esterases (45) and contains a plurality of isoenzymes (α , β , and γ -PLE) (46).

To solve the problems associated with heterogeneous commercial PLE, many studies involving the production of recombinant γ -PLE have been reported. Brüsehaber et al. (47) have described the expression of the γ -PLE gene with the Thioredoxin-tag (Trx-

tag) in *Escherichia coli*. Böttcher et al. (48) have described co-expression with the molecular chaperones GroEL and GroES in *E. coli* to produce γ -PLE. These methods have the drawback that the activity in whole cell is low for industrial applications. Böttcher et al. (48) have also described that the γ -PLE gene was expressed with *ompA* (outer membrane protein A secretion signal) and *relB* (pectate lyase B signal sequence for periplasmic translocation) for periplasmic expression of the γ -PLE gene; however, the majority of γ -rPLE (recombinant γ -PLE) exists in an insoluble form as inclusion bodies in the cytoplasm. In the study with yeast as a host, Lange et al. (49) have described that active γ -rPLE was secreted into the culture supernatant using recombinant *Pichia pastoris* expressing the γ -PLE gene. This method is limited by the fact that the activity of the culture supernatant is low for industrial applications. In this study, I sought to identify a novel esterase, EstBT, that substitutes for PLE and constructed a scheme to synthesize the pharmaceutical intermediate ASI-2 in a process in which chemical synthesis and bioconversion are combined.

REFERENCES

1. **Menon, V. and Rao, M.:** Trends in bioconversion of lignocellulose: Biofuels, platform chemicals & biorefinery concept, *Prog. Energy Combust. Sci.*, **38**, 522–550 (2012).
2. **Takeuchi M., Kishino S., Park S.B., Hirata A., Kitamura N., Saika A., and Ogawa J.:** Efficient enzymatic production of hydroxy fatty acids by linoleic acid $\Delta 9$ hydratase from *Lactobacillus plantarum* AKU 1009a. *J Appl Microbiol.*, **120**, 1282–1288 (2016).
3. **Kozono, I., Mihara, K., Minagawa, K., Hibi, M., and Ogawa, J.:** Engineering of the cytochrome P450 monooxygenase system for benzyl maltol hydroxylation, *Appl. Microbiol. Biotechnol.*, **101**, 6651–6658 (2017).
4. **Kato, Y., Tsuda, T., and Asano, Y.:** Nitrile hydratase involved in aldoxime metabolism from *Rhodococcus* sp. strain YH3-3 purification and characterization, *Eur. J. Biochem.*, **263**, 662-670 (1999).
5. **Stancu, M.M.:** Physiological cellular responses and adaptations of *Rhodococcus erythropolis* IBBP01 to toxic organic solvents, *J. Environ. Sci.*, **26**, 2065-2075 (2014).
6. **Urano, N., Fukui, S., Kumashiro, S., Ishige, T., Kita, S., Sakamoto, K., Kataoka, M., and Shimizu, S.:** Directed evolution of an aminoalcohol dehydrogenase for efficient production of double chiral aminoalcohols, *J. Biosci. Bioeng.*, **111**, 266–271 (2011).
7. **Kimura, T., Ishikawa, C., Osorio-Lozada, A., Robins, K.T., Hibi, M., and Ogawa, J.:** Production of a pharmaceutical intermediate via biohydroxylation using whole cells of *Rhodococcus rubropertinctus* N82, *Biosci. Biotechnol. Biochem.*, **78**, 1772–

- 1776 (2014).
8. **Hashimoto, Y., Nishiyama, M., Yu, F., Watanabe, I., Horinouchi, S., and Beppu, T.:** Development of a host-vector system in a *Rhodococcus* strain and its use for expression of the cloned nitrile hydratase gene cluster, *J. Gen. Microbiol.*, **138**, 1003–1010 (1992).
 9. **Stolt, P., and Stoker, N.G.:** Functional definition of regions necessary for replication and incompatibility in the *Mycobacterium fortuitum* plasmid pAL5000, *Microbiology*, **142**, 2795–2802 (1996).
 10. **Nakashima, N. and Tamura, T.:** A novel system for expressing recombinant proteins over a wide temperature range from 4 to 35 degrees C, *Biotechnol. Bioeng.*, **86**, 136–148 (2004).
 11. **Nakashima, N. and Tamura, T.:** Isolation and characterization of a rolling-circle-type plasmid from *Rhodococcus erythropolis* and application of the plasmid to multiple-recombinant-protein expression, *Appl. Environ. Microbiol.*, **70**, 5557–5568 (2004).
 12. **Metz, T.O., Alderson, N.L., Thorpe, S.R., and Baynes, J.W.:** Pyridoxamine, an inhibitor of advanced glycation and lipoxidation reactions: a novel therapy for treatment of diabetic complications, *Arch. Biochem. Biophys.*, **419**, 41–49 (2003).
 13. **Voziyan, P.A., Metz, T.O., Baynes, J.W., and Hudson, B.G.:** A post-amadori inhibitor pyridoxamine also inhibits chemical modification of proteins by scavenging carbonyl intermediates of carbohydrate and lipid degradation, *J. Biol. Chem.*, **277**, 3397–3403 (2002).
 14. **Jayakumar, R. V.:** Risk factors in diabetic nephropathy, *Int. J. Diabetes Dev. Ctries.*, **32**, 1–3 (2012).
 15. **Balyakina, M.V., Yakovleva, N.L., and Gunar, V.I.:** Synthesis of pyridoxamine and

- its 5'-phosphate ester, *Pharm. Chem. J.*, **14**, 407–409 (1980).
16. **Menon, V. and Rao, M.:** Trends in bioconversion of lignocellulose: Biofuels, platform chemicals & biorefinery concept, *Prog. Energy Combust. Sci.*, **38**, 522–550 (2012).
 17. **Yuan, B., Yoshikane, Y., Yokochi, N., Ohnishi, K., and Yagi, T.:** The nitrogen-fixing symbiotic bacterium *Mesorhizobium loti* has and expresses the gene encoding pyridoxine 4-oxidase involved in the degradation of vitamin B₆, *FEMS Microbiol. Lett.*, **234**, 225–230 (2004).
 18. **Mugo, A.N., Kobayashi, J., Yamasaki, T., Mikami, B., Ohnishi, K., Yoshikane, Y., and Yagi, T.:** Crystal structure of pyridoxine 4-oxidase from *Mesorhizobium loti*, *Biochim. Biophys. Acta.*, **1834**, 953–963 (2013).
 19. **Bousquet, A. and Musolino, A., inventors; Sanofi-Synthelabo, assignee:** Hydroxyacetic ester derivatives, preparation method and use as synthesis intermediates, United States patent US 6,573,381 B1. 2003 Jun 3.
 20. **Bousquet, A. and Musolino, A., inventors; Sanofi-Synthelabo, assignee:** Hydroxyacetic ester derivatives, preparation method and use as synthesis intermediates, United States patent US 6,894,186 B2. 2005 May 17.
 21. **Bousquet, A. and Musolino, A., inventors; Sanofi-Aventis, assignee:** Hydroxyacetic ester derivatives, preparation method and use as synthesis intermediates, United States patent US 7,153,969 B2. 2006 Dec 26.
 22. **Wang, H., Sun, H., Gao, W., and Wei, D.:** Efficient production of (*R*)-*o*-chloromandelic acid by recombinant *Escherichia coli* cells harboring nitrilase from *Burkholderia cenocepacia* J2315, *Org. Process Res. Dev.*, **14**, 767–773 (2014).
 23. **Wang, H., Gao, W., Sun, H., Chen, L., Zhang, L., Wang, X., and Wei, D.:** Protein engineering of a nitrilase from *Burkholderia cenocepacia* J2315 for efficient and

- enantioselective production of (*R*)-*o*-chloromandelic acid, *Appl. Environ. Microbiol.*, **81**, 8469–8477 (2015).
24. **Bálint, J., Nagy, M.C., Dombrády, Z., Fogassy, E., Gajáry, A., and Subaet, C., inventors; Sanofi-Aventis, assignee:** Resolution process for (*R*)-(-)-2-hydroxy-2-(2-chlorophenyl)acetic acid, United States patent US 7,381,835 B2. 2008 Jun 3.
25. **Yamaguchi, T. and Asano, Y.:** Draft genome sequence of an aldoxime degrader, *Rhodococcus* sp. Strain YH3-3, *Genome Announc.*, **4**, e00406–16 (2016).
26. **Kataoka, M., Ishige, T., Urano, N., Nakamura, Y., Sakuradani, E., Fukui, S., Kita, S., Sakamoto, K., and Shimizu, S.:** Cloning and expression of the l-1-amino-2-propanol dehydrogenase gene from *Rhodococcus erythropolis*, and its application to double chiral compound production, *Appl. Microbiol. Biotechnol.*, **80**, 597–604 (2008).
27. **Kimoto, N. and Yamamoto, H., inventors; Daicel Chemical Industries, Ltd., assignee:** α -Keto acid reductase, method for producing the same, and method for producing optically active α -hydroxy acids using the same, United States patent US 7,250,278 B2. 2007 Jul 31.
28. **Negoro, T., Murata, M., Ueda, S., Fujitani, B., Ono, Y., Kuromiya, A., Komiya, M., Suzuki, K., and Matsumoto J.:** Novel, highly potent aldose reductase inhibitors: (*R*)-(-)-2-(4-bromo-2-fluorobenzyl)-1,2,3,4-tetrahydropyrrolo[1,2-a]pyrazine-4-spiro-3'-pyrrolidine-1,2',3,5'-tetrone (AS-3201) and its congeners, *J. Med. Chem.*, **41**, 4118–4129 (1998).
29. **Hamada, Y., Kitoh, R., and Raskin, P.:** Crucial role of aldose reductase activity and plasma glucose level in sorbitol accumulation in erythrocytes from diabetic patients, *Diabetes*, **40**, 1233–1240 (1991).
30. **Toyoda, F., Tanaka, Y., Ota, A., Shimmura, M., Kinoshita, N., Takano, H.,**

- Matsumoto, T., Tsuji, J., and Kakehashi, A.:** Effect of ranirestat, a new aldose reductase inhibitor, on diabetic retinopathy in SDT rats, *J. Diabetes Res.*, article ID 672590, 1–7 (2014). DOI:10.1155/2014/672590
31. **Tanaka, D., inventor; Dainippon Sumitomo Pharma Co., Ltd., assignee:** 3-Hydrazino-2,5-dioxopyrrolidine-3-carboxylates, process for production of the same, and use of the same, United States patent US 8,003,808 B2. 2011 Aug 23.
32. **Tanaka, D. and Negoro, T., inventors; Dainippon Sumitomo Pharma Co., Ltd., assignee:** Optically active 3-amino-2,5-dioxopyrrolidine-3-carboxylate, process for production of the compound, and use of the compound, United States patent US 8,058,456 B2. 2011 Nov 15.
33. **Kudo, Y., Yamada, O., inventors; Nissan Chemical Industries, Ltd., Dainippon Sumitomo Pharma Co., Ltd., assignees:** Method for producing optically active succinimide compound, United States patent US 7,994,342 B2. 2011 Aug 9.
34. **Inagaki, T. and Yamakawa, Y., inventors; Dainippon Sumitomo Pharma Co., Ltd., and Katayama Seiyakusyo Co., Ltd., assignees:** Succinic acid diester derivative, process for production thereof, and use of the derivative in the production of pharmaceutical preparation, United States patent US 8,030,486 B2. 2011 Oct 4.
35. **Kasai, M., Kita, S., Ogawa, T., Tokai, H., inventors; Dainippon Sumitomo Pharma Co., Ltd., and Kyowa Hakko Bio Co., Ltd., assignees:** Process for producing optically active succinimide derivatives and intermediates thereof, United States patent US 8,633,001 B2. 2014 Jan 21.
36. **Hayashi, Y., Onaka, H., Itoh, N., Seto, H., and Dairi, T.:** Cloning of the gene cluster responsible for biosynthesis of KS-505a (longestin), a unique tetraterpenoid, *Biosci. Biotechnol. Biochem.*, **71**, 3072–3081 (2007).
37. **Okazaki, R., Kiyota, H., and Oritani, T.:** Enzymatic resolution of (\pm)-epoxy- β -

- cyclogeraniol, a synthetic precursor for abscisic acid analogs, *Biosci. Biotechnol. Biochem.*, **64**,1444–1447 (2000).
38. **Kanjanavas, P., Khuchareontaworn, S., Khawsak, P., Pakpitcharoen, A., Pothivejkul, K., Santiwatanakul, S., Matsui, K., Kajiwara, T., and Chansiri, K.:** Purification and characterization of organic solvent and detergent tolerant lipase from thermotolerant *Bacillus* sp. RN2, *Int. J. Mol. Sci.*, **11**, 3783–3792 (2010).
39. **Park, E.Y., Sato, M., and Kojima, S.:** Lipase-catalyzed biodiesel production from waste activated bleaching earth as raw material in a pilot plant, *Bioresour. Technol.*, **99**, 3130–3135 (2008).
40. **Bornscheuer, U.T. and Kazlauskas, R.J.:** Hydrolases in organic synthesis -regio- and stereoselective biotransformations, 2nd edn. Weinheim: Wiley-VCH; 2006.
41. **Faber, K.:** Biotransformations in organic chemistry, 5th edn. Berlin, Heidelberg, New York: Springer; 2004.
42. **de Maria, P.D., Kossmann, B., Potgrave, N., Buchholzc, S., Trauthweinc, H., Maya, O., and Gröger, H.:** Improved process for the enantioselective hydrolysis of prochiral diethyl malonates catalyzed by pig liver esterase, *Synlett.*, **11**, 1746–1748 (2005).
43. **Lam, L.K.P., Hui, R.A.H.F., and Jones, J.B.:** Enzymes in organic synthesis. 35. Stereoselective pig liver esterase catalyzed hydrolyses of 3-substituted glutarate diesters. Optimization of enantiomeric excess via reaction conditions control, *J. Org. Chem.*, **51**, 2047–2050 (1986).
44. **Bornscheuer U, Hummel A, Böttcher D, Brisehaber, E., Doderer, K., and Trauthwein, H., inventors; Enzymicals AG, assignee:** Isoforms of pig liveresterase. United States patent US 8,304,223 B2. 2012 Nov 6.
45. **Seebach, D. and Eberle, M.:** Enantioselective cleavage of meso-nitrodiol diacetates

- by an esterase concentrate from fresh pig liver: Preparation of useful nitroaliphatic building blocks for EPC syntheses, *Chimia.*, **40**, 315–318 (1986).
46. **Faber, D. and Jencks, W.P.:** Different forms of pig liver esterase, *Arch. Biochem. Biophys.*, **203**, 214–226 (1980).
47. **Brüsehabe, E., Schwiebs, A., Schmidt, M., Böttcher, D., Bornscheuer, U.T.:** Production of pig liver esterase in batch fermentation of *E. coli* Origami, *Appl. Microbiol. Biotechnol.*, **86**, 1337–1344 (2010).
48. **Böttcher, D., Brüsehabe, E., Doderer, K., and Bornscheuer, U.T.:** Functional expression of the γ -isoenzyme of pig liver carboxyl esterase in *Escherichia coli*, *Appl. Microbiol. Biotechnol.*, **73**, 1282–1289 (2007).
49. **Lange, S., Musidlowska, A., Schmidt-Dannert, C., Schmitt, J., and Bornscheuer, U.T.:** Cloning, functional expression, and characterization of recombinant pig liver esterase, *Chembiochem.*, **2**, 576–582 (2001).

CHAPTER I

Molecular biological studies on novel expression system using *Rhodococcus* sp.

SECTION 1

Isolation of two plasmids, pRET1100 and pRET1200, from *Rhodococcus erythropolis* IAM1400 and construction of a *Rhodococcus–Escherichia coli* shuttle vector

Compatible expression vectors are advantageous in that they can be used to produce compounds from bacteria that co-express multiple genes. Therefore, I sought to discover novel compatible plasmids for co-expressing multiple genes and isolated two plasmid species, pRET1100 and pRET1200, from *R. erythropolis* IAM1400. Here, I describe the new cryptic pRET1100 plasmid and a shuttle vector that is compatible with pRE2895.

Materials and methods

Strains and plasmids The properties of the strains and plasmids used in this study are summarized in Tables 1 and 2. *Rhodococcus erythropolis* strains IAM1400 and IAM1503 were obtained from the Institute of Applied Microbiology (Tokyo, Japan). *R. erythropolis* strains JCM2893, JCM2894, and JCM2895 (1) were obtained from the Japan Collection of Microorganisms (Ibaraki, Japan). *Escherichia coli* and *R. erythropolis* were

cultured in Luria-Bertani broth (1% Bacto tryptone, 0.5% Bacto yeast extract, and 1% NaCl) in the presence or absence of appropriate antibiotics. The antibiotics used to select transformants in the culture media were 100 µg/ml ampicillin, 100 µg/ml kanamycin, and 30 µg/ml chloramphenicol. The preparation of plasmids from *R. erythropolis* followed the method of Denis-Larose et al. (2).

Enzymes and chemicals All restriction enzymes and DNA modification enzymes were purchased from TOYOBO Co., Ltd. (Osaka, Japan), New England Biolabs, Inc. (Ipswich, MA, USA), and Roche Molecular Systems, Inc. (Basel, Switzerland). All chemicals were purchased from Tokyo Chemical Industry Co., Ltd. (Tokyo, Japan), Sigma-Aldrich (St. Louis, MO, USA), and Wako Pure Chemical Industries, Ltd. (Osaka, Japan).

Standard genetic manipulations Cloning was performed by standard genetic manipulation (3). The transformation of *R. erythropolis* followed the method of Hirasawa et al. (4). The transformation of *E. coli* was performed with the *E. coli* Transformation Buffer Set (Zymo Research Corp., Irvine, CA, USA). Genomic DNA was prepared with a Genomic DNA Buffer set and Genomic-tip 500/G (Qiagen, Hilden, Germany). PCR fragments were prepared with KOD -plus- (Toyobo Co., Ltd.).

Sequence determination and analysis pRET1100 and pRET1200 DNAs were digested with the appropriate restriction enzymes and then inserted into the *E. coli* vector pBluescript II KS (-). Determination of the DNA sequences of the plasmid inserts was accomplished by the primer walking method with an ABI PRISM 310NT DNA Genetic Analyzer (Applied Biosystems, Carlsbad, CA, USA). Sequence assembly and analysis were performed with Genetyx (Genetyx Corp., Tokyo, Japan) and DNASIS Pro (Hitachi Software Corp., Tokyo, Japan)

Construction of the *Rhodococcus–E. coli* shuttle vectors The construction scheme for the shuttle vectors is shown in Fig. 1. To construct the pRET1102 plasmid, the DNA of pRET1100 was digested with *Alw44I*, blunt-ended, and ligated with pHSG299 digested with *HincII*. To construct the pRET1200 plasmid, the DNA of pRET1200 was digested with *BspLU11I*, blunt-ended, and ligated with pHSG299 digested with *HincII*.

Estimation of plasmid copy number Estimation of plasmid copy number was performed using the methods of Projan et al. (5) and Nakashima and Tamura (6). To estimate DNA band intensities, ImageJ was used (National Institutes of Health, Bethesda, MD, USA).

Nucleotide sequence accession numbers The sequence data for the pRET1100 and pRET1200 plasmids have been submitted to the DDBJ/EMBL/GenBank databases under accession numbers LC331663 (pRET1100) and LC331662 (pRET1200).

TABLE 1. Bacterial strains used in this study

Species	Strains	Source	Application
<i>E. coli</i>	JM109	Toyobo Co., Ltd.	General cloning
	DH5alpha	Toyobo Co., Ltd.	General cloning
<i>R. erythropolis</i>	IAM1400	Institute of Applied Microbiology	Source of pRET1100 and pRET1200
	IAM1503	Institute of Applied Microbiology	Source of pRET1300 and pRET1400
	JCM2893	Japan Collection of Microorganisms	Source of pRET1500 and pRET1600
	JCM2894	Japan Collection of Microorganisms	Source of pRET1700 and pRET1800
	JCM2895	Japan Collection of Microorganisms	Source of pRET0500
			Host strain to transform with the shuttle vector
	MAK-34	This study	Host strain to transform with the shuttle vector

TABLE 2. Plasmids used in this study

Plasmids	Characteristics	Source/Reference
Cloning vectors		
pUC18	Ap ^r	Takara Bio Inc.
pHSG299	Km ^r	Takara Bio Inc.
pHSG398	Cm ^r	Takara Bio Inc.
pBluescript II KS(-)	Ap ^r	Toyobo Co., Ltd.
pRET vectors		
pRET0500	Same as pRE2895	1
pRET1100	5.4 kbp plasmid isolated from <i>R. erythropolis</i> IAM1400	This study
pRET1200	5.4 kbp plasmid isolated from <i>R. erythropolis</i> IAM1400	This study
pRET1300	5.4 kbp plasmid isolated from <i>R. erythropolis</i> IAM1503	This study
pRET1400	5.4 kbp plasmid isolated from <i>R. erythropolis</i> IAM1503	This study
pRET1500	5.4 kbp plasmid isolated from <i>R. erythropolis</i> JCM2893	This study
pRET1600	5.4 kbp plasmid isolated from <i>R. erythropolis</i> JCM2893	This study
pRET1700	5.4 kbp plasmid isolated from <i>R. erythropolis</i> JCM2894	This study
pRET1800	5.4 kbp plasmid isolated from <i>R. erythropolis</i> JCM2894	This study
pRET1101	Ap ^r ; DNA fragment of pRET1100 digested with <i>Alw44 I</i> and blunt ended in <i>Sma I</i> site of pUC18	This study
pRET1102	Km ^r ; DNA fragment of pRET1100 digested with <i>Alw44 I</i> and blunt ended in <i>Hinc II</i> site of pHSG299	This study
pRET1103	Cm ^r ; DNA fragment of pRET1100 digested with <i>Alw44 I</i> and blunt ended in <i>Hinc II</i> site of pHSG398	This study
pRET1201	Ap ^r ; DNA fragment of pRET1200 digested with <i>BspLU11 I</i> and blunt ended in <i>Sma I</i> site of pUC18	This study
pRET1202	Km ^r ; DNA fragment of pRET1200 digested with <i>BspLU11 I</i> and blunt ended in <i>Hinc II</i> site of pHSG299	This study
pRET1203	Cm ^r ; DNA fragment of pRET1200 digested with <i>BspLU11 I</i> and blunt ended in <i>Hinc II</i> site of pHSG398	This study
pRET1123	Km ^r ; 2.7 kbp DNA fragment of pRET1102 digested with <i>BamH I</i> and <i>Hinc II</i> in <i>BamH I</i> and <i>Hinc II</i> sites of pHSG299	This study
pRET1127	Km ^r ; PCR fragment of pRET1100 (nucleotides 468 to 2768) in <i>Hinc II</i> site of pHSG299	This study
pRET1128	Km ^r ; PCR fragment of pRET1100 (nucleotides 468 to 2684) in <i>Hinc II</i> site of pHSG299	This study
pRET1129	Km ^r ; PCR fragment of pRET1100 (nucleotides 628 to 3144) in <i>Hinc II</i> site of pHSG299	This study
pRET1130	Km ^r ; PCR fragment of pRET1100 (nucleotides 877 to 3144) in <i>Hinc II</i> site of pHSG299	This study

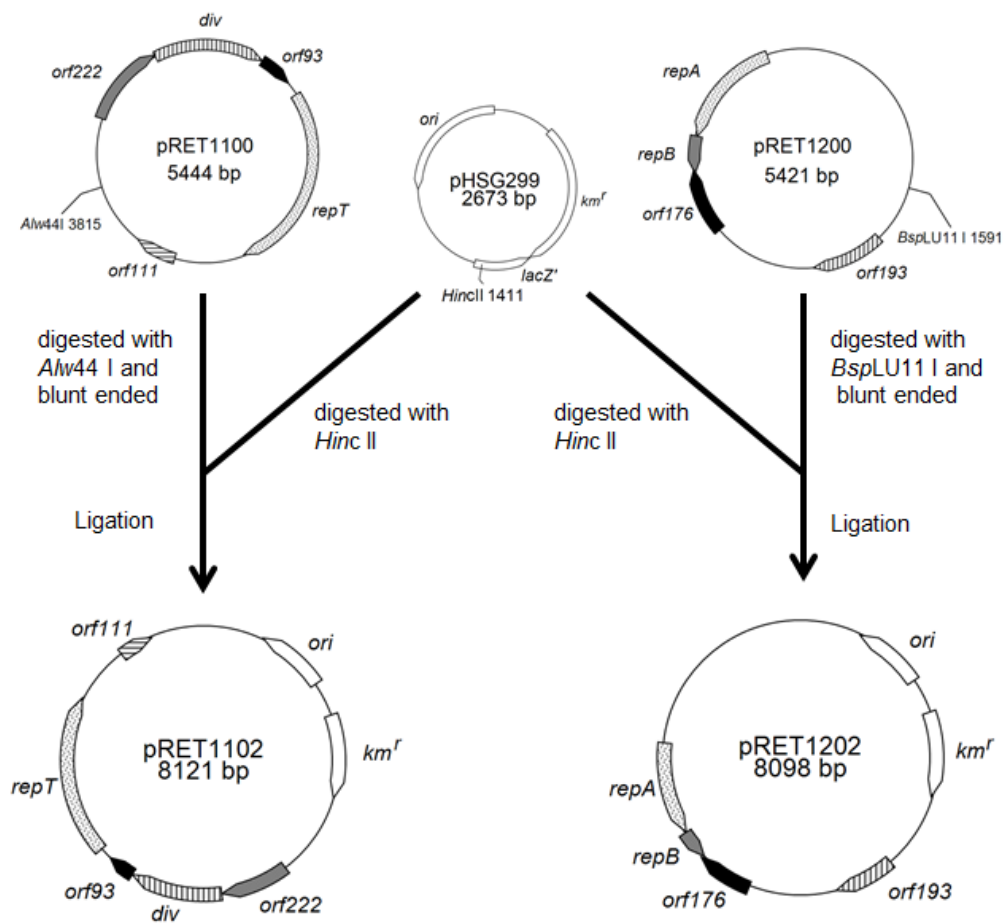


FIG. 1. *Rhodococcus*–*E. coli* shuttle vectors construction. Cloning sites are displayed. The orfs are shown as arrows. *repT*, *repA*, and *repB*, are the predicted RepT, RepA, and RepB proteins involved in plasmid replication, respectively, in *Rhodococcus erythropolis*. *ori* is ColE1 ori. *kmr* is kanamycin resistance gene.

Results

Isolation of plasmids from *R. erythropolis*

I isolated cryptic circular plasmids from *R. erythropolis* strains IAM1400, IAM1503, JCM2893, and JCM2894. *R. erythropolis* IAM1400 harbored two plasmid species, designated as pRET1100 and pRET1200. These plasmids were the nearly same size (5.4 kb). pRET1100 harbors one

recognition site for *KpnI* and no recognition site for *PstI*, while pRET1200 harbors one recognition site for *PstI* and no recognition site for *KpnI*. After digestion of these plasmids with *PstI* or *KpnI*, the resulting fragments were separated by agarose gel electrophoresis (Fig. 2).

When the pRET1200 DNA was digested with *PstI*, the resulting amount of pRET1200 linear DNA was the same as that of the remaining pRET1100 closed circular DNA (Fig. 2, lane 2) and was approximately half the amount of the undigested pRET1100 and pRET1200 closed circular DNA (Fig. 2, lane 1). After *PstI* treatment, the pRET1200 linear DNA (Fig. 2, lane 2) was able to be digested with ATP-dependent DNase, which selectively hydrolyzes linear dsDNA to deoxynucleotides, but the remaining pRET1100 DNA was not digested (data not shown). In contrast, the *KpnI*-digested pRET1100 linear DNA (Fig. 2, lane 3) was able to be digested with ATP-dependent DNase, but the remaining pRET1200 DNA was not (data not shown). These results suggest that both pRET1100 and pRET1200 are circular closed dsDNAs in *R. erythropolis*.

R. erythropolis strains IAM1503, JCM2893, and JCM2894 each harbored two plasmid species, designated as pRET1300 and pRET1400, pRET1500 and pRET1600, and pRET1700 and pRET1800, respectively. The size of each plasmid was 5.4 kb (Table 2). I also isolated pRE2895 (1) from *R. erythropolis* JCM2895, which harbored one plasmid species.

The pRET1100 and pRET1200 DNAs were digested with a variety of restriction enzymes (Table 3), as were the pRET0500 (pRE2895), pRET1300, pRET1400, pRET1500, pRET1600, pRET1700, and pRET1800 DNAs. The band patterns of pRET1300, pRET1500, and pRET1700 after digestion with the restriction enzymes were almost the same as that of pRET1100. Likewise, the patterns of pRET1400, pRET1600, pRET1800, and pRET0500 were almost the same as that of pRET1200.

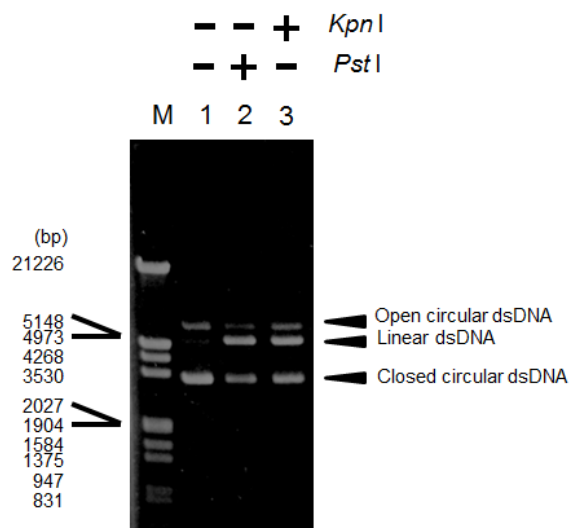


FIG. 2. Agarose gel electrophoresis of the plasmid DNAs isolated from *R. erythropolis* IAM 1400. The plus signs indicate the plasmid treated with the restriction enzyme. The minus signs indicate the plasmid not digested with the restriction enzyme. Lane M, size marker (lambda DNA digested with *EcoR* I and *Hind* III); lane 1, the plasmid DNAs isolated from *R. erythropolis* IAM 1400 (control); lane 2, the isolated plasmid DNAs that were treated with *Pst* I; lane 3, the isolated plasmid DNAs that were treated with *Kpn* I.

TABLE 3. The number of fragments and the fragment sizes digested with the restriction enzyme

	pRET1100		pRET1200	
	Number of cleavage sites	Fragment sizes (kbp)	Number of cleavage sites	Fragment sizes (kbp)
<i>Bam</i> H I	2	0.4, 5.0	1	5.4
<i>Eco</i> R I	2	0.3, 5.1	1	5.4
<i>Hind</i> III	0	-	0	-
<i>Kpn</i> I	1	5.4	0	-
<i>Pvu</i> II	1	5.4	2	0.9, 4.5
<i>Sac</i> I	1	5.4	1	5.4
<i>Sca</i> I	0	-	0	-
<i>Sph</i> I	0	-	0	-
<i>Sma</i> I	1	5.4	2	0.4, 5.0

Genome structures of pRET1100 and pRET1200

Determination of

the DNA sequences of pRET1100 and pRET1200 was accomplished by the primer walking method. As shown in Fig. 3, the pRET1100 plasmid is a closed circular dsDNA molecule of 5444 bp with a G+C content of 59.4%. The pRET1100 plasmid has two possible open reading frames (ORFs), designated as *repT* and *div*, as well as three minor ORFs (*orf93*, *orf111*, and *orf222*), whose functions are presently unclear. The pRET1200 DNA molecule consists of 5421 bp with a G+C content of 62.3%. The pRET1200 plasmid is highly homologous to pN30 (13) from *R. erythropolis*, with an identity of 98.82% according to Genetyx analysis. The pRET1200 plasmid contains *repA* and *repB*, which encode the replication proteins RepA and RepB, respectively, as well as two minor ORFs (*orf176* and *orf193*), whose functions are presently unclear. The predicted RepA and RepB proteins are highly homologous to proteins from pN30 (7), pNit-QC2 (6), and pREC2 (8) with identities of 100% according to Genetyx analysis. The pRET1200 RepB protein has a characteristic helix-turn-helix motif 1 and a characteristic helix-turn-helix motif 2 (9).

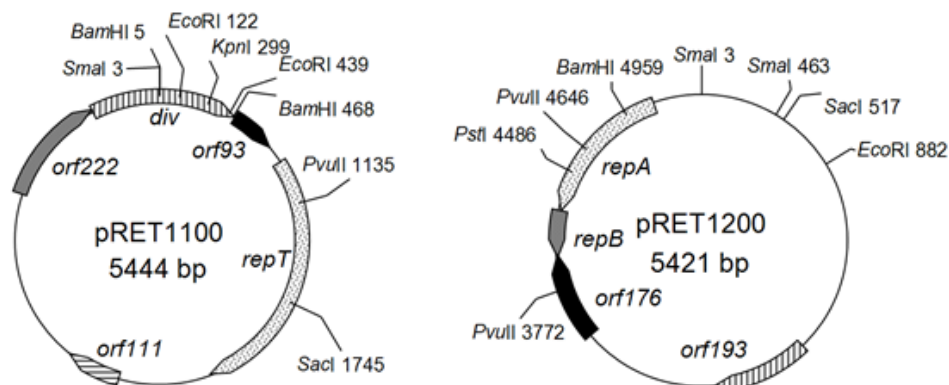


FIG. 3. Structure of pRET1100 and pRET1200 from *Rhodococcus erythropolis* IAM1400. The orfs are shown as arrows. *repT*, *repA*, and *repB*, are the predicted RepT, RepA, and RepB proteins involved in plasmid replication, respectively. *div* is a putative cell division protein.

Homology between pRET1100 RepT and other plasmid replication proteins

The pRET1100 *repT* gene encodes a novel replication protein, RepT. The predicted RepT protein is not highly homologous to proteins from other plasmids that have been reported. For example, the identity between RepT and the pRE8424 Rep was only 5% according to a Genetyx analysis. Using the BLAST program (10), I identified the plasmid proteins that are most homologous to RepT as pDYM4.3k Rep (11) from *Streptomyces* sp. X335, pTSC1 Rep (12) from *Streptomyces* sp. x4, and pCAZ1 Rep (13) from *Couchioplanes caeruleus* subsp. *azureus*, with E-values of 1e-143, 3e-91, and 2e-84, respectively. As shown in Fig. 4, homology is relatively low among the Rep proteins.

pRET1100	RepT	1	MHFHDNAEVGQEGRTAVLSPLRGVAAKRDVSDDAAKRSRQARHAPGLVTSATTVRESLPA	60
pDYM4.3k	Rep	0	-----	0
pTSC1	Rep	0	-----	0
pCAZ1	Rep	1	-----MTQPFRRGRVISRPEKQRRAGAPTFTPPHGSCPNLCFDR	39
pRET1100	RepT	61	PETAGQGLAESVTADDFWSHSFPRADDVVGAAASFQSVANWDGREGPRPRFVVVAPGVVRL	120
pDYM4.3k	Rep	0	-----	0
pTSC1	Rep	1	-----MSAAVGLFDRRPSSASARGLADGRGRDA	28
pCAZ1	Rep	40	KQNPMFVLRRLADACSRSHVSPVTVDTADSVTSLQWWTFRFPSPAGLDLAARMFNPREGWGG	99
pRET1100	RepT	121	EVCDLARRERTAERAYLAARARVDMAAARHNSPYDFDVEDDEELAEELASLOGLEDDDDIGGW	180
pDYM4.3k	Rep	1	-----MAKRERALEAQHRRQVDAEILGAWLHATGSFPADA	36
pTSC1	Rep	29	VAAVDRATIGAEGPRPLLTIAIPGVVSLSWPDAARKKERAERQOEAARKSASALGRYWAAY	88
pCAZ1	Rep	100	APGLRRDRDAEEGPRWRVFLSAGAFATIGAPDLAAERRYERAMQARQKTADALAAHLATH	159
pRET1100	RepT	181	SAEREIVGWSARSRSRMILRMAELDWAPMMDLPGIPAMVTLTYPGDWLTVAPTGAEVKKH	240
pDYM4.3k	Rep	37	EPSREITGWSRRSRSMIRRLAELDWTPILSAACLPCMITLTYPGDWLTVAPDGETSKKH	96
pTSC1	Rep	89	VGD-----PAEPEPTRVTVEWSRKSRSRMTRRLAELDYTFLLRMGLRLP-MTT	135
pCAZ1	Rep	160	PTDAKGRMAARCCDDCPTDPEPCREITSWRSKSRANMVRALCELDYRPLLNDRTRVPAAMV	219
pRET1100	RepT	241	LQTFKFRFORANGIAWGWAKMEFQSRGAPHFHLYMVPVPHGKAGDSRKLRLHDAELLKWEI	300
pDYM4.3k	Rep	97	INAFYKRYERANGVDVFGPWKFEFOHRRGAPHYHLYCVPPQGIAGELRRKBDIRVNDWHN	156
pTSC1	Rep	136	LTYPGDWLTVAPTGKAVKEHLKIWRRRERERAWGFPPIGIWKLEFQRRGAPHHIFWGPEPE	195
pCAZ1	Rep	220	LTYPGDWLTVAPTGDGKAAKRHLQMERKRFVKAAGHDVTGVWVKLEFQERGAHFHLLMVPPH	279
pRET1100	RepT	301	ARAEGEDPGRRPYFREAPSEGLKFRFWLSAVWADVVDHPDPEKEKEKHSAGTGVVDYNEGT	360
pDYM4.3k	Rep	157	MKAAGIDPGPKPRFRKAIGDGLKFAQWLSITWADIVDHPDPEERAKHQAGTGVVDYREGM	216
pTSC1	Rep	196	GLAGELRKLTKRRYRPAVGDGLPYRQWLSVWVADIVVHPDPEERRRHLLDAGTAVDREGE	255
pCAZ1	Rep	280	GLS-RIPG-KKARLGSWVGAKPFREWLSLVWADIVVHPDPEQRRRHERAGTGLDWSEGL	337
			←-----Region 1-----→	
pRET1100	RepT	361	RGSDFRRLAVYFESKHGTFADKEYQHVFQWQKTGGGGRFGWYRGLSPATAATEISWDE	420
pDYM4.3k	Rep	217	RTSDFRRLAVYFESKHGTYADKEYQNRVFEWQAFGGGGRFGWYRGLNVLVAQVEIDWPE	276
pTSC1	Rep	256	RMRDFRRLAVYFESKHGTYSAKEYQHVFQWAEFGGGRFGWYRGLSPATAGVELDPAA	315
pCAZ1	Rep	338	RATDFRRLAVYFESKHGFRKEYQNVFEAWQEEGGGGRFGWYRGLQRVIVGVEVEHDD	397
			←-----Region 2-----→	
pRET1100	RepT	421	YLLSRTLRRLS-ARTKIWDPALRGGSGGHRWVKAMRRVTRHR-LDVTGEILGTKTR	478
pDYM4.3k	Rep	277	YQLMSRTLRKLA-ARTRVWDSLNAGRGGHRWVKAMRTIEVPRRPFDDQDTGEVGHQFR	335
pTSC1	Rep	316	AVWAGRLLRRYARSQGVTTQRTVRRVGG-VPIPTDRVMGLA----GAQLVTGPERVRYR	370
pCAZ1	Rep	398	AVRAARLVRRWARAQGTTRETVTRTGGGAIRSELAEVEGLA----GAQTIAARTTRR-R	452
pRET1100	RepT	479	KVRAFVRRFVRTSGYLOVNDGPALARTLSRLRSTCLS-----	515
pDYM4.3k	Rep	336	KVREVEVRFVRTSGFLOVNDGPALASTLSRLRESCLT-----	372
pTSC1	Rep	371	TVRRFVRLAENRGFLOVNDGGLASLRLRALDPDRAAVAPADRAWGAIGTTPPRETETE	430
pCAZ1	Rep	453	SVRRRVCRMKGGKGFVSVNNGEEFAIMLRALDVVARDVHEPGSPQMRLELRAQRANQE	512
			←-----Region 3-----→ ←-----Region 4-----→	
pRET1100	RepT	515	-----	515
pDYM4.3k	Rep	372	-----	372
pTSC1	Rep	431	TETEHQGRGAYD	442
pCAZ1	Rep	513	SVLQ-----	516

FIG. 4. Alignment of amino acid sequences of RepT of pRET1100 with plasmid replication proteins. Black highlighting denotes amino acids that are conserved in four sequences. Gray highlighting denotes amino acids that highly conserved in many sequences. The arrows indicate high conserved regions. The accession numbers for each Rep protein are as follows: pDYM4.3K, JQ621947 (DDBJ), I3RM63 (UniProt); pTSC1, GU271942 (DDBJ), D3JSU0 (UniProt); pCAZ1, AB981620 (DDBJ), A0A0K2RW21 (UniProt).

Construction of the *Rhodococcus-E. coli* shuttle vectors I constructed the pRET1101 (Ap^r), pRET1102 (Km^r), pRET1103 (Cm^r), pRET1201 (Ap^r), pRET1202 (Km^r), and pRET1203 (Cm^r) plasmids (Table 2). The construction scheme for the pRET1102 and pRET1202 plasmids is shown in Fig. 1. pRET1102 and pRET1202 were successfully transformed into *R. erythropolis* MAK-34, but the other plasmids, pRET1101, pRET1103, pRET1201, and pRET1203, could not be transformed into *R. erythropolis* MAK-34 with high efficiency. The pRET1102 plasmid was also successfully transformed into *R. erythropolis* JCM2895. The obtained recombinant *R. erythropolis* JCM2895 harbored the pRE2895 and pRET1102 plasmids. In contrast, while the pRET1202 plasmid was successfully transformed into *R. erythropolis* JCM2895 with low efficiency, the obtained recombinant *R. erythropolis* JCM2895 harbored only the pRET1202 plasmid.

To examine the minimal region necessary for replication, I reduced the size of the pRET1102 plasmid (Table 2 and Fig. 5). *R. erythropolis* MAK-32 was transformed successfully with the pRET1123 plasmid encoding the pRET1100 *repT* gene. *R. erythropolis* MAK-32 was also transformed successfully with the pRET1127 and pRET1129 plasmids, but not with the pRET1128 and pRET1130 plasmids. These results suggest that the pRET1100 DNA region from nucleotides 628 to 2768 is required for replication in *R. erythropolis*.

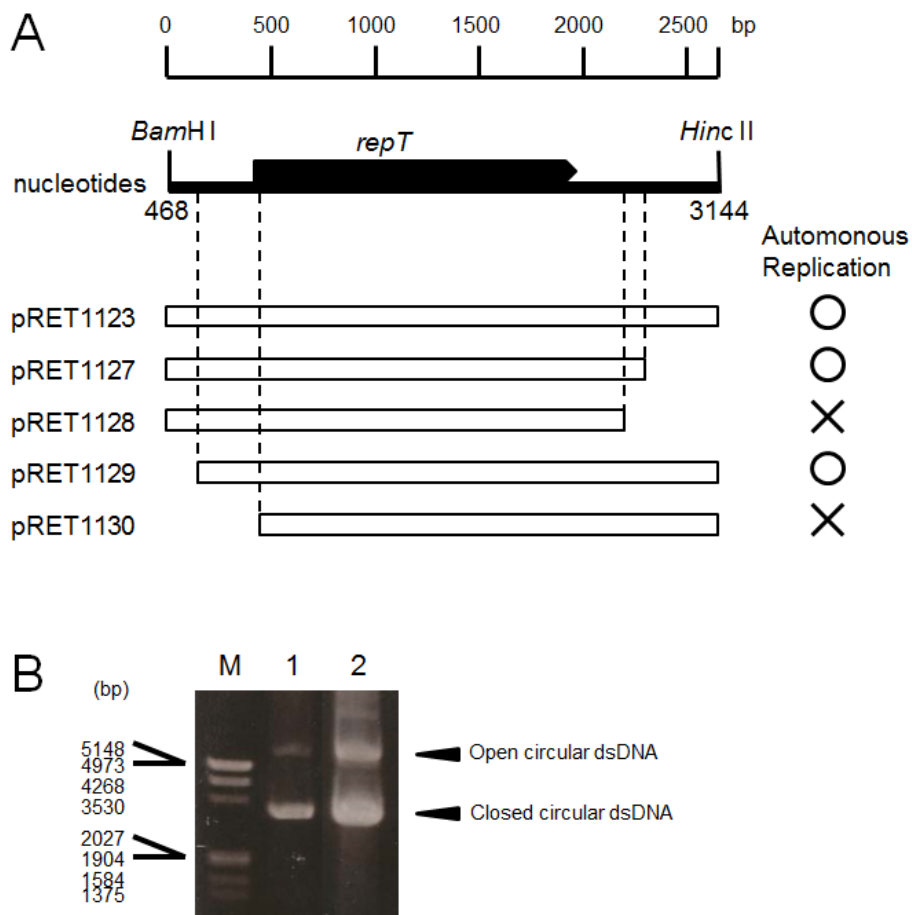


FIG. 5. Determination of the minimum region required for autonomous replication of pRET1100 (A), and agarose gel electrophoresis of the plasmid DNA isolated from recombinant *R. erythropolis* MAK-34 (B). (A) The reduced plasmids derived from pRET1100. The circles indicate the plasmid replicates in *R. erythropolis* MAK-34. The crosses indicate the plasmid do not replicate in *R. erythropolis* MAK-34. (B) agarose gel electrophoresis of the plasmid DNA isolated from recombinant *R. erythropolis* MAK-34 harboring the pRET1123 plasmid or the pRET1129 plasmid. Lane M, size marker (lambda DNA digested with *Eco*RI and *Hind*III); lane 1, the pRET1123 plasmid isolated from recombinant *R. erythropolis* MAK-34; lane 2, pRET1129 plasmid isolated from recombinant *R. erythropolis* MAK-34.

Estimation of plasmid copy number Estimation of plasmid copy number was performed using the methods of Projan et al. (5) and Nakashima and Tamura (6). The estimated copy number of pRET1202 in *R. erythropolis* was $50 \pm 5/\text{cell}$, which is almost the same as that of pNit-QC2 (6), derived from pRE2895 from *R. erythropolis* JCM2895; this is reasonable, as pRET1202 contains the same replication region. The estimated copy number of pRET1102 was $40 \pm 4/\text{cell}$, which is 1.25 times lower than that of pRET1202. The estimated copy number of the reduced shuttle vectors pRET1123 and pRET1127 was $50 \pm 5/\text{cell}$ for both plasmids. The estimated copy number of the reduced shuttle vector pRET1129 in *R. erythropolis* was $138 \pm 6/\text{cell}$, which is 3.46 times higher than those of pRET1123 and pRET1127.

Stabilities of constructed vectors in *Rhodococcus* cells The obtained colony of the recombinant *R. erythropolis* JCM2895 that harbored the pRE2895 and pRET1102 plasmids was inoculated into 10 mL Luria-Bertani broth in the absence of antibiotics and was cultured to an OD₆₁₀ of 3.5 for four days. After three passages, more than 95% of the obtained cells in stationary phase harbored the pRE2895 and pRET1102 plasmids. In contrast, I was unable to obtain a recombinant *R. erythropolis* that harbored the pRET1100 and pRET1202 plasmids, as a competent *R. erythropolis* that harbored only the pRET1100 plasmid could not be obtained.

Discussion

Plasmids have important uses in bioscience, biotechnology, and biochemistry. In this study, I successfully isolated two plasmid species of approximately the same size from the *R. erythropolis* strains IAM1400, IAM1503, IAM1503, JCM2893, and

JCM2894. Nakashima and Tamura (6) reported the isolation of pRE2893 and pRE2894 from *R. erythropolis* JCM2893 and *R. erythropolis* JCM2894, respectively, but other plasmids have not been described. It is assumed that pRE2893 and pRE2894 are similar to the plasmids pRET1600 and pRET1800, respectively, which are described here. Likewise, it is assumed that pRET1200 is similar to pRE2895, isolated from *R. erythropolis* JCM2895 (1), as these plasmids exhibit almost the same band patterns when digested with restriction enzymes.

R. erythropolis JCM2895 was transformed with pRET1102, a newly developed *Rhodococcus-E. coli* shuttle vector, resulting in a strain harboring the pRE2895 and pRET1102 plasmids. These results suggest that the plasmids pRET1100 and pRE2895 are compatible in *R. erythropolis*. The pRE2895 plasmid is similar to the ColiE2 plasmids and is predicted to replicate by a θ -type mechanism (6); however, the replication mechanism of pRET1100 remains unclear. In addition, pRET1102 stably replicates in *R. erythropolis*, as demonstrated by the fact that when the recombinant *R. erythropolis* cells were cultivated in Luria-Bertani broth without antibiotics, more than 95% harbored the pRET1102 plasmid.

The pRET1200 plasmid is also similar to the ColiE2 plasmids, as the pRET1200 RepA and RepB proteins are identical to the pRET2895 RepA and RepB proteins. However, pRET1200 differs from other ColiE2 plasmids from Actinomycetes in that pRET1200 has the replication origin (5'-CATCTGA-3') of the ColiE2 plasmid (9) within the *repA* gene, rather than upstream of the *repA* gene. The minimum sequence region required for the autonomous replication of pRE2895 has been previously reported (6).

pRET1103, carrying the chloramphenicol resistance gene from pHSG398, was not successfully transformed into *R. erythropolis* MAK-34 at high efficiency. Nakashima and Tamura (6) have reported that this recombinant *R. erythropolis* harbors the pNit-RC2

plasmid carrying the chloramphenicol resistance gene from pHN346, which functions as a selective marker in *R. erythropolis*. It is presumed that the chloramphenicol resistance gene within pHSG398, which is derived from *E. coli*, does not function in *R. erythropolis*. I was unable to identify a selective marker that functions both in *R. erythropolis* and *E. coli*, except for the kanamycin resistance gene.

In this study, I also described the high-copy plasmid pRET1129, derived from pRET1100. As this result is a new finding, however, the mechanism underlying its high copy number is unclear. Additionally, I found that *R. erythropolis* strains IAM1400, IAM1503, IAM1503, JCM2893, and JCM2894 harbored similar plasmids. These strains were isolated from different soils in petroleum zones in Japan (14).

In conclusion, I successfully isolated the compatible and stable plasmids pRET1100 (a cryptic plasmid) and pRET1200 from *R. erythropolis* IAM1400. In the future, these plasmids should be useful for the co-expression of multiple genes.

REFERENCES

1. **Nakashima, N. and Tamura, T.:** A novel system for expressing recombinant proteins over a wide temperature range from 4 to 35 degrees C, *Biotechnol. Bioeng.*, **86**, 136-148 (2004).
2. **Denis-Larose, C., Labbé, D., Bergeron, H., Jones, A.M., Greer, C.W., al-Hawari, J., Grossman, M.J., Sankey, B.M., and Lau, P.C.:** Conservation of plasmid-encoded dibenzothiophene desulfurization genes in several rhodococci, *Appl. Environ. Microbiol.*, **63**, 2915-2919 (1997).
3. **Sambrook, J., Fritsch, E.F., and Maniatis, T.:** *Molecular cloning: a laboratory manual*, 2nd ed. Cold Spring Laboratory, Cold Spring Harbor, NY (1989).
4. **Hirasawa, K., Ishii, Y., Kobayashi, M., Koizumi, K., and Maruhashi, K.:** Improvement of desulfurization activity in *Rhodococcus erythropolis* KA2-5-1 by genetic engineering, *Biosci. Biotechnol. Biochem.*, **65**, 239-246 (2001).
5. **Projan, S.J., Carleton, S., and Novick, R.P.:** Determination of plasmid copy number by fluorescence densitometry, *Plasmid*, **9**, 182-190 (1983).
6. **Nakashima, N. and Tamura, T.:** Isolation and characterization of a rolling-circle-type plasmid from *Rhodococcus erythropolis* and application of the plasmid to multiple-recombinant-protein expression, *Appl. Environ. Microbiol.*, **70**, 5557-5568 (2004).
7. **Riabchenko, L.E., Novikov, A.D., Golyshin, P.N., and Ianenko, A.S.:** Sequence and structure analysis of cryptic plasmid pN30 from oil-oxidizing strain *Rhodococcus erythropolis* 30, *Genetika*, **41**, 1725-1727 (2005).
8. **Sekine, M., Tanikawa, S., Omata, S., Saito, M., Fujisawa, T., Tsukatani, N., Tajima, T., Sekigawa, T., Kosugi, H., Matsuo, Y., Nishiko, R., Imamura, K., Ito,**

- M., Narita, H., Tago, S., Fujita, N., and Harayama, S.:** Sequence analysis of three plasmids harboured in *Rhodococcus erythropolis* strain PR4, *Environ. Microbiol.*, **8**, 334-346 (2006).
9. **Toda, H., Koyanagi, T., Enomoto, T., and Itoh, N.:** Characterization of two cryptic plasmids from *Kocuria palustris* IPUFS-1 and construction of novel *Escherichia coli*-*Kocuria* shuttle vector for biocatalysis, *J. Biosci. Bioeng.*, **124**, 255-262 (2017).
10. **Altschul, S.F., Madden, T.L., Schäffer, A.A., Zhang, J., Zhang, Z., Miller, W., and Lipman, D.J.:** Gapped BLAST and PSI-BLAST: a new generation of protein database search programs, *Nucleic Acids Res.*, **25**, 3389-3402 (1997).
11. **Zhou, M., Dai, Y., Zhong, L., and Qin, Z.:** Replication and conjugation of *Streptomyces* small plasmid pDYM4.3k, *Wei. Sheng. Wu. Xue. Bao.*, **52**, 916-920 (2012).
12. **Chen, W. and Qin, Z.:** Development of a gene cloning system in a fast-growing and moderately thermophilic *Streptomyces* species and heterologous expression of *Streptomyces* antibiotic biosynthetic gene clusters, *BMC Microbiol.*, **11**, 243-252 (2011).
13. **Jang, M.S., Fujita, A., Ikawa, S., Hanawa, K., Yamamura, H., Tamura, T., Hayakawa, M., Tezuka, T., Ohnishi, Y.:** Isolation of a novel plasmid from *Couchioplanes caeruleus* and construction of two plasmid vectors for gene expression in *Actinoplanes missouriensis*, *Plasmid*, **77**, 32-38 (2015).
14. **Iizuka, H. and Komagata, K.:** Microbiological studies on petroleum and natural gas. I. Determination of hydrocarbon-utilizing bacteria, *J. Gen. Appl. Microbiol.*, **10**, 207-221 (1964).

SUMMARY

With the aim of being able to co-express multiple genes, I searched for novel compatible plasmids and isolated two plasmid species, pRET1100 and pRET1200, from *Rhodococcus erythropolis* IAM1400. Sequencing analysis revealed that the pRET1100 plasmid is a double-stranded DNA molecule of 5444 bp with two possible open reading frames (ORFs), *repT* and *div*, and three minor ORFs. The cryptic replication protein, RepT, is not highly homologous to those from other plasmids that have been reported. The *Rhodococcus–Escherichia coli* shuttle vector pRET1102 was transformed into *R. erythropolis* JCM2895 harboring the pRE2895 plasmid. The recombinant *R. erythropolis* JCM2895 harbored two plasmid species. These results suggest that plasmid derivatives of pRET1100 and pRE2895 are fully compatible in *R. erythropolis*. I determined the minimum region of pRET1100 required for autonomous replication in *R. erythropolis* and constructed a high-copy plasmid, pRET1129, in *R. erythropolis*.

SECTION 2

Construction of *Rhodococcus* expression vectors and expression of the aminoalcohol dehydrogenase gene in *Rhodococcus erythropolis*

In SECTION 1 of CHAPTER I, I described that the pRET1123 plasmid carrying the minimum region required for autonomous replication in *Rhodococcus erythropolis* was constructed. In this study, I constructed a *Rhodococcus* expression vector using the pRET1123 plasmid and a strong constitutive promoter. This *Rhodococcus* expression vector enables the overexpression of a desired gene and has a broad host range

Materials and methods

Strains and plasmids The characteristics of the plasmids used in this study are summarized in Table 1. Actinomycete strains were obtained from the Institute of Applied Microbiology (Tokyo, Japan), the Japan Collection of Microorganisms (Ibaraki, Japan), the National Institute of Technology and Evaluation (Tokyo, Japan), and the National Institute of Advanced Industrial Science and Technology (Tokyo, Japan). These strains were cultured in Luria-Bertani (LB) broth (1% Bacto tryptone, 0.5% Bacto yeast extract, and 1% NaCl) in the presence or absence of the appropriate antibiotics. Kanamycin (100 µg/mL) was used to select transformants in the culture media.

TABLE 1. Plasmids used in this study

Plasmid	Characteristics	Source/Reference
<i>E. coli</i> vector		
pQE-70	Ap ^r	Qiagen
pMAK8417-2	Ap ^r ; PCR fragment (<i>aadh</i> gene) amplified with MAKPstF and MAKHisBglIIR primers from <i>R. erythropolis</i> MAK154 and digested with <i>Bgl</i> II in <i>Bgl</i> II and blunt-ended <i>Sph</i> I site of pQE-70	This study
pMAK8417-13	Ap ^r ; PCR fragment (<i>hscI</i> promoter) amplified with PhrdB1F and PhrdB1F-R primers and digested with <i>Eco</i> RI and <i>Pst</i> I in <i>Eco</i> RI and <i>Pst</i> I sites of pMAK8417-2	This study
pRET vector		
pRET1102	Km ^r ; <i>Rhodococcus-E. coli</i> shuttle vector derived from pRET1100	(1)
pRET1202	Km ^r ; <i>Rhodococcus-E. coli</i> shuttle vector derived from pRET1200	(1)
pRET1104	Km ^r ; PCR fragment of <i>aadh</i> gene (nucleotides 8170 to 9526 amplified with MAKF1-Pst and MAKR2-del primers from <i>R. erythropolis</i> MAK154) digested with <i>Pst</i> I in <i>Pst</i> I and <i>Hinc</i> II sites of pRET1102	This study
pRET1123	Km ^r ; <i>Rhodococcus-E. coli</i> reduced shuttle vector	(1)
pRET1132	Km ^r ; Δ <i>Pst</i> I site; pRET1123 digested with <i>Pst</i> I, blunt-ended, and self-ligated	This study
pRET1135	Km ^r ; PCR fragment (<i>hscI</i> promoter and <i>aadh</i> gene) amplified with pQE70F1 and pQE70R1135Bm primers from pMAK8417-13 and digested with <i>Eco</i> RI and <i>Bam</i> HI in <i>Eco</i> RI and <i>Bam</i> HI sites of pRET1132	This study
pRET1138	Km ^r ; PCR fragment (<i>I200rep</i> promoter) amplified with P1200rep-Pst5195 and P1204rep-Ec2958 primers from pRET1202 and digested with <i>Eco</i> RI and <i>Pst</i> I in <i>Eco</i> RI and <i>Pst</i> I sites of pRET1135	This study
pRET1172	Km ^r ; PCR fragment (<i>TRR</i> promoter) amplified with PTRRPst-F2 and PTRREco-R primers from synthetic oligonucleotides PTRR and digested with <i>Eco</i> RI and <i>Pst</i> I in <i>Eco</i> RI and <i>Pst</i> I sites of pRET1135	This study
pRET1172-st	Km ^r ; PCR fragment (<i>aadh</i> gene) amplified with MAKPstF and MAKstBglIIR primers from <i>R. erythropolis</i> MAK154 and digested with <i>Pst</i> I in <i>Pst</i> I and blunt-ended <i>Kpn</i> I site of pRET11100	This study

Enzymes and chemicals

All restriction enzymes and DNA modification enzymes were purchased from Toyobo Co., Ltd. (Osaka, Japan) and New England Biolabs, Inc. (Ipswich, MA, USA). All chemicals were purchased from Sigma-Aldrich (St. Louis, MO, USA) and Wako Pure Chemical Industries, Ltd. (Osaka, Japan). The synthetic oligonucleotides used in this study were purchased from Hokkaido System Science Co., Ltd. (Hokkaido, Japan) and are summarized in Table 2.

TABLE 2. Synthetic oligonucleotides used in this study

Primer designation	Nucleotide sequence (5'→3')	Application
MAKF1-Pst	ATGCC <u>CTGCAGG</u> TCGACTCTAGAGGATCCCGAATCTTCTCGTTGATGCAGATCAGGTC	Construction of the pRET1104 plasmid
MAKR2-del	GGGAGGCAATGCTCCGGAATTGATCTCGG	Construction of the pRET1104 plasmid
MAKPstF	GACCA <u>CTGCAG</u> ATCAATCAACTCTGTGAGGTC	Construction of the pMAK8417–2 and pRET1172-st plasmids
MAKHsBglIIR	CGCTTAGATC <u>TCAG</u> TTCCGCCGAGCGCCATCGCCG	Construction of the pMAK8417–2 plasmid
MAKsBglIIR	CGCTTAGATC <u>TTAC</u> AGTTCCGCCGAGCGCCATCGCCG	Construction of the pRET1172-st plasmid
PhrδB1F	GACCGGA <u>AATTC</u> GTCTGTTGACTCCGGCGTCGGCGTCATGCATTCTTGAGT <u>CTGCAG</u> CTGGG	Amplification of the promoter <i>hsp</i> (<i>P_{hsp}</i>)
PhrδB1F-R	CCCAG <u>CTGCAG</u> ACTCAAGAATAC	Amplification of the promoter <i>hsp</i> (<i>P_{hsp}</i>)
P1200rep-Pst5195	AGCCG <u>CTGCAG</u> AAAGCAACACCCGCATCCGCCATTG	Amplification of the promoter <i>1200rep</i> (<i>P_{1200rep}</i>)
P1204rep-Ec2958	CGCGGA <u>AATTC</u> GACCACCACGCACGCACACCGCAC	Amplification of the promoter <i>1200rep</i> (<i>P_{1200rep}</i>)
PTRR	TTAATGGATATTAATGTATCAGTATAGATACATTGTGTATCGGTTCAATCAATGATACAAA AAGTTTCTAAAAACACTTGACGATCTTAAAGTATCGTTTATTATAAATGTTGATACGAT ATGTATCGGAAATGGAGGTGCAAAAATGAAGCGTGAGCGACTTATTG	Amplification of the promoter <i>TRR</i> (<i>P_{TRR}</i>)
PTRRPst-F2	GTTA <u>CTGCAG</u> ACAATAAGTCCCTCACGCTTCATTTT	Amplification of the promoter <i>TRR</i> (<i>P_{TRR}</i>)
PTRRco-R	TGGAGAA <u>TTC</u> TTAATGGATATTATATGTATCAGTA	Amplification of the promoter <i>TRR</i> (<i>P_{TRR}</i>)
pQE70F1	GGCGTATCACGAGGCCCTTTCGTCTTCACC	Construction of the pRET1135 plasmid
pQE70R1135Bm	GGTTGGATCCGTCATCACCGAAACGCGCGAGGCGAG	Construction of the pRET1135 plasmid
pRET1144R560EvKp	TCAATGGTACCGAAGATATCGACCTCATCAGAGTTGATGATCTGCAG	Construction of the pRET1199 and pRET11100 plasmids
pRET1144F1405Kp	GAACTGGGTACCATCACCATCACCATCACTAAGCTTAATTAGC	Construction of the pRET1199 and pRET11100 plasmids

Note: Nucleotide sequences with underlines show that restriction sites (*CTGCAG*, *Pst* I; *AGATCT*, *Bgl* II; *GAATTC*, *EcoR* I; *GGATCC*, *Bam*H I, *GGTACC*, *Kpn* I).

Standard genetic manipulations and sequence analysis Cloning was performed by standard genetic manipulation techniques (2). Actinomycete strains were transformed using the method described by Hirasawa et al. (3). Actinomycete cells were grown in 100 mL of LB at 25–30°C with shaking and harvested at mid-log phase. The cells were washed twice with ice-cold water and suspended with 2.4 mL of ice-cold 10% glycerol. These cells were stored in small portions at –80°C. Portions of 90 µL of cells were mixed with plasmid DNA in 1-mm gap cuvettes and pulsed at 20 kV/cm (400Ω external resistance, 25 µF capacitor) with a Gene Pulser II system (Bio-Rad Laboratories, Inc., Hercules, CA, USA). Pulsed cells were diluted with 0.3 mL of LB and incubated for 3 h at 25°C and spread on LB plates with 100 µg/mL kanamycin. *E. coli* transformation

was performed using the *E. coli* Transformation Buffer Set (Zymo Research Corp., Irvine, CA, USA). Genomic DNA was isolated using a Genomic DNA Buffer set and Genomic-tip 500/G (Qiagen, Hilden, Germany). PCR fragments were prepared with KOD-plus (Toyobo Co., Ltd.). Sequence assembly and analysis were performed using GENETYX Ver.12 (GENETYX Corp., Tokyo, Japan) and DNASIS Pro Ver.2.0 (Hitachi Software Corp., Tokyo, Japan).

AADH activity analysis The substrates of AADH are (*S*)-1-phenyl-1-keto-2-methylaminopropane and 3-pyrrolidinone (3-PLD). In this study, AADH activity was measured in terms of the bioconversion rate of 3-PLD to (*S*)-3-hydroxypyrrolidine (HPD) because 3-PLD detects the activity of AADH six times more sensitively than (*S*)-1-phenyl-1-keto-2-methylaminopropane. Actinomycete strains were cultured in 5 mL of Luria-Bertani broth at 25°C for 4 days. Cells were then harvested and suspended in 1 mL of 200 mM phosphate buffer (pH 6.0) containing 2% glucose and 3% 3-PLD and incubated at 30°C with shaking for 2 h. The cell suspension was then centrifuged at 12,000 ×*g* (MX-307; TOMY SEIKO CO., LTD., Tokyo, Japan) for 5 min at 4°C, and the resulting supernatant was analyzed by HPLC (4).

Construction of the *Rhodococcus* expression vectors To remove the *aadh* gene from the pRET1138 and pRET1172 plasmids, PCR fragments were generated using inverse PCR with the primers, pRET1144R560EvKp and pRET1144F1405Kp. Each of the PCR fragments amplified from pRET1138 and pRET1172 plasmids was digested with *Kpn*I and ligated. The obtained plasmids were designated as pRET1199 and pRET11100, respectively.

Results

Transformation efficiency of the pRET1102 plasmid for actinomycete strains

The pRET1102 plasmid is the *Rhodococcus*–*E. coli* shuttle vector carrying the *repT* gene (1), which codes for a cryptic replication protein and is required for the autonomous replication of the plasmid in *R. erythropolis*. To survey the transformation efficiency of the pRET1102 plasmid, it was transformed into actinomycete strains, including *R. erythropolis* (Table 3). *R. erythropolis* MAK154 was transformed with high efficiency (4.0×10^5 CFU/ μg of DNA). The transformation efficiency of *R. opacus* JCM9703, a closely related species of *R. erythropolis*, was almost the same as that of *R. erythropolis* MAK154 (2.2×10^5 CFU/ μg of DNA). In contrast, *R. rhodnii* JCM3203, *R. ruber* NBRC15591, and *R. zopfii* JCM9919 were transformed with low efficiency (3.7×10^2 , 2.3×10^2 , and 5.2×10^2 CFU/ μg of DNA, respectively; Fig. 1).

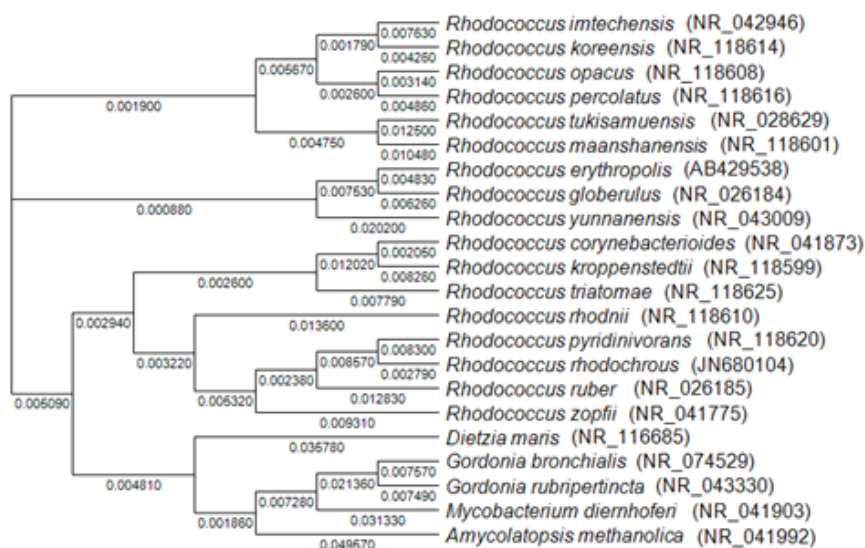


FIG. 1. Phylogenetic tree showing the related species of *Rhodococcus erythropolis* based on 16S rRNA gene sequences. The tree was constructed from an evolutionary distance matrix using GENETYX Ver.12 software. The DDBJ/EMBL/GenBank database accession numbers of the 16S rRNA genes are shown in parentheses.

TABLE 3. Transformation efficiency of pRET1102 for actinomycete strains

Strain	Transformation efficiency
	(CFU/ μ g DNA)
<i>Rhodococcus imtechensis</i> JCM13270	3.1×10^5
<i>Rhodococcus koreensis</i> JCM10743	3.4×10^5
<i>Rhodococcus opacus</i> JCM9703	2.2×10^5
<i>Rhodococcus percolatus</i> JCM10087	3.8×10^5
<i>Rhodococcus tukisamuensis</i> JCM 11308	3.6×10^5
<i>Rhodococcus maanshanensis</i> JCM 11374	1.9×10^5
<i>Rhodococcus erythropolis</i> MAK154	4.0×10^5
<i>Rhodococcus globerulus</i> NBRC14531	3.9×10^5
<i>Rhodococcus yunnanensis</i> JCM13366	1.0×10^5
<i>Rhodococcus corynebacterioides</i> JCM3376	9.7×10^4
<i>Rhodococcus kroppenstedtii</i> JCM13011	1.2×10^5
<i>Rhodococcus triatomae</i> JCM13396	3.1×10^5
<i>Rhodococcus rhodnii</i> JCM3203	3.7×10^2
<i>Rhodococcus pyridinivorans</i> JCM10940	6.6×10^4
<i>Rhodococcus rhodochrous</i> NBRC15564	4.8×10^4
<i>Rhodococcus ruber</i> NBRC15591	2.3×10^2
<i>Rhodococcus zopfii</i> JCM9919	5.2×10^2
<i>Gordonia bronchialis</i> JCM3231	6.1×10^4
<i>Gordonia rubripertincta</i> JCM3199	3.9×10^4
<i>Amycolatopsis methanolica</i> NBRC15065	5.7×10^3
<i>Mycobacterium diernhoferi</i> NBRC3707	1.5×10^4
<i>Dietzia maris</i> NBRC15801	8.4×10^3

Note: *R. ruber* JCM3205 and *R. jostii* JCM11615 were unable to be transformed with pRET1102.

Expression of the *aadh* gene in *R. erythropolis* MAK154

The

genome of *R. erythropolis* MAK154 has a single copy of the *aadh* gene. To increase the copy number of the *aadh* gene, *R. erythropolis* MAK154 was transformed with the pRET1104 plasmid (Fig. 2), which carries the *aadh* gene with the 405-bp upstream region, including the putative ribosomal binding site. The activity of recombinant *R. erythropolis* MAK154 harboring the pRET1104 plasmid was almost the same as that of the wild-type strain.

Therefore, to increase the expression level of the *aadh* gene, I constructed *aadh* expression vectors containing the ribosomal binding site of *aadh* and a promoter (Fig. 3). The promoters from Gram-positive bacteria used in this study are listed in Table 4. These promoters have been reported to function in each bacteria. The *aadh* gene expression vectors pRET1135, pRET1138, and pRET1172 have the promoters *hsp* (5), *1200rep* (1), and *TRR* (6), respectively. The HPD concentration of recombinant *R. erythropolis* MAK154 harboring the pRET1135 plasmid was 0.38 mg/mL, which was approximately three times higher than that of the recombinant *R. erythropolis* MAK154 harboring the pRET1104 plasmid (0.13 mg/mL). The HPD concentrations of recombinant *R. erythropolis* MAK154 harboring the pRET1138 and pRET1172 plasmids were 1.76 and 2.50 mg/mL, respectively. The promoter activity of the *TRR* was stronger than that of *hsp* and *1200rep*.

TABLE 4. Promoters that express *aadh* gene in *R. erythropolis*

Promoter	Origin	GenBank accession no.	Position	Length	Template of PCR	Primer of PCR	Ref.
<i>1200rep</i>	<i>Rhodococcus erythropolis</i>	LC331662	204–5073 (Complement)	553 bp	pRET1202 plasmid	P1204rep-Ec2958 ^a P1200rep-Pst5195 ^a	(1)
<i>hsp</i>	<i>Streptomyces griseus</i>	D14499	49–87	39 bp	PhrdB1F ^(a,b)	PhrdB1F-R ^(a) (PhrdB1F)	(5)
<i>TRR</i>	<i>Lactobacillus plantarum</i>	X98106	730–557 (Complement)	174 bp	PTRR ^(a)	PTRRPst-F2 ^(a) PTRREco-R ^(a)	(6)

^(a) Synthetic oligonucleotide, ^(b) Concentration of template is equal to that of primer in PCR

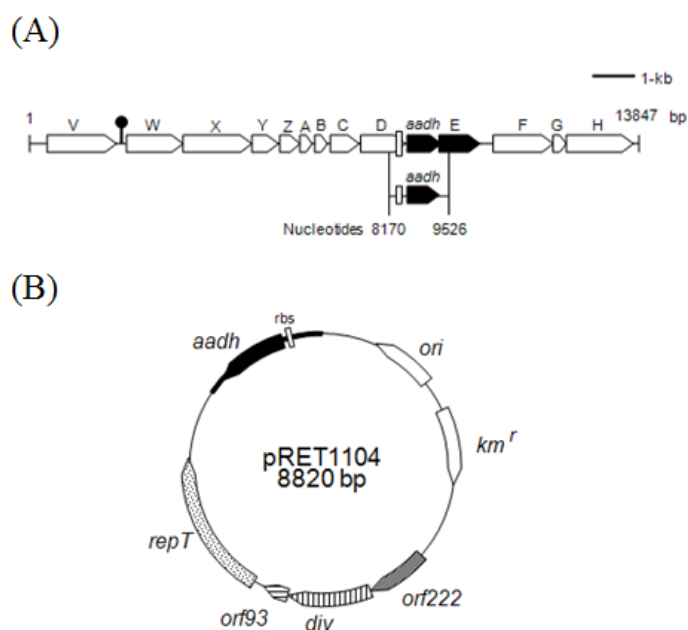


FIG. 2. Structure of pRET1104. (A) ORF map around *aadh* isolated from *Rhodococcus erythropolis* MAK154. The DDBJ/EMBL/GenBank database accession number is AB573180. The *aadh* and *orfE* are shown in solid gray. A closed circle with a bold line indicates the putative OrfE binding site. An open square indicates the putative ribosomal binding site (rbs) of *aadh*. (B) ORF map of pRET1104. The pRET1104 plasmid carries the *aadh* gene with a 405-bp upstream region, including the putative ribosomal binding site (nucleotides 8170 to 9526). *repT*, *ori*, *div*, and *km^r* are the gene involved in plasmid replication in *R. erythropolis*, ColE1 *ori*, the gene involved in cell division, and the kanamycin resistance gene, respectively.

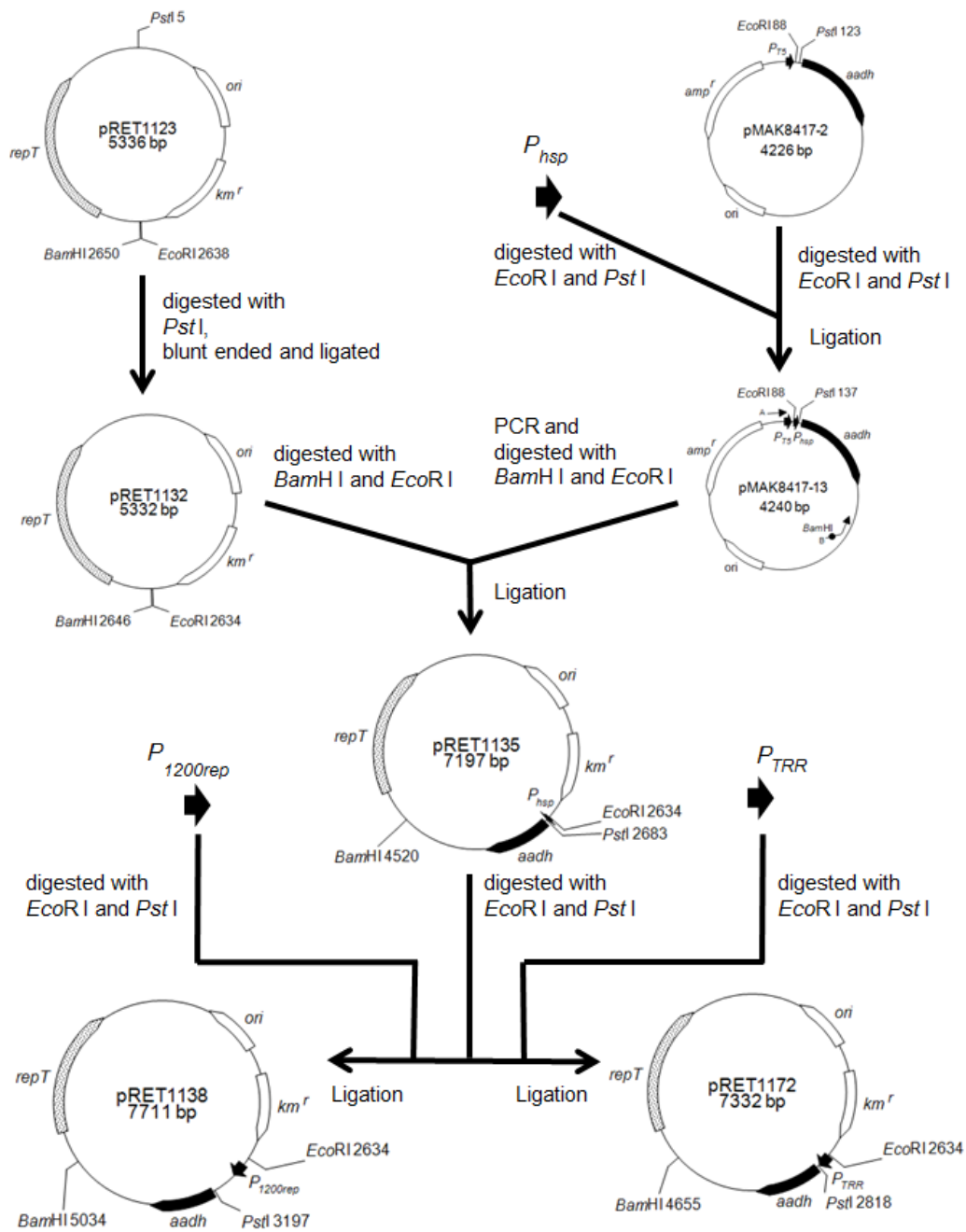


FIG. 3. Construction of *aadH* gene expression vectors. DNA insert containing *aadH* with the putative ribosomal binding site. Cloning sites are displayed. *repT*, *ori*, *div*, and *km^r* are the gene involved in plasmid replication in *Rhodococcus erythropolis*, ColE1 ori, the gene involved in cell division, and the kanamycin resistance gene, respectively. P_{T5} , P_{hsp} , $P_{1200rep}$, and P_{TRR} are the promoters *T5*, *hsp*, *1200rep*, and *TRR*, respectively.

Host range of *TRR* promoter

The plasmid pRET1172 containing the *TRR* promoter was transformed into the actinomycete strains listed in Table 3. The AADH activities of all the strains transformed with the plasmid pRET1172 were higher than those of strains transformed with the pRET1102 plasmid (Fig. 4). Of all the recombinant strains studied, recombinant *R. koreensis* JCM10743 harboring pRET1172 showed the highest HPD concentration (6.2 mg/mL), whereas recombinant *R. maanshanensis* JCM 11374 harboring pRET1172 showed the lowest (0.3 mg/mL; Fig. 4).

The AADHs shown in Fig. 3 are the enzymes with C-terminal 6xHis tags. I constructed AADH without the C-terminal 6xHis tags (pRET1172-st). The activity of the recombinant *R. erythropolis* MAK154 harboring the pRET1172 plasmid was 2.3 ± 0.21 mg/mL. The activity of the AADH without the C-terminal 6xHis tag was almost the same as that of the AADH with C-terminal 6xHis tag. The estimated copy number of pRET1172 in *R. erythropolis* MAK154 is 35 ± 6 /cell, which is almost the same as that of pRET1102.

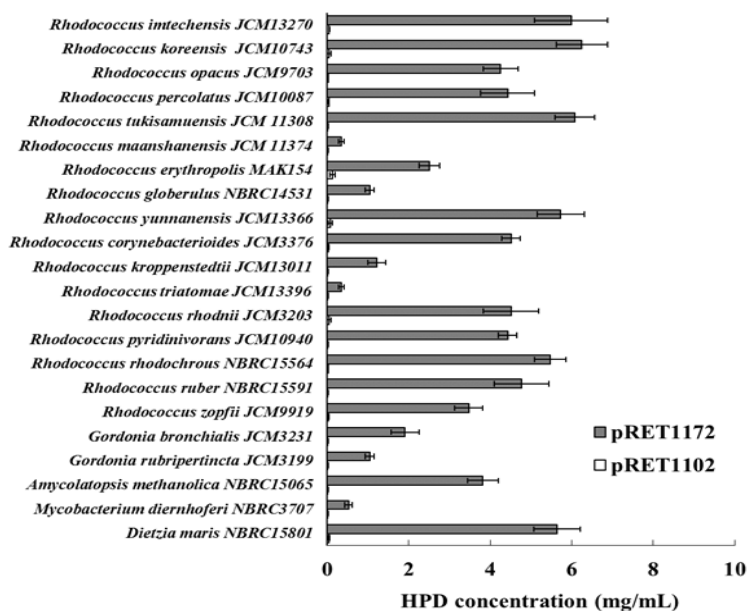


FIG. 4. (*S*)-3-hydroxypyrrolidine (HPD) concentrations of recombinant actinomycete strains. HPD concentrations were analyzed by the bioconversion rate of 3-pyrrolidinone (3-PLD) to HPD. Vertical bars indicate SD from three independent experiments.

Discussion

Although *Rhodococcus* sp. are known to produce many industrially important enzymes, genetic manipulation of *Rhodococcus* strains using *Rhodococcus* expression vectors is not well studied. Therefore, I constructed *Rhodococcus* expression vectors derived from the *Rhodococcus*–*Escherichia coli* shuttle vector pRET1102 and different promoters to increase the expression of *aadh*. The pRET1102 plasmid carries the *repT* gene that codes for a cryptic replication protein and is required for the autonomous replication in *R. erythropolis* (1). The pRET1102 plasmid was successfully transformed into many actinomycete strains, including *R. erythropolis*. The species closely related to *R. erythropolis* [e.g., *R. opacus* (7)] were transformed with high efficiency. In addition, the pRET1102 transformation efficiency for *R. erythropolis* was almost the same as that for the *Rhodococcus*–*E. coli* shuttle vector pNit-QC2(8) carrying the *repA* and *repB* genes, which encode the replication protein for *R. erythropolis*. These results suggest that the pRET1102 plasmid has a broad host range.

The HPD concentration of recombinant *R. erythropolis* MAK154 harboring the pRET1104 plasmid was almost the same as that of the wild-type strain. In contrast, the HPD concentration of recombinant *R. erythropolis* MAK154 harboring the pRET1135 plasmid was approximately three times higher than that of recombinant *R. erythropolis* MAK154 harboring the pRET1104 plasmid. These results suggest that the 405-bp upstream region of the *aadh* gene has no promoter.

The promoter activity of the promoter *TRR*, which is derived from *Lactobacillus plantarum*, was stronger than that of the promoters *hsp* and *1200rep*. Many actinomycete strains transformed with pRET1172 having the *TRR* promoter showed increased AADH activities. These results suggest the broad host range of the *TRR* promoter. These

promoters are constitutive promoters of varying strengths and are useful for developing whole cell biocatalysts in manufacturing industries. Therefore, to express genes other than *aadh*, I constructed the *Rhodococcus* expression vectors pRET1199 and pRET11100 without *aadh*, derived from the plasmids pRET1138 and pRET1172, respectively. The differences in recombinant AADH expression in different host strains might be due to differences in copy number, promoter activity, and membrane permeability. I have not yet collected sufficient data to explain this phenomenon.

Activity of AADH was found in actinomycete strains harboring pRET1102, which has no *aadh* gene, except for *R. erythropolis* MAK154. This result suggests that the actinomycete strains shown in Fig. 4, except for *R. erythropolis* MAK154, are unable to produce HPD. Actinomycete strains except for *R. erythropolis* MAK154 might have no *aadh* (4). The recombinant *R. erythropolis* MAK154 harboring pRET1172 was cultivated with aminopropanol, as AADH expression in *R. erythropolis* MAK154 is known to be induced by aminopropanol (4). The activity of AADH increased slightly (3.1 ± 0.29 mg/mL), suggesting that intrinsic AADH is induced by aminopropanol. The enantiopurity of the product was $> 98\%$ enantiomeric excess (*ee*) of (*S*)-enantiomer.

The AADH of *R. erythropolis* MAK154 is a valuable enzyme that produces double chiral compounds (4,9), which are used as pharmaceuticals. Many actinomycete strains transformed with pRET1172 having the *TRR* promoter showed high AADH activities. In this study, I successfully constructed *Rhodococcus* expression vectors and expressed the *aadh* gene in many actinomycete strains.

REFERENCES

1. **Yamamura, E.-T.:** Isolation of two plasmids, pRET1100 and pRET1200, from *Rhodococcus erythropolis* IAM1400 and construction of a *Rhodococcus*–*E. coli* shuttle vector, *J. Biosci. Bioeng.* **125**, 625–631 (2018).
2. **Sambrook, J., Fritsch, E.F., and Maniatis, T.:** *Molecular cloning: a laboratory manual*, 2nd ed. Cold Spring Laboratory, Cold Spring Harbor, NY (1989).
3. **Hirasawa, K., Ishii, Y., Kobayashi, M., Koizumi, K., and Maruhashi, K.:** Improvement of desulfurization activity in *Rhodococcus erythropolis* KA2-5-1 by genetic engineering, *Biosci. Biotechnol. Biochem.*, **65**, 239–246 (2001).
4. **Urano, N., Kataoka, M., Ishige, T., Kita, S., Sakamoto, K., and Shimizu, S.:** Genetic analysis around aminoalcohol dehydrogenase gene of *Rhodococcus erythropolis* MAK154: a putative GntR transcription factor in transcriptional regulation, *Appl. Microbiol. Biotechnol.* **89**, 739–744 (2011).
5. **Hatada, Y., Shinkawa, H., Kawamoto, K., Kinashi, H., and Nimi O.:** Cloning and nucleotide sequence of a *hsp70* gene from *Streptomyces griseus*, *J. Ferment. Bioeng.* **77**, 461–467 (1997).
6. **Kodaira, K.-I., Oki, M., Kakikawa, M., Watanabe, N., Hirakawa, M., Yamada, K., and Taketo, A.:** Genome structure of the *Lactobacillus* temperate phage ϕ gle: the whole genome sequence and the putative promoter/repressor system, *Gene*, **187**, 45–53 (1997).
7. **Maruyama, T., Ishikura, M., Taki, H., Shindo, K., Kasai, H., Haga, M., Inomata, Y., and Misawa, N.:** Isolation and characterization of *o*-xylene oxygenase genes from *Rhodococcus opacus* TKN14, *Appl. Environ. Microbiol.*, **71**, 7705–7715 (2005).

8. **Nakashima, N. and Tamura, T.:** Isolation and characterization of a rolling-circle-type plasmid from *Rhodococcus erythropolis* and application of the plasmid to multiple-recombinant-protein expression, *Appl. Environ. Microbiol.*, **70**, 5557–5568 (2004).
9. **Kataoka, M., Nakamura, Y., Urano, N., Ishige T, Shi, G., Kita, S., Sakamoto, K., and Shimizu, S.:** A novel NADP⁺-dependent L-1-amino-2-propanol dehydrogenase from *Rhodococcus erythropolis* MAK154: a promising enzyme for the production of double chiral aminoalcohols, *Lett. Appl. Microbiol.*, **43**, 430–435 (2006).

SUMMARY

NADP⁺-dependent aminoalcohol dehydrogenase (AADH) of *Rhodococcus erythropolis* MAK154 produces double chiral aminoalcohols, which are used as pharmaceuticals. However, the genetic manipulation of *Rhodococcus* strains to increase their production of such industrially important enzymes is not well studied. Therefore, I aimed to construct *Rhodococcus* expression vectors, derived from the *Rhodococcus*–*Escherichia coli* shuttle vector pRET1102, to express *aadh*. The plasmid pRET1102 could be transformed into many actinomycete strains, including *R. erythropolis*. The transformation efficiency for a species closely related to *R. erythropolis* was higher than that for other actinomycete strains. Promoters of various strengths, *hsp*, *1200rep*, and *TRR*, were obtained from Gram-positive bacteria. The activity of *TRR* was stronger than that of *hsp* and *1200rep*. The *aadh*-expressing plasmid pRET1172 with *TRR* could be transformed into many actinomycete strains to increase their AADH production. The *Rhodococcus* expression vector, pRET11100, constructed by removing *aadh* from the pRET1172 plasmid may be useful for bioconversion.

CHAPTER II

Biochemical and molecular biological studies on enzymatic synthesis of vitamin B₆ derivatives and optically active carboxylic acids

SECTION 1

Bioconversion of pyridoxine to pyridoxamine through pyridoxal using a *Rhodococcus* expression system

In this study, with the aim of producing pyridoxamine (PM), two enzymes, pyridoxine 4-oxidase (PNO) and pyridoxamine-pyruvate aminotransferase (PPAT), were derived from *Mesorhizobium loti* and used for bioconversion. PNO is expressed in *Escherichia coli* and recombinant PNO has been purified and characterized. However, the expression of *pno* in *E. coli* has the disadvantage that it needs coexpression of the chaperonins, GroEL and GroES. In the SECTION I, I described that the novel *Rhodococcus* expression system was constructed. The present study investigates the bioconversion of pyridoxine (PN) to PM through pyridoxal (PL), using the *Rhodococcus* expression system without chaperonins.

Materials and methods

Strains and plasmids

Actinomycete strains were obtained from the Institute of Applied Microbiology (Tokyo, Japan), the National Institute of Technology and Evaluation (Tokyo, Japan), and the Japan Collection of Microorganisms (Ibaraki, Japan). *E. coli* BL21 (DE3) was obtained from Nippon Gene Co., Ltd. (Tokyo, Japan). These strains were cultured in Luria-Bertani (LB) medium (0.5% Bacto yeast extract, 1% Bacto tryptone, and 1% NaCl) in the presence or absence of the appropriate antibiotics. Ampicillin (100 µg/mL) and kanamycin (50 µg/mL) were used to select transformants in the culture media. The plasmids, pET-mll6785 (*pno* expression vector for *E. coli*), pET6806 (*ppat* expression vector for *E. coli*), and pRET11100 (*Rhodococcus* expression vector), were constructed as previously described (1–3).

Enzymes and chemicals

All restriction enzymes and DNA modification enzymes were purchased from Toyobo Co., Ltd. (Osaka, Japan) and New England Biolabs, Inc. (Ipswich, MA, USA). All chemicals were purchased from Sigma-Aldrich (St. Louis, MO, USA), Wako Pure Chemical Industries, Ltd. (Osaka, Japan), and Tokyo Chemical Industry Co., Ltd. (Tokyo, Japan). The synthetic oligonucleotides used in this study were purchased from Hokkaido System Science Co., Ltd. (Hokkaido, Japan).

Standard genetic manipulations and sequence analysis

Cloning was performed by standard genetic manipulation techniques (4). Actinomycete strains were transformed using the method described by Yamamura (3). *E. coli* transformation was performed using the *E. coli* Transformation Buffer Set (Zymo Research Corp., Irvine, CA, USA). PCR fragments were prepared with KOD -Plus- (Toyobo Co., Ltd.), according to the manufacturer's instructions. Sequence analysis and assembly were performed using GENETYX Ver.12 (GENETYX Corp., Tokyo, Japan).

Molecular mass measurement

Crude extracts from recombinant *R.*

erythropolis were analyzed on SDS–PAGE (12% gel) by the method of Laemmli (5) and were visualized by staining with Coomassie Brilliant Blue R-250. Crude extracts were prepared by the method described by Yuan et al. (1). Size marker was used the SDS-PAGE Molecular Weight Standards (Broad Range) purchased from Bio-Rad Laboratories, Inc. (Hercules, CA, USA).

Construction of *pno* and *ppat* expression vectors for *R. erythropolis*

The present study investigates the bioconversion of PN to PM through PL (Fig. 1), using a *Rhodococcus* expression system. To construct *pno* and *ppat* expression vectors for *R. erythropolis*, the plasmid pRET11100 was used because it has a strong constitutive promoter and broad actinomycetes host range (3). The *pno* gene, which was derived from *M. loti*, was amplified with the primers: PNO3F50Pt: 5'-GATGGCTGCAGGGATGACCA GGGCCAAGTTGAGCACGCACCGAATTG-3' (*Pst* I site is underlined) and mllR(st)Kp: 5'-GGCCGGTACCTTGTCGACTTAGTACTGTCGGGCGAAAGTCTC GG-3' (*Kpn* I site is underlined), from the plasmid pET-mll6785 using a Mastercycler gradient thermal cycler (Eppendorf, Hamburg, Germany). The PCR fragment containing *pno* was digested with *Pst* I and *Kpn* I and then ligated into the *Pst* I and *Kpn* I sites of pRET11100 to prepare the plasmid pRET-PNO9, which is the *pno* expression vector for *R. erythropolis*. To prepare the *ppat* expression vector for *R. erythropolis*, the *M. loti*-derived *ppat* gene was amplified with the primers: mlr6806PtF1: 5'-GGAGACTGCGATGCGCTATCCCGAACATGCCGATCCGGTCATC-3' (*Pst* I site is underlined) and mlr6806KpR1200St: 5'-TCAGGGGTACCTTAAATTAAGCTGAG GGAAAGTTCAGGCGTC-3' (*Kpn* I site is underlined), from the plasmid pET6806 and digested with *Pst* I and *Kpn* I. The DNA fragment containing *ppat* was ligated into the *Pst* I and *Kpn* I sites of pRET11100, and designated pRET-PPAT1.

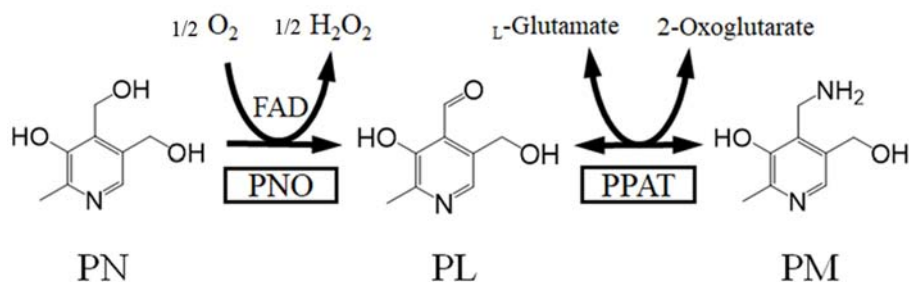


FIG. 1 Scheme for the bioconversion of PN to PM through PL. PL is produced from PN by PNO, while PM is produced from PL by PPAT. FAD is flavin adenine dinucleotide.

Construction of the *pno* and *ppat* coexpression vector for *R. erythropolis*

The *ppat* gene was amplified with the primers: mlr6806PtF1: 5'-GGAGACTGCAGGATGCGCTATCCCGAACATGCCGATCCGGTCATC-3' (*Pst* I site is underlined) and mlr6806KpR1200His: 5'-GAAAGTGGTACCGTCGGCGTCGATTACGGCCAGCGCCGCCTC-3' (*Kpn* I site is underlined), from the plasmid pET6806 and was digested with *Pst* I and *Kpn* I. The DNA fragment containing *ppat* was ligated into the *Pst* I and *Kpn* I sites of pRET11100, which was designated pRET-PPAT2. The *pno* gene was amplified with the primers: PNO9-FKp: 5'-CCGAGGAGGTATACATATGACCAGGGCCAAGGTTGAGCACGCACC-3' (*Kpn* I site is underlined) and R1135Bm: 5'-GGTTGGATCCGTCATCACCGAAACGCGCGAGGCAG-3'), from the plasmid pET-PNO9. The *pno*-containing PCR fragment was digested with *Kpn* I and *Xba* I and was ligated into the *Kpn* I and *Xba* I sites of pRET-PPAT2 to prepare the plasmid pRET-PPP1 which is the *pno* and *ppat* coexpression vector for *R. erythropolis* (Fig. 2).

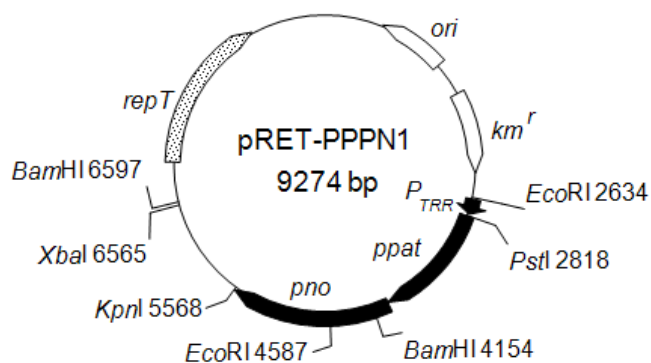


FIG. 2 Structure of pRET-PPP1 co-expressing *pno* and *ppat*. *km^r* is the kanamycin resistance gene. *P_{TRR}* is the promoter *TRR*. *ppat* and *pno* are the gene encoding pyridoxamine-pyruvate aminotransferase (PPAT) and the gene encoding pyridoxine 4-oxidase (PNO), respectively. *repT* is the gene involved in plasmid replication in *R. erythropolis*. *ori* is ColE1 ori.

Screening of *R. erythropolis* strains as a host cell

Recombinant *R.*

erythropolis cells were inoculated into 5 mL of LB medium with kanamycin (50 µg/mL) and incubated at 25°C with shaking for 3 days. The cells were harvested and suspended in 1 mL of 300 mM phosphate buffer (pH 7.0) containing 2% glucose and 100 mM PN and incubated at 30°C with shaking for 10 h. Cell suspensions were then centrifuged at 12,000 × *g* for 5 min at 4°C, and the resulting supernatants were analyzed by high-performance liquid chromatography (HPLC) as described below. Recombinant *E. coli* cells used in control experiments were incubated as previously described (1) and treated as described above.

Analysis of PN, PL, and PM by HPLC

PN, PL, and PM were

determined by HPLC on an Inertsil ODS-3 column (ϕ 4.6 × 75 mm; GL Sciences Inc., Tokyo, Japan). The mobile phase was 0.1% trifluoroacetic acid-acetonitrile, the gradient of acetonitrile concentration was from 1 to 80% for 8 min, the flow rate was 1.0 mL/min,

and the detection wavelength was at 294 nm.

Cultivation of recombinant *R. erythropolis* by a jar fermenter

Recombinant *R. erythropolis* cells were propagated in LB medium as described by Kozono et al. (6). Recombinant *R. erythropolis* cells were inoculated into 5 mL of LB medium with kanamycin and incubated at 25°C with shaking for 3 days. Five milliliters of seed medium were transferred into 3.6 L of LB medium in a 5 L jar fermenter (LS-5, Sakura Seiki Co., Ltd., Tokyo, Japan) and incubated at 30°C with 500-rpm agitation, 1-vvm aeration, and a pH maintained at 7.0 ± 0.5 for 3 days.

Reactor bioconversion using the *Rhodococcus* expression system

Bioconversion of PN and PL was performed in three ways. First, for the bioconversion of PN to PL, 3.5 L of the culture medium of recombinant *R. erythropolis* was harvested and suspended in 700 mL of tap water containing 500 mM (approximately 10%) PN and 0–2% glucose (standard reaction condition was 2% glucose). The cell suspension was transferred into a 1.8 L reactor (TBR-2-3, Sakura Seiki Co., Ltd.) and incubated at 27.5–40.0°C with 500-rpm agitation, 0.1–1.5-vvm aeration, and a pH maintained at 5.5–7.5 for 2–6 days (standard reaction condition: 30°C, 1 vvm, and pH 6.5 for 2 days). Second, for bioconversion of PL to PM, 12 L of the culture medium of recombinant *R. erythropolis* was harvested and suspended in 700 mL of tap water containing 100 mM PL and 400 mM L-glutamate. The cell suspension was transferred into a 1.8 L reactor and incubated at 30°C with 500-rpm agitation, 1-vvm aeration, and a pH maintained at 6.5 for 2 days. Third, for the bioconversion of PN to PM through PL, 33 L of the culture medium of recombinant *R. erythropolis* was harvested and suspended in 700 mL of tap water containing 200 mM (approximately 4%) PN, 2% glucose, and 800 mM L-glutamate. The cell suspension was transferred into a 1.8 L reactor and incubated at 30°C with 500-rpm agitation, 1-vvm aeration, and a pH maintained at 6.5 for 2 days.

Nucleotide sequence accession number The nucleotide sequences reported in this paper appear in the DDBJ/GenBank/EMBL nucleotide sequence databases under accession number NC_002678.

Results

Construction of a *pno* expression vector for *R. erythropolis* and screening of *R. erythropolis* strains as a host cell PNO catalyzes the oxidation of PN to PL. The PNO enzyme from *M. loti* is monomeric and has a molecular mass of 56 kDa. It shows a high specificity for PN and no activity toward PM (1). For overexpression of *pno* in *R. erythropolis* cells, *pno* was inserted downstream of the *TRR* promoter of pRET11100. The plasmid pRET-PNO9 was transformed into many *R. erythropolis* strains for screening and identification of a host cell (Fig. 3A).

The strain with the lowest PL production was recombinant *R. erythropolis* JCM6827 (1.1 ± 0.1 mM), while the strain with the highest PL production was recombinant *R. erythropolis* JCM3191 (45.9 ± 4.6 mM). In control experiments using the recombinant *E.coli* BL21 (DE3) harboring pET-mll6785, the production of PL was 0.05 ± 0.01 mM. The activity of recombinant *R. erythropolis* JCM3191 was 918 times higher than that of recombinant *E.coli* BL21 (DE3). The PL production of recombinant *R. erythropolis* JCM3191 with 5 μ M FAD was 45.2 ± 3.9 mM and almost the same as that without FAD. All recombinant *R. erythropolis* strains harboring pRET11100 did not produce PL. Regarding PNO, it was overexpressed in *R. erythropolis* JCM3191. The protein had a molecular weight of 56 kDa, which is in agreement with the predicted molecular weight. The overexpressed PNO was detected as a soluble form on SDS-PAGE (Fig. 3B).

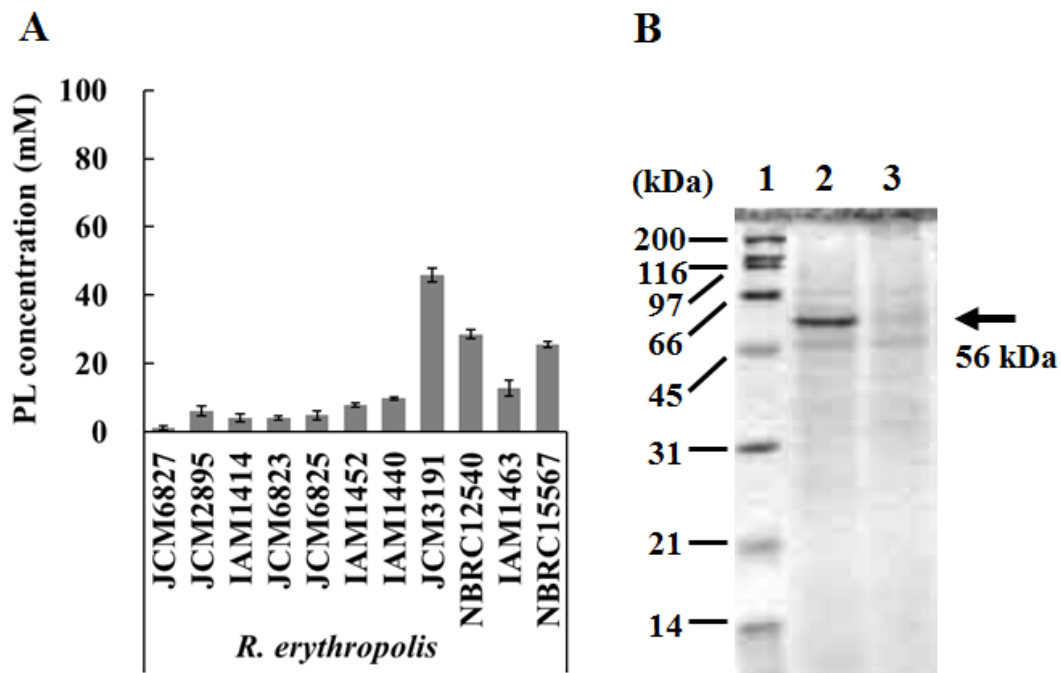


FIG. 3 Screening of *R. erythropolis* strains as a host cell. (A) PL concentrations of recombinant *R. erythropolis* strains harboring the pRET-PNO9 plasmid. Vertical bars indicate SD from three independent experiments. (B) SDS-PAGE of crude extracts from recombinant *R. erythropolis* cells. Lane 1, standard proteins; lane 2, the crude extract from recombinant *R. erythropolis* JCM3191 harboring the pRET-PNO9 plasmid; lane 3, the crude extract from recombinant *R. erythropolis* JCM3191 harboring the pRET11100 plasmid.

Optimization of reaction conditions for bioconversion of PN to PL

The bioconversion of PN to PL using recombinant *R. erythropolis* JCM3191 harboring the plasmid pRET-PNO9 is an oxidation reaction requiring oxygen. PL production increased with increasing aeration; an optimal reaction aeration was determined to be >1 vvm (Fig. 4A). The effects of pH were also examined, and it was determined that a pH of 6.5 was optimal (Fig. 4B). Similarly, an optimal reaction temperature of 30.0–32.5°C was determined based on evaluation of a range of temperatures from 27.5–40.0°C (Fig. 4C). Further, the production of PL increased with increasing glucose as an energy source. The optimal reaction concentration of glucose was found to be >1.0% glucose. PL concentration increased over time by the addition of >1.0% glucose, and was approximately 450 mM in 84 h (Fig. 4D).

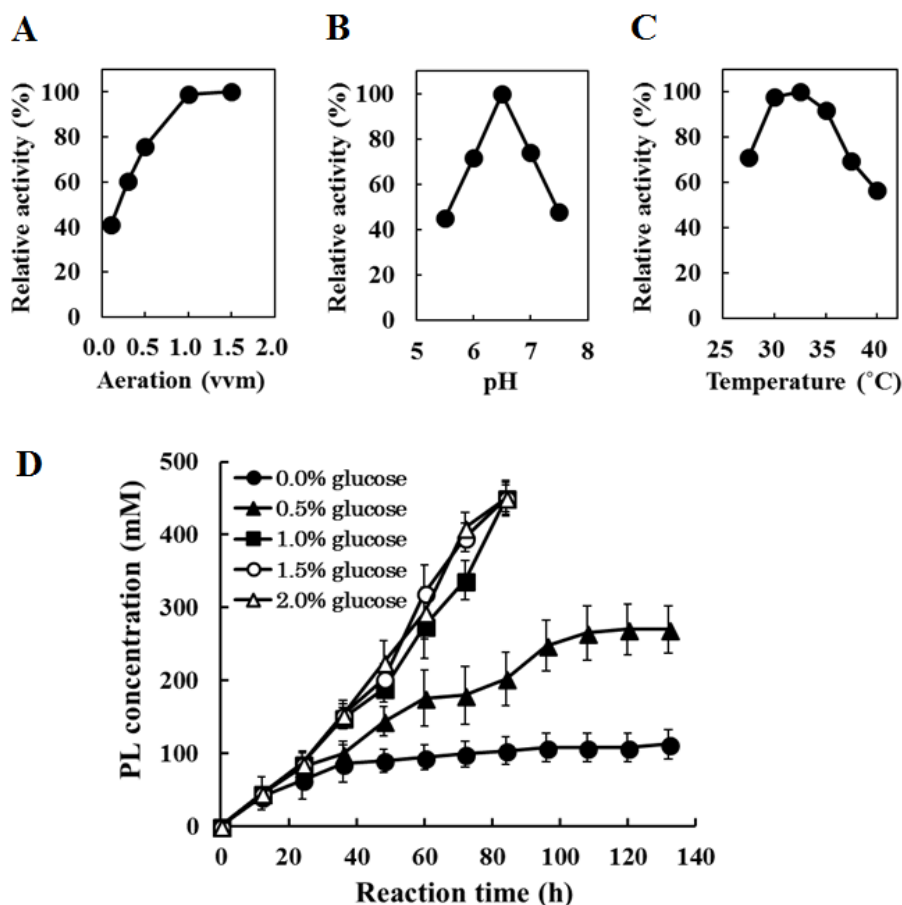


FIG. 4 Effects of aeration, pH, temperature, and glucose concentrations on the bioconversion of PN to PL by recombinant *R. erythropolis* JCM3191 harboring the pRET-PNO9 plasmid. (A) Effect of aeration. Activity was assayed under standard reaction conditions, except for the aeration. (B) Effect of pH. Activity was assayed under standard reaction conditions, except for pH. pH was adjusted with 28% sodium hydroxide (NaOH). (C) Effect of temperature. Activity was assayed under standard reaction conditions, except for the temperature. (D) Effect of glucose addition. Activity was assayed under standard reaction conditions, except for reaction time and glucose concentration. Vertical bars indicate SD from three independent experiments. Closed circle, closed triangle, closed square, open circle, and open triangle indicates no glucose, 0.5% glucose, 1.0% glucose, 1.5% glucose, and 2.0% glucose, respectively.

Construction of a *ppat* expression vector for *R. erythropolis* and conditional

production of PM dependent on PL production

PPAT is a pyridoxal 5'-phosphate-independent aminotransferase that catalyzes the transfer of an amino group between PL and L-glutamate to PM and 2-oxoglutarate. For overexpression of *ppat* in *R. erythropolis* cells, *ppat* was inserted downstream of the *TRR* promoter of pRET11100. The plasmid pRET-PPAT1 was transformed into *R. erythropolis* JCM3191. The recombinant *R. erythropolis* JCM3191 strain harboring the pRET-PPAT1 plasmid overexpressed *ppat*. The bioconversion rate of PL to PM using recombinant *R. erythropolis* JCM3191 was approximately 80% (Fig. 5A) using the same conditions as those of PL production (1 vvm, pH 6.5, and 30°C). Overexpression of PPAT was detected as a soluble form on SDS-PAGE, with a molecular weight of 42 kDa, which is in agreement with the predicted molecular weight (Fig. 5B).

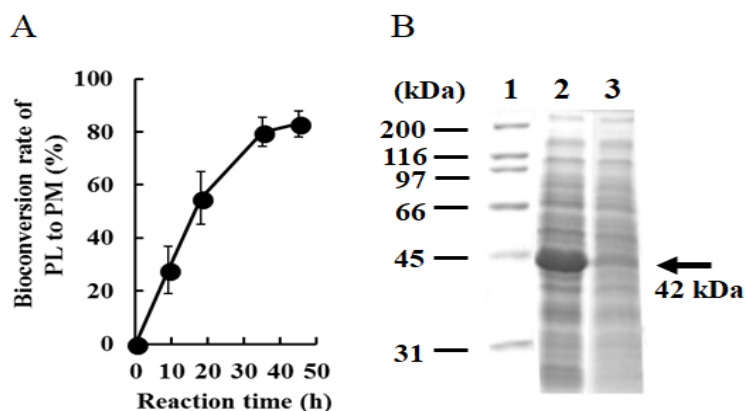


FIG. 5 Bioconversion of PL to PM using recombinant *R. erythropolis* JCM3191 harboring the pRET-PPAT1 plasmid. (A) Bioconversion rate of PL to PM of recombinant *R. erythropolis* JCM3191 harboring the plasmid pRET-PPAT1. Vertical bars indicate SD from three independent experiments. (B) SDS-PAGE of crude extracts from recombinant *R. erythropolis* cells. Lane 1, standard proteins; lane 2, the crude extract from recombinant *R. erythropolis* JCM3191 harboring the pRET-PPAT1 plasmid; lane 3, the crude extract from recombinant *R. erythropolis* JCM3191 harboring the pRET11100 plasmid.

Bioconversion of PN to PM through PL To coexpress *ppat* and *pno* in *R. erythropolis* cells, *ppat* was inserted downstream of the *TRR* promoter of pRET11100, while *pno* was inserted downstream of *ppat*. The obtained plasmid was designated as pRET-PPPN1 (Fig. 2), which was then transformed into *R. erythropolis* JCM3191. The recombinant *R. erythropolis* JCM3191 strain harboring pRET-PPPN1 had bioconversion activity producing PM from PN. The PN concentration decreased over 5 h, while the PL concentration increased and PM production started. After 20 h from the start of the reaction, PN and PL concentrations decreased and PM concentration increased. After 48 h from the start of the reaction, the PM concentration was 145 mM (bioconversion rate of 75%), while PN and PL concentrations were <1 mM. The production of PM from 400 mM PN was approximately 150 mM, which is almost the same as that from 200 mM PN. PM was efficiently produced by bioconversion of PN (Fig.6).

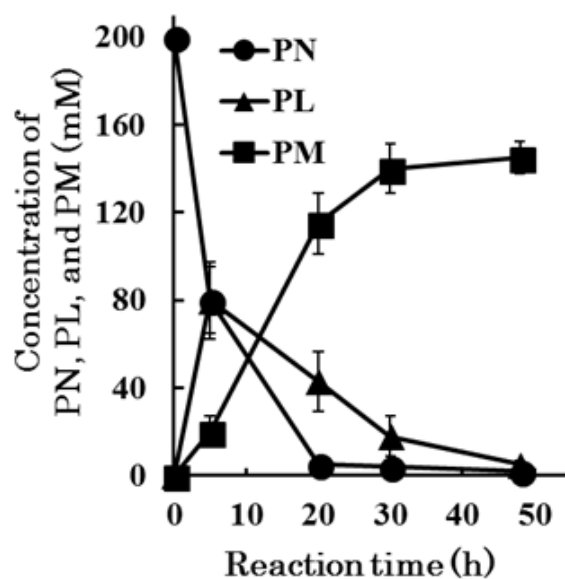


FIG. 6 Bioconversion of PN to PM through PL using the recombinant *R. erythropolis* JCM3191 strain harboring the pRET-PPPN1 plasmid. Vertical bars indicate SD from three independent experiments. Closed circle, closed triangle, and closed square indicates PN, PL, and PM concentrations, respectively.

Discussion

R. erythropolis strains have broad metabolic diversity and an array of unique enzymatic capabilities that are beneficial for several manufacturing industries (7, 8). Several scientists developed many genetic tools to analyze *Rhodococcus* (9) including gene disruption systems (10, 11, 12); however, little study has been done to actually screen *R. erythropolis* strains as a host cell. Screening *R. erythropolis* strains, I demonstrated that *R. erythropolis* JCM3191 was a good host for PL production (Fig. 3A), and that the activities of PL production were significantly different between *R. erythropolis* strains. In fact, the activity of recombinant *R. erythropolis* JCM3191 was 41 times higher than that of recombinant *R. erythropolis* JCM6827. Moreover, the activity of recombinant *R. erythropolis* JCM3191 was 918 times higher than that of recombinant *E.coli* BL21 (DE3). The PL production of recombinant *R. erythropolis* JCM3191 was almost the same as that without FAD. *R. erythropolis* JCM3191 may have sufficient amounts of FAD for PNO. Although these differences of activities may be attributed to the broad metabolic diversities of *R. erythropolis* strains, I was not able to obtain data on differences of intrinsic enzyme activities (e.g. catalase activity). Further, *R. erythropolis* may lack vitamin B₆ metabolic enzymes, such as PNO and PPAT, as all recombinant *R. erythropolis* strains harboring pRET11100 did not produce PL.

The characterization of purified PNO has been described by Yuan et al. (1), in which the optimal reaction pH and temperature of purified PNO were found to be between 8.0–8.5 and 40°C, respectively. However, little study has been done to examine the optimal reaction pH and temperature of the whole-cell reaction. I determined that the optimal reaction pH and temperature of the whole-cell reaction were 6.5 and 30.0–32.5°C respectively, which differ from those of purified PNO. These differences in optimal

reaction pH and temperature may be due to differences in membrane permeability of the substrate and enzyme stability. Further, the production of PL increased with increasing aeration requiring >1 vvm, suggesting bioconversion of PN to PL is an oxidation reaction needing active aeration.

Previously, I described the possibility that *R. erythropolis* has high intrinsic enzymatic activities (e.g., cofactor-regenerating enzymatic activity) that increased by the addition of glucose (3). For this reason, glucose was added in the bioconversion of PN to PL in the *Rhodococcus* expression system. The production of PL increased by the addition of glucose and the bioconversion rate was approximately 90% from 500 mM PN (approximately 10% PL). Although I have not yet collected sufficient data to explain this phenomenon, intrinsic enzymatic activities such as catalase activity in *R. erythropolis* may account for the production increase by glucose addition.

The expression level of *ppat* in recombinant *R. erythropolis* JCM3191 was almost the same as that in *E. coli* described by Yoshikane et al. (13). With the aim of PN bioconversion to PM through PL using *R. erythropolis* JCM3191 coexpressing *ppat* and *pno*, PM was produced from PL using this recombinant strain expressing *ppat* using the same conditions for PL production (1 vvm, pH 6.5, and 30°C). The bioconversion rate of PL to PM was approximately 80%.

Using recombinant *R. erythropolis* JCM3191 harboring pRET-PPP1, thereby possessing the bioconversion activity to produce PM from PN, the production of PM in this strain was 145 mM from 200 mM PN. PM production from 400 mM PN was comparable to that found from 200 mM PN, suggesting there is little substrate inhibition below 400 mM PN. After reaction completion, the total concentration of vitamin B₆ (PN, PL, and PM) from 200 mM PN was approximately 145 mM (PN, <1 mM; PL, <1 mM; PM, 145 mM). This observed decrease in the total amount may be due to PL forming a

Schiff base with primary amines such as proteins, L-glutamate, and PM (13, 14).

If PL does not accumulate during the bioconversion reaction of PN to PM through PL, there is a possibility that the amount of PM production will increase. Further study to investigate increasing PM production will be conducted by making *ppat* activity higher than *pno* activity so that PL is not accumulated during the reaction. Recently, I reported the weak constitutive promoters, *hsp* and *1200rep* (3), the compatible and stable plasmid pRET1202, and the high copy plasmid pRET1129 derived from pRET1102 (15). Furthermore, we previously reported many mutated PPATs with high activity toward L-glutamate (2). Thus, the coexpression vector pRET-PPPN1 expressing *ppat* and *pno* can be reconstructed using these promoters, plasmids, and mutated PPATs.

In conclusion, using a *Rhodococcus* expression system, approximately 145 mM PM was produced from 200 mM PN through PL demonstrating a bioconversion rate of 75%. Moreover, recombinant *R. erythropolis* overexpressing *pno* produced approximately 450 mM PL from 500 mM PN (approximately 10% PN). Based on these findings, pyridoxamine production by bioconversion using a *Rhodococcus* expression system may be of interest for future industrial applications.

REFERENCES

1. **Yuan, B., Yoshikane, Y., Yokochi, N., Ohnishi, K., and Yagi, T.:** The nitrogen-fixing symbiotic bacterium *Mesorhizobium loti* has and expresses the gene encoding pyridoxine 4-oxidase involved in the degradation of vitamin B₆, *FEMS Microbiol. Lett.*, **234**, 225–230 (2004).
2. **Yoshikane, Y., Tamura, A., Yokochi, N., Ellouze, K., Yamamura, E., Mizunaga, H., Fujimoto, N., Sakamoto, K., Sawa, Y., and Yagi, T.:** Engineering *Mesorhizobium loti* pyridoxamine–pyruvate aminotransferase for production of pyridoxamine with L-glutamate as an amino donor, *J. Mol. Cat. B-Enzym.*, **67**, 104–110 (2010).
3. **Yamamura, E.-T.:** Construction of *Rhodococcus* expression vectors and expression of the aminoalcohol dehydrogenase gene in *Rhodococcus erythropolis*, *Biosci. Biotechnol. Biochem.*, **82**, 1396–1403 (2018).
4. **Sambrook, J., Fritsch, E.F., and Maniatis, T.:** *Molecular cloning: a laboratory manual*, 2nd ed. Cold Spring Laboratory, Cold Spring Harbor, NY (1989).
5. **Laemmli, U.K.:** Cleavage of structural proteins during the assembly of the head of bacteriophage T4, *Nature*, **227**, 680–685 (1970).
6. **Kozono, I., Mihara, K., Minagawa, K., Hibi, M., and Ogawa, J.:** Engineering of the cytochrome P450 monooxygenase system for benzyl maltol hydroxylation, *Appl. Microbiol. Biotechnol.*, **101**, 6651–6658 (2017).
7. **Makino, Y., Dairi, T., and Itoh, N.:** Engineering the phenylacetaldehyde reductase mutant for improved substrate conversion in the presence of concentrated 2-propanol, *Appl. Microbiol. Biotechnol.*, **77**, 833–843 (2007).
8. **Nakashima, N. and Tamura, T.:** Isolation and characterization of a rolling-circle-

- type plasmid from *Rhodococcus erythropolis* and application of the plasmid to multiple-recombinant-protein expression, *Appl. Environ. Microbiol.*, **70**, 5557–5568 (2004).
9. **Finnerty, W.R.:** The biology and genetics of the genus *Rhodococcus*, *Annu. Rev. Microbiol.*, **46**, 193–218 (1992).
 10. **Urano, N., Kataoka, M., Ishige, T., Kita, S., Sakamoto, K., and Shimizu, S.:** Genetic analysis around aminoalcohol dehydrogenase gene of *Rhodococcus erythropolis* MAK154: a putative GntR transcription factor in transcriptional regulation, *Appl. Microbiol. Biotechnol.*, **89**, 739–746 (2011).
 11. **Kikukawa, H., Sakuradani, E., Nakatani, M., Ando, A., Okuda, T., Sakamoto, T., Ochiai, M., Shimizu, S., and Ogawa, J.:** Gene targeting in the oil-producing fungus *Mortierella alpina* 1S-4 and construction of a strain producing a valuable polyunsaturated fatty acid, *Curr. Genet.*, **61**, 579–589 (2015).
 12. **van der Geize, R., Hessels, G.I., van Gerwen, R., Vrijbloed, J.W., van der Meijden, P., and Dikhuizen, L.:** Targeted disruption of the *kstD* gene encoding a 3-ketosteroid Δ^1 -dehydrogenase isoenzyme of *Rhodococcus erythropolis* strain SQ1, *Appl. Environ. Microbiol.*, **66**, 2029–2036 (2000).
 13. **Yoshikane, Y., Yokochi, N., Ohnishi, K., Hayashi, H., and Yagi, T.:** Molecular cloning, expression and characterization of pyridoxamine–pyruvate aminotransferase, *Biochem. J.*, **396**, 499–507 (2006).
 14. **Balyakina, M.V., Yakovleva, N.L., and Gunar, V.I.:** Synthesis of pyridoxamine and its 5'-phosphate ester, *Pharm. Chem. J.*, **14**, 407–409 (1980).
 15. **Yamamura, E.-T.:** Isolation of two plasmids, pRET1100 and pRET1200, from *Rhodococcus erythropolis* IAM1400 and construction of a *Rhodococcus–E. coli* shuttle vector, *J. Biosci. Bioeng.*, **125**, 625–631 (2018).

SUMMARY

Pyridoxamine, which is a form of vitamin B₆, is a promising candidate for a prophylactic and/or remedy for diabetic complications. Pyridoxamine is chemically synthesized by an oxidative method in manufacturing. However, pyridoxamine production by bioconversion, which is generally preferable for environmental and energetic aspects, has been little investigated. Therefore, I aimed to produce pyridoxamine from pyridoxine, which is a readily and economically available starting material, by bioconversion using a *Rhodococcus* expression system. I found in the bioconversion of pyridoxine to pyridoxal, approximately 450 mM pyridoxal was produced from 500 mM pyridoxine using recombinant *Rhodococcus erythropolis* expressing the pyridoxine 4-oxidase gene derived from *Mesorhizobium loti*. Next, in the bioconversion of pyridoxal to pyridoxamine using recombinant *R. erythropolis* expressing the pyridoxamine-pyruvate aminotransferase gene derived from *M. loti*, the bioconversion rate was approximately 80% under the same conditions as pyridoxal production. Finally, in the bioconversion of pyridoxine to pyridoxamine through pyridoxal using recombinant *R. erythropolis* coexpressing the genes for pyridoxine 4-oxidase and pyridoxamine-pyruvate aminotransferase, the bioconversion rate was approximately 75%. Based on these findings, pyridoxamine production by bioconversion using a *Rhodococcus* expression system may be of interest for future industrial applications.

SECTION 2

A novel method of producing the pharmaceutical intermediate

(R)-2-chloromandelic acid by bioconversion

Many esterases are valuable to manufacturing industries, and they are effective for use in bioconversion. Therefore, in this study, with the aim of producing (R)-2-chloromandelic acid (R-CM), I sought to identify an esterase that hydrolyzes racemic 2-chloromandelic acid methyl ester (CMM), which is a readily and economically available starting material, to R-CM, and purified a novel esterase EstE from *Exophiala dermatitidis* NBRC6857 (former name: *Exophiala jeanselmei* until August 2009). In addition, I described a novel method of producing R-CM from CMM by a bioconversion using recombinant cells harboring the esterase EstE.

Materials and methods

Strains and plasmids *Exophiala dermatitidis* NBRC6857 (former name: *E. jeanselmei* until August 2009) was obtained from the National Institute of Technology and Evaluation (Tokyo, Japan). *E. dermatitidis* NBRC6857 was cultured in GPY broth (1% glucose, 0.5% Bacto peptone, and 0.3% Bacto yeast extract). *Rhodococcus erythropolis* JCM3191 was obtained from the Japan Collection of Microorganisms (Ibaraki, Japan). *Escherichia coli* JM109 was obtained from Toyobo Co., Ltd. (Osaka, Japan). These strains were cultured in Luria-Bertani broth (1% Bacto tryptone, 0.5% Bacto yeast extract, and 1% NaCl) in the presence or absence of the appropriate antibiotics. Kanamycin (100 µg/mL) and ampicillin (100 µg/mL) were used

to select transformants in the culture media. The *E. coli* expression vector pQE-70 was obtained from Qiagen (Hilden, Germany). The *Rhodococcus* expression vector pRET11100 was constructed as previously described (1,2).

Enzymes and chemicals All restriction enzymes and DNA modification enzymes were purchased from Toyobo Co., Ltd. (Osaka, Japan) and New England Biolabs, Inc. (Ipswich, MA, USA). All chemicals were purchased from Sigma-Aldrich (St. Louis, MO, USA) and FUJIFILM Wako Pure Chemical Corp. (Osaka, Japan). The synthetic oligonucleotides used in this study were purchased from Hokkaido System Science Co., Ltd. (Hokkaido, Japan).

Standard genetic manipulations and sequence analysis Cloning was performed by standard genetic manipulation techniques (3). Actinomycete strains were transformed using the method described by Yamamura (2). *E. coli* transformation was performed using the *E. coli* Transformation Buffer Set (Zymo Research Corp., Irvine, CA, USA). Genomic DNA was isolated using a Genomic DNA Buffer set and Genomic-tip 500/G (Qiagen, Hilden, Germany). RNA was isolated using an RNeasy Mini Kit (Qiagen, Hilden, Germany). cDNA was prepared with ReverTra -Plus- (Toyobo Co., Ltd.). PCR fragments were prepared with KOD -plus- (Toyobo Co., Ltd.). DNA sequences of the plasmid inserts were determined by the primer walking method described by Yamamura (2). Sequence assembly and analysis were performed using GENETYX Ver.12 (GENETYX Corp., Tokyo, Japan) and DNASIS Pro Ver.2.0 (Hitachi Software Corp., Tokyo, Japan).

Screening of a bacterial library for CMM-asymmetric hydrolyzing activity

The microorganisms were inoculated into 5 mL of GPY broth and incubated at 25°C with shaking for 3–6 days. The cells were harvested and suspended in 1 mL of 50 mM MES (2-morpholinoethanesulfonic acid) buffer (pH 6.5) containing 1% CMM, then

incubated at 30°C with shaking for 20 h. The reactions were stopped by the addition of perchloric acid to acidify. Cell suspensions were centrifuged at $12,000 \times g$ for 5 min at 4°C, and the resulting supernatants were analyzed by high-performance liquid chromatography (HPLC) as described below.

Analysis of CMM, R-CM, and (S)-2-chloromandelic acid by HPLC

The hydrolysis rate of CMM and optical purity of the product were determined by HPLC on a MCI GEL packed column CRS10W (ϕ 4.6 \times 50 mm; Mitsubishi Chemical Corp., Tokyo, Japan). The mobile phase was 0.2 mM copper (II) sulfate solution/acetonitrile (85/15, v/v), the flow rate was 2.0 mL/min, column temperature was 25°C, and the detection wavelength was at 254 nm. Calibration curves were prepared using CMM, R-CM, and (S)-2-chloromandelic acid.

Purification of an esterase EstE

E. dermatitidis NBRC6857 cells

were propagated in GPY broth as described by Kozono et al. (4). *E. dermatitidis* NBRC6857 cells were inoculated into 100 mL of GPY broth and were incubated at 30°C with shaking for 4 days. Seed medium (100 mL) was transferred into 3 L of GPY broth in a 5-L jar fermenter (LS-5, Sakura Seiki Co., Ltd., Tokyo, Japan) and incubated at 30°C with 400-rpm agitation and 1-vvm aeration for 2 days. Twelve liters of the culture broth of *E. dermatitidis* NBRC6857 was harvested and suspended in 50 mM MES buffer (pH 6.5). 30 wt% cell suspension was disrupted by ultrasonication for 3 h with an ultrasonic homogenizer US-300 (Nihonseiki Kaisha Ltd., Tokyo, Japan). The disrupted cell suspension was centrifuged at $14,000 \times g$ for 20 min and the resulting supernatant was used as the crude extracts. Solid ammonium sulfate (24.3 g) was added to 100 mL of crude extracts containing 0.1% polyethylene glycol mono-4-octylphenyl ether ($n =$ approximately 10, Triton X-100) and cOmplete (protease inhibitor, F. Hoffmann-La Roche, Ltd.). After stirring at 4°C for 1 h, the crude extracts were centrifuged at $14,000$

× g for 30 min and the resulting supernatant was combined with 13.2 g of solid ammonium sulfate. After stirring at 4°C for 1 h, the precipitate with 60% saturation of solid ammonium sulfate was collected by centrifugation and was dissolved in 18 mL of 50 mM MES-OS buffer (MES buffer (pH 6.5) containing 0.1% Triton X-100 and cOmplete). The enzyme solution was dialyzed against 2 L of 50 mM MES-OS buffer and was applied to 40 mL of DEAE Sepharose Fast Flow (GE Healthcare UK Ltd., Buckinghamshire, England) equilibrated with 25 mM MES-OS buffer. The enzyme was eluted with a linear gradient of 0–0.2 M NaCl in 25 mM MES-OS buffer. The active fractions containing the enzyme were collected and combined with an equal volume of 25 mM MES-OS buffer containing 2 M NaCl. The enzyme solution containing approximately 1 M NaCl was applied to 30 mL of Phenyl Sepharose 6 Fast Flow (GE Healthcare UK Ltd., Buckinghamshire, England) equilibrated with 25 mM MES-OS buffer containing 1 M NaCl. The enzyme was eluted with a linear gradient of 0.1–0 M NaCl in 25 mM MES-OS buffer. The active fractions containing the enzyme were collected, concentrated by ultrafiltration using Vivaspin 6 (MWCO 10000, Sartorius, Gottingen, Germany), and were dialyzed against 2 L of 20 mM acetate buffer (pH 5.0). The concentrated sample was applied to SOURCE 15S 4.6/100 PE (GE Healthcare UK Ltd., Buckinghamshire, England) equilibrated with 20 mM acetate buffer (pH 5.0) and was eluted with 5 mL of 20 mM acetate buffer (pH 5.0). After being concentrated by ultrafiltration using Vivaspin 6 (MWCO 10000), the sample was applied to HiLoad 16/60 Superdex 200 Prep Grade (GE Healthcare UK Ltd., Buckinghamshire, England) equilibrated with 20 mM phosphate buffer (pH 7.0) and was eluted with 20 mM phosphate buffer (pH 7.0). When measuring molecular mass by gel filtration, 20 mM phosphate buffer (pH 7.0) containing 0.85% NaCl was used instead of 20 mM phosphate buffer (pH 7.0). Protein purity was analyzed on SDS-PAGE (10% gel) by the method described by Laemmli (5) and was

visualized by staining with Coomassie Brilliant Blue R-250. The SDS-PAGE Molecular Weight Standards (Broad Range) purchased from Bio-Rad Laboratories, Inc. (Hercules, CA, USA) was used as a size marker.

Enzyme and protein assays The reaction mixture consisting of 0.05% substrates (standard substrate was CMM), 100 mM buffer (standard buffer was phosphate buffer (pH 7.0)), and enzyme was incubated at 10–50°C (standard reaction condition was 30°C) for 30 min. The reactions were stopped by addition of perchloric acid to acidify and were centrifuged at $12,000 \times g$ for 5 min at 4°C. The resulting supernatants were analyzed by high-performance liquid chromatography (HPLC) as described above. Proteins were measured using a Bio-Rad Protein Assay (Bio-Rad Laboratories, Inc., Hercules, CA, USA) with bovine serum albumin as a standard.

Synthesis of substrates for investigating substrate specificity Racemic 3-chloromandelic acid methyl ester, racemic 4-chloromandelic acid methyl ester, racemic 4-methoxymandelic acid methyl ester, racemic atrolactic acid methyl ester, and racemic phenyllactic acid methyl ester were synthesized by esterification with methanol from racemic 3-chloromandelic acid, racemic 4-chloromandelic acid, racemic 4-methoxymandelic acid, racemic atrolactic acid, and racemic phenyllactic acid, respectively. Racemic 2-chloromandelic acid ethyl ester was synthesized by esterification with ethanol from racemic 2-chloromandelic acid. Racemic 2-chloromandelic acid isopropyl ester was synthesized by esterification with isopropanol from racemic 2-chloromandelic acid. Racemic 2-chloromandelic acid benzyl ester was synthesized by esterification with benzyl alcohol from racemic 2-chloromandelic acid.

Amino acid sequencing The purified enzyme that was eluted from the gel filtration was digested with Lysyl Endopeptidase (FUJIFILM Wako Pure Chemical Corp., Osaka, Japan) at 37°C for 6 h. The digested enzyme was applied to a Sephasil

Peptide C18 5 µm ST 4.6/100 column (GE Healthcare UK Ltd., Buckinghamshire, England) equilibrated with 0.1% trifluoroacetic acid and was eluted with a linear gradient of 0–80% acetonitrile in 0.1% trifluoroacetic acid. The amino acid sequence of the internal peptide (the digested enzyme) that was eluted from the column was determined by automated Edman degradation with a PPSQ-21A Protein Sequencer (Shimadzu Corp., Kyoto, Japan).

Sequence determination and analysis of the *estE* gene

The

oligonucleotide primer pools were designed based on the amino acid sequences of the internal peptides (6). The degenerate primers were 5'-AC(G/A/T/C)GT(G/A/T/C)GT(G/A/T/C)GA(T/C)AT(A/T/C)TGGGG(G/A/T/C)GG(G/A/T/C)TGGGC(G/A/T/C)GA(T/C)GA(G/A)GA(G/A)CA(T/C)AC(G/A/T/C)CA(G/A)CC(G/A/T/C)TGGAC-3' (sense strand) and 5'-GTCCA(G/A/T/C)GG(T/C)TG(G/A/T/C)GT(G/A)TG(T/C)TC(T/C)TC(G/A)TC(G/A/T/C)GCCCA(G/A/T/C)CC(G/A/T/C)CCCCA(G/A/T)AT(G/A)TC(G/A/T/C)AC(G/A/T/C)AC(G/A/T/C)GT-3' (antisense strand). The *estE* gene was obtained using the degenerate primers and the TaKaRa LA PCR *in vitro* Cloning Kit (Takara Bio Inc., Shiga, Japan). DNA sequences of the *estE* gene were determined by the primer walking method with an ABI PRISM 310NT DNA Genetic Analyzer (Applied Biosystems, Carlsbad, CA, USA). Sequence assembly and analysis were performed with Genetyx Ver.12 (Genetyx Corp., Tokyo, Japan) and DNASIS Pro Ver. 2.9 (Hitachi Software Corp., Tokyo, Japan).

Construction of *estE* expression vectors

The *estE* gene was

amplified with the following primers: CMMF1Sp: 5'-ATCATCAGCATGCCAGCCGAAGTCCAAGGACACACCGAAG-3' (*Sph* I site is underlined) and CMMR1170Bgl(st): 5'-CGTCCAAGATCTCCTTCACTGTCCTTTCAGTATCCTTC-3' (*Bgl* II site is underlined), from the genomic DNA of *E. dermatitidis* NBRC6857 using a

Mastercycler gradient thermal cycler (Eppendorf, Hamburg, Germany). The PCR fragment containing *estE* was digested with *Sph* I and *Bgl* II and then ligated into the *Sph* I and *Bgl* II sites of pQE-70 to prepare the plasmid pECM-G65, which is the *estE* expression vector for *E. coli*. To express the *estE* gene in *R. erythropolis*, the plasmid pRET11100 was used because it has a strong constitutive promoter and broad actinomycetes host range (2). The *estE* gene was amplified with the primers: CMMF1Pt(1138): 5'-ACTCCCTGCAGCTCAGGATCATTATCGATCATCATCATGG CAGC-3' (*Pst* I site is underlined) and CMMR1170Kp(st): 5'-TTTCACGGGTACCGT CTCCTTCACTGTCCTTTCAGTATCCTTC-3' (*Kpn* I site is underlined), from the genomic DNA of *E. dermatitidis* NBRC6857 using a Mastercycler gradient thermal cycler. The PCR fragment containing *estE* was digested with *Pst* I and *Kpn* I and then ligated into the *Pst* I and *Kpn* I sites of pRET11100 to prepare the plasmid pRET-CMM3.

Activity measurements of recombinant cells

Recombinant *E.*

coli JM109 cells harboring the plasmid pECM-G65 were inoculated into 5 mL of Luria-Bertani broth with ampicillin (100 µg/ml) and isopropyl-β-D-thiogalactopyranoside (1 mM) and was incubated at 37°C with shaking for 16 h, while recombinant *R. erythropolis* JCM3191 harboring the plasmid pRET-CMM3 was inoculated into 5 mL of Luria-Bertani broth with kanamycin and was incubated at 25°C with shaking for 7 days. The reaction mixture consisting of 1% CMM, 100 mM phosphate buffer (pH 7.0), and a portion of the cultured cells was incubated at 30°C with shaking for 30 min. The reaction was stopped by adding perchloric acid to acidify. The production of *R*-CM was analyzed as described above.

Producing *R*-CM by bioconversion

Recombinant *E. coli* JM109 cells

harboring the plasmid pECM-G65 were inoculated into 5 mL of Luria-Bertani broth with ampicillin (100 µg/mL) and isopropyl-β-D-thiogalactopyranoside (1 mM) and was

incubated at 37°C with shaking for 16 h. The cultured cells were harvested and suspended in 100 mL of 0.85% saline solution containing 10 g CMM. The reaction mixture containing approximately 4.5 mg-dry-cell of Recombinant *E. coli* JM109 was stirred and incubated at 30°C for 24 h. The pH of the reaction mixture was maintained at 7.0 with 14% NaOH. Production of *R*-CM was analyzed as described above.

Nucleotide sequence accession number The sequence of the *estE* gene has been submitted to the DDBJ/EMBL/GenBank databases under accession number LC387563. The nucleotide sequences reported in this paper appear in the DDBJ/GenBank/EMBL nucleotide sequence databases under accession number LC331663 (pRET1100).

Results

Screening for CMM-asymmetric hydrolyzing microorganisms To screen for CMM-asymmetric hydrolyzing microorganisms, a total of 910 strains from our bacterial library were used, consisting of 262 strains of yeasts, 132 strains of actinomycetes, 212 strains of fungi, and 304 strains of bacteria. Among the microbial strains, 21 strains exhibited CMM-hydrolyzing activity, while 5 strains exhibited an optical purity of 90% *ee* or more of the (*R*)-enantiomer (Table 1). *E. dermatitidis* NBRC6857 had the highest stereoselectivity. The enantiopurity of the product was 99.9% enantiomeric excess (*ee*) of the (*R*)-enantiomer. For this reason, *E. dermatitidis* NBRC6857 was used for further study.

TABLE 1. Strains exhibited an optical purity of 90% *ee* or more of the (*R*)-enantiomer

Strain	Optical purity (<i>R</i>) (% <i>ee</i>)
<i>Exophiala dermatitidis</i> NBRC6857	99.9
<i>Cylindrocarpon</i> sp. NBRC31855	96.7
<i>Mycobacterium smegmatis</i> NBRC3154	95.6
<i>Mycobacterium phlei</i> NBRC3158	95.2
<i>Leifsonia aquatica</i> NBRC15710	90.4

Identification of a CMM-asymmetric hydrolyzing enzyme from *E.*

***dermatitidis* NBRC6857**

To identify the enzyme that hydrolyzes CMM to *R*-CM asymmetrically, the crude extracts of *E. dermatitidis* NBRC6857 were subjected to five purification steps (Table 2). In Superdex steps, which was the final purification step, the specific activity and the purification fold were 795.8 mU/mg and 79.7, respectively, in reaction mixtures without Triton X-100, which is a surfactant. Here, 0.1% Triton X-100 was added to a reaction mixture, since from the ammonium sulfate precipitation step to Phenyl Sepharose step, each buffer contained 0.1% Triton X-100. The specific activity measured by adding Triton X-100 was almost the same as that measured without adding it (776.8 mU/mg). The purified EstE hydrolyzed CMM to *R*-CM at optical purity of 99.9% *ee* of the (*R*)-enantiomer.

The purified enzyme, called EstE, showed the single protein band with a molecular weight of 42 kDa (Fig. 1). The molecular weight of the native enzyme was 41 kDa as determined by gel filtration, suggesting that EstE is a monomeric protein.

TABLE 2. Purification of EstE from *Exophiala dermatitidis* NBRC6857

Purification step	Total activity (mU)	Total protein (mg)	Specific activity (mU/mg)	Yield (%)	Purification fold
Crude extract	3340	334	10.0	100	1.00
Ammonium sulfate precipitation 40-60%	2430	45.1	53.9	72.9	5.40
DEAE Sepharose Fast Flow	2420	5.3	453	72.4	45.4
Phenyl Sepharose 6 Fast Flow	1930	2.9	669	58.0	67.0
SOURCE 15S PE 4.6/100	695	0.9	781	20.8	78.3
HiLoad 16/60 Superdex 200 prep grade	279	0.4	796	8.3	79.7

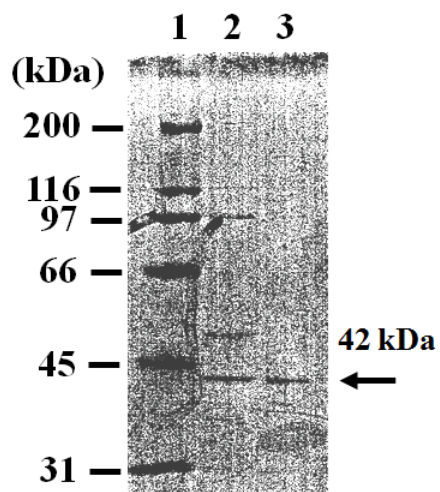


FIG. 1. SDS-PAGE of EstE from *Exophiala dermatitidis* NBRC6857.

Lane 1, size marker; lane 2, the active fraction of SOURCE 15S PE; lane 3, the active fractions of HiLoad 16/60 Superdex.

optimal reaction conditions of EstE were investigated to produce *R*-CM efficiently. The effect of pH on the activity of EstE was examined from pH 3.0 to 11.0, the optimal pH was found to be 7.0 (Fig. 2A). The effect of reaction temperature was also examined, and maximum activity was observed at 40°C (Fig. 2B). However, the optimal reaction temperature was 30°C or lower, as EstE was more stable at 30°C (relative activity was 100%) than at 40°C (relative activity was 98%, Fig. 2C).

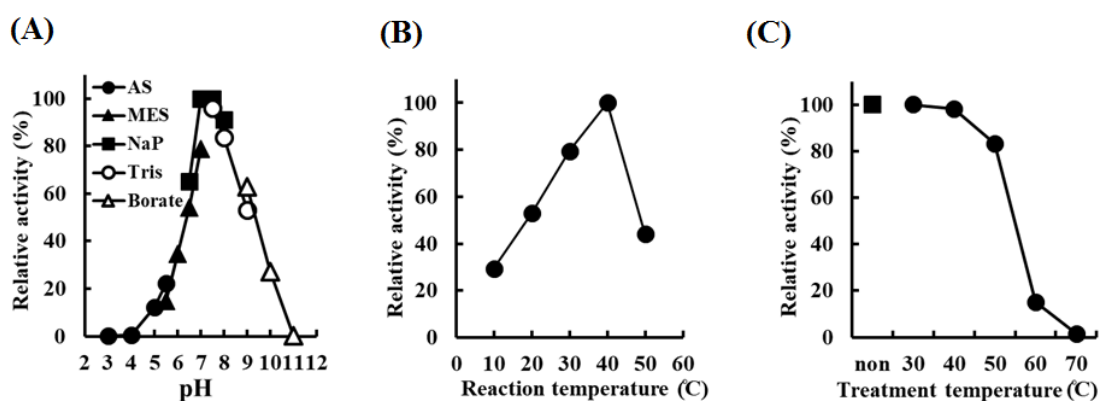


FIG. 2. Determining optimal pH and temperature for EstE activity.

(A) Effect of pH on EstE activity. Activity was assayed under standard reaction conditions, except for the buffer. Closed circle, closed triangle, closed square, open circle, and open triangle indicate acetic acid-sodium acetate buffer (AS), MES buffer (MES), sodium phosphate buffer (NaP), Tris buffer (Tris), and borate buffer (Borate), respectively. (B) Effect of temperature on EstE activity. Activity was assayed under standard reaction conditions, except for temperature. (C) Effect of temperature on stability. Activity was assayed under standard reaction conditions. EstE was incubated for 30 min at 30–70°C before adding the reaction mixture. Closed square indicates no temperature treatment. Closed circle indicates temperature treatment from 30 to 70°C.

Substrate specificity of hydrolysis by EstE

Fig. 3 shows the substrate specificity of EstE. In the general formula (I) in Fig. 3, the values of specific activity were in the order of 2-chloromandelic acid ethyl ester > 2-chloromandelic acid isopropyl ester > 2-chloromandelic acid benzyl ester > CMM. Optical purity was over 90% for all substrates. In the general formula (II) in Fig. 3, the values of specific activity were in the order of 4-methoxymandelic acid methyl ester > 4-chloromandelic acid methyl ester > CMM > 3-chloromandelic acid methyl ester > mandelic acid methyl ester > phenyllactic acid methyl ester. CMM exhibited the highest optical purity. As the specific activity differs from CMM, optical purity tended to decrease. In the general formula (III) in Fig. 3, the values of specific activity were in the order of atrolactic acid methyl ester > mandelic acid methyl ester. When atrolactic acid methyl ester was used as a substrate, the optical purity was 96.7% *ee*.

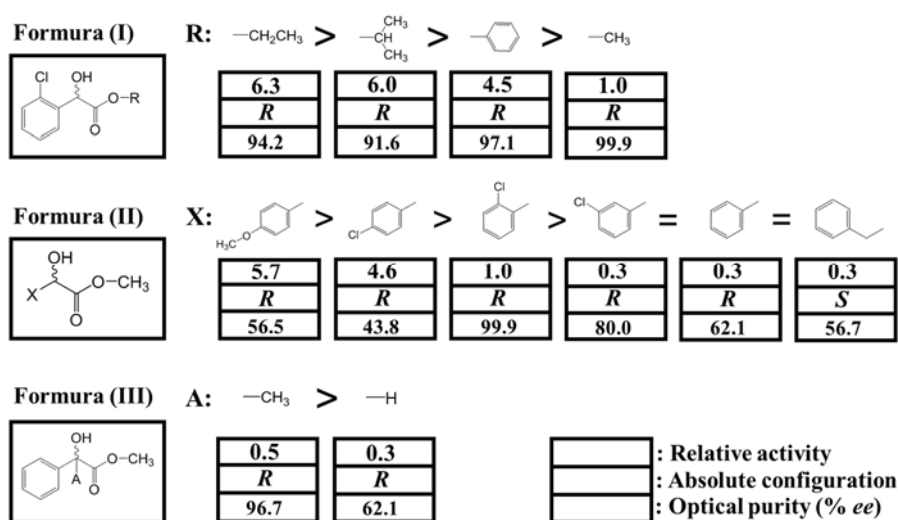


Fig. 3. Substrate specificity of hydrolysis of EstE.

The top, middle, and bottom of the box indicate relative activity, absolute configuration, and optical purity, respectively. The inequality sign indicates the relationship between magnitudes of the relative activities. An equal sign indicates that the relative activities were equal. Specific activity is defined as the hydrolysis rate of CMM as 1.0.

Amino acid and nucleotide sequences of EstE

Purified EstE was

digested with Lysyl Endopeptidase. Two internal peptides were obtained. The amino acid sequence of one of the internal peptides was determined by automated Edman degradation (TVVDIWGGWADEEHTQPWTR). Using the oligonucleotide primer pools designed based on the amino acid sequence of the internal peptides, the nucleotide sequence of *estE* that encodes EstE was determined. Here, the *estE* gene was not amplified by PCR with the oligonucleotide primer pools designed based on the amino acid sequence of another internal peptide. The *estE* gene comprised 1176 bp and encoded a protein of 392 amino acid residues (accession number LC387563). The amino acid sequence of EstE had the Lysyl endopeptidase cleavage site (Lys-X) and the sequence of the internal peptide. The predicted molecular weight was 42 kDa, which is in good agreement with the results of SDS-PAGE in Fig. 1. As *E. dermatitidis* NBRC6857 is a fungus, the nucleotide sequence of the cDNA of *estE* was analyzed simultaneously. The nucleotide sequence of cDNA of *estE* is in agreement with that of genomic DNA of *estE*. These results suggest that *estE* has no intron. Using the TBLASTN 2.2.26 program (protein–translated nucleotide Basic Local Alignment Search Tool, <https://www.ddbj.nig.ac.jp/index-e.html>) (7), the EstE protein is homologous to the esterase derived from Actinomycetes (Table 3).

TABLE 2. Features and similarities between EstE and known proteins

GenBank Accession No.	Product	Organism	E-value	Similarity	Ref.
KF601763	Fenoxaprop-ethyl hydrolase	<i>Rhodococcus</i> sp. JPL-2	1e-148	73%	(8)
JF970231	Fenoxaprop-ethyl hydrolase	<i>Rhodococcus</i> sp. T1(2011)	1e-146	73%	(9)
CP015163	Serine hydrolase	<i>Amocolatopsis albispora</i> strain WP1	1e-137	72%	
AY052630	Lactone hydrolase	<i>Rhodococcus ruber</i> SC1	1e-136	71%	(10)
ALU68731	β -Lactamase	<i>Rhodococcus erythropolis</i> R138	1e-132	73%	(11)
AGT95066	β -Lactamase	<i>Rhodococcus erythropolis</i> CCM2595	1e-132	73%	(12)

Expression of *estE* in *R. erythropolis* cells and *E. coli* cells

For

overexpression of the *estE* gene in *R. erythropolis*, which is a type of Actinomycetes, *estE* was inserted downstream of the *TRR* promoter of the *Rhodococcus* expression vector pRET11100 (pRET-CMM3). The plasmid pRET-CMM3 was transformed into *R. erythropolis* JCM3191. The activity per culture broth of recombinant *R. erythropolis* JCM3191 harboring pRET-CMM3 was 4 U/mL of culture broth (U = $\mu\text{mol}/\text{min}$), which was 105 times higher than that of *E. dermatitidis* NBRC6857 (0.038 U/mL-culture broth). Next, to overexpress the *estE* gene in *E. coli*, *estE* was inserted downstream of the *T5* promoter of pQE-70 (pECM-G65). The plasmid pECM-G65 was transformed into *E. coli* JM109. The activity per culture broth of recombinant *E. coli* JM109 harboring pECM-G65 was 21 U/mL-culture broth (U = $\mu\text{mol}/\text{min}$), which was 553 times higher than that of *E. dermatitidis* NBRC6857. EstE was overexpressed in *E. coli* JM109 and was detected in a soluble form on SDS-PAGE, with a molecular weight of 42 kDa, which is in agreement with the predicted molecular weight (Fig. 4).

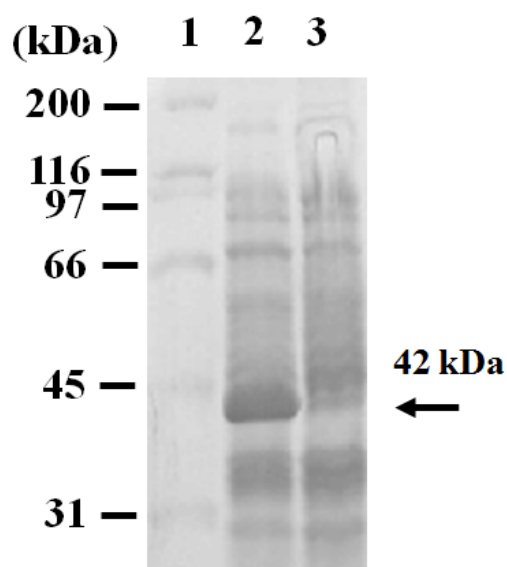


FIG. 4. SDS-PAGE of crude extracts from *Escherichia coli* JM109 harboring a EstE expression plasmids.

Lane 1, size marker; lane 2, the crude extract from *E. coli* JM109 harboring pECM-G65; lane 3, the crude extract from *E. coli* JM109 harboring pQE-70.

Bioconversion of CMM to R-CM

The activity per culture broth of recombinant *E. coli* JM109 was higher than those of recombinant *R. erythropolis* JCM3191 and *E. dermatitidis* NBRC6857. The bioconversion ability of CMM to R-CM was examined using recombinant *E. coli* JM109 harboring the plasmid pECM-G65 (Fig. 5). A solution of 10% CMM containing equal amounts of (*R*)-2-chloromandelic acid methyl ester and (*S*)-2-chloromandelic acid methyl ester was converted to approximately 5% R-CM (conversion rate 49%) in 24 h. At the end of the reaction, (*R*)-2-chloromandelic acid methyl ester was not detected in the reaction mixture, and the product of optical purity of 2-chloromandelic acid was 97% *ee*. R-CM was efficiently produced by bioconversion of CMM using recombinant *E. coli* JM109 cells overexpressing *estE* derived from *E. dermatitidis* NBRC6857.

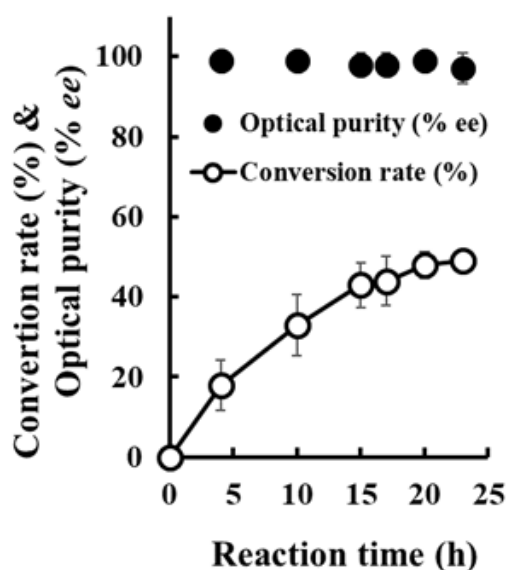


Fig. 5. Bioconversion of CMM to R-CM using recombinant *Escherichia coli* JM109 harboring the pECM-G65 plasmid. Vertical bars indicate SD from three independent experiments. Open circle and closed circle indicate conversion rate and optical purity, respectively.

Discussion

α -Hydroxycarboxylic acids and derivatives thereof are useful intermediates for manufacturing various kinds of medicines or agricultural chemicals (13–15). Especially, since various biologically active compounds can be produced using optically active α -hydroxycarboxylic acids and derivatives thereof with an asymmetric center at the α -position, various methods for efficiently producing optically active α -hydroxycarboxylic acids and derivatives thereof with high optical purity have been developed. *R*-CM is one such intermediate for industrial synthesis of clopidogrel. Upon screening for CMM-asymmetric hydrolyzing microorganisms, I found that *E. dermatitidis* NBRC6857 had the highest stereoselectivity (97.1% *ee* of (*R*)-enantiomer).

EstE was purified from the crude extracts of *E. dermatitidis* NBRC6857 by five purification steps. From the ammonium sulfate precipitation step to Phenyl Sepharose step, each buffer contained 0.1% Triton X-100, which is a surfactant, as EstE was stabilized by the addition of Triton X-100 in purification steps. In SOURCE 15S and Superdex steps, each buffer lacked Triton X-100, as EstE was not separated from other proteins by the addition of Triton X-100. In the final purification step, the specific activity and the purification fold were not increased sufficiently, as the buffer contained no Triton X-100. Due to the interaction between the resin and EstE without Triton X-100, the specific activity may not be increased sufficiently. The activity of EstE was not decreased without Triton X-100 in the reaction, suggesting that Triton X-100 is not necessary for the enzyme assay described in this paper.

Many bioconversion reactions occur at ambient temperature, neutral pH, and ambient pressure (4,16–18), which are good for environmental conservation. I investigated whether EstE is suitable for bioconversion. The effects of temperature and

pH on the activity of EstE were examined, and the optimal temperature and pH of CMM-asymmetric hydrolyzing reaction were 30°C and 7.0, respectively, which are ambient temperature and neutral pH. These results suggested that EstE is suitable for bioconversion.

EstE showed high optical purity to the substrate in general formula (I) in Fig. 3, as optical purity was over 90% in all substrates. In the general formula (II) in Fig. 3, since the specific activity differs from CMM, optical purity tended to decrease. These results suggested that the substrate in general formula (I) is suitable for EstE. By analyzing the crystal structure of EstE and these substrates, interesting findings may be obtained.

To isolate the *estE* gene, the amino acid sequence of the internal peptides of EstE were determined. Here, I was not able to determine the amino acid sequence of the N-terminus of EstE by Edman degradation. The N-terminus of purified EstE from *E. dermatitidis* NBRC6857 may be blocked with an N-formyl group, N-pyroglutamyl group, or N-acetyl group. Based on the obtained amino acid sequence of the internal peptides, the *estE* gene was isolated. Upon analyzing the nucleotide sequences of *estE*, EstE may be closer to prokaryotic enzymes, as *estE* has no intron and EstE is homologous to the esterase derived from Actinomycetes (Table 3).

The *estE* gene was overexpressed in *E. coli* JM109. The activity per culture broth of the recombinant *E. coli* JM109 was 5.25 times higher than that of recombinant *R. erythropolis* JCM3191. I cannot yet fully explain this phenomenon, but it may be due to membrane permeability of CMM or the expression level of *estE*.

Methods of producing *R*-CM have been reported by some researchers and a patent has been applied for (13,19,20). The method I described in this paper is a novel method of producing *R*-CM from CMM by a bioconversion using EstE that hydrolyzes CMM asymmetrically. *R*-CM was produced at conversion rate of 49% and at optical

purity of 97% *ee* from 10% CMM in 24 h with 0.45 mg-dry-cell/L recombinant *E. coli* JM109 cells. Since (*S*)-2-chloromandelic acid methyl ester is racemized in the presence of sodium methoxide easily, unreacted (*S*)-2-chloromandelic acid methyl ester is able to be reused for a bioconversion, and the method in this paper is efficient. Based on these findings, *R*-CM production by bioconversion of CMM may be of interest for future industrial applications.

REFERENCES

1. **Yamamura, E.-T.:** Isolation of two plasmids, pRET1100 and pRET1200, from *Rhodococcus erythropolis* IAM1400 and construction of a *Rhodococcus*–*E. coli* shuttle vector, *J. Biosci. Bioeng.* **125**, 625–631 (2018).
2. **Yamamura, E.-T.:** Construction of *Rhodococcus* expression vectors and expression of the aminoalcohol dehydrogenase gene in *Rhodococcus erythropolis*, *Biosci. Biotechnol. Biochem.*, **82**, 1396–1403 (2018).
3. **Sambrook, J., Fritsch, E.F., and Maniatis, T.:** *Molecular cloning: a laboratory manual*, 2nd ed. Cold Spring Laboratory, Cold Spring Harbor, NY (1989).
4. **Kozono, I., Mihara, K., Minagawa, K., Hibi, M., and Ogawa, J.:** Engineering of the cytochrome P450 monooxygenase system for benzyl maltol hydroxylation, *Appl. Microbiol. Biotechnol.*, **101**, 6651–6658 (2017).
5. **Laemmli, U.K.:** Cleavage of structural proteins during the assembly of the head of bacteriophage T4, *Nature*, **227**, 680–685 (1970).
6. **Kataoka, M., Nakamura, Y., Urano, N., Ishige T, Shi, G., Kita, S., Sakamoto, K., and Shimizu, S.:** A novel NADP⁺-dependent L-1-amino-2-propanol dehydrogenase from *Rhodococcus erythropolis* MAK154: a promising enzyme for the production of double chiral aminoalcohols, *Lett. Appl. Microbiol.*, **43**, 430–435 (2006).
7. **Altschul, S.F., Madden, T.L., Schäffer, A.A., Zhang, J., Zhang, Z., Miller, W., and Lipman, D.J.:** Gapped BLAST and PSI-BLAST: a new generation of protein database search programs, *Nucleic Acids Res.*, **25**, 3389–3402 (1997).
8. **Hongming, L., Xu, L., Zhaojian, G., Fan, Y., Dingbin, C., Jianchun, Z., Jianhong, X., Shunpeng, L., and Qing, H.:** Isolation of an aryloxyphenoxy propanoate (AOPP) herbicide-degrading strain *Rhodococcus ruber* JPL-2 and the cloning of a

- novel carboxylesterase gene (*feh*), *Braz. J. Microbiol.*, **46**, 425–432 (2015).
9. **Hou, Y., Tao, J., Shen, W., Liu, J., Li, J., Li, Y., Cao, H., and Cui, Z.:** Isolation of the fenoxaprop-ethyl (FE)-degrading bacterium *Rhodococcus* sp. T1, and cloning of FE hydrolase gene *feh*, *FEMS Microbiol. Lett.*, **323**, 196–203 (2011).
 10. **Kostichka, K., Thomas, S.M., Gibson, K.J., Nagarajan, V., and Cheng, Q.:** Cloning and characterization of a gene cluster for cyclododecanone oxidation in *Rhodococcus ruber* SC1, *J. Bacteriol.*, **183**, 6478–6486 (2001).
 11. **Kwasiborski, A., Mondy, S., Beury-Cirou, A., and Faure, D.:** Genome sequence of the quorum-quenching *Rhodococcus erythropolis* strain R138, *Genome Announc.*, **2**, e00224–14 (2014). DOI:10.1128/genomeA.00224-14
 12. **Strnad, H., Patek, M., Fousek, J., Szokol, J., Ulbrich, P., Nesvera, J., Paces, V., Vlcek, C.:** Genome sequence of *Rhodococcus erythropolis* strain CCM2595, a phenol derivative-degrading bacterium, *Genome Announc.*, **2**, e00208–14 (2014). DOI:10.1128/genomeA.00208-14
 13. **Wang, H., Gao, W., Sun, H., Szokol, J., Ulbrich, P., Nesvera, J., Paces, V., Vlcek, C.:** Protein engineering of a nitrilase from *Burkholderia cenocepacia* J2315 for efficient and enantioselective production of (*R*)-*o*-chloromandelic acid, *Appl. Environ. Microbiol.*, **81**, 8469–8477 (2015).
 14. **Groger, H.:** Enzymatic routes to enantiomerically pure aromatic α -hydroxy carboxylic acids: A further example for the diversity of biocatalysis, *Adv. Synth. Catal.*, **343**, 547–558 (2001).
 15. **De Santis, G., Zhu, Z., Greenberg, W.A., Wong, K., Chaplin, J., Hanson, S.R., Farwell, B., Nicholson, L.W., Rand, C.L., Weiner, D.P., Robertson, D.E., and Burk, M.J.:** An enzyme library approach to biocatalysis: Development of nitrilases for enantioselective production of carboxylic acid derivatives, *J. Am. Chem. Soc.*,

124, 9024–9025 (2002).

16. **Kataoka, M., Ishige, T., Urano, N., Nakamura, Y., Sakuradani, E., Fukui, S., Kita, S., Sakamoto, K., and Shimizu, S.:** Cloning and expression of the 1-1-amino-2-propanol dehydrogenase gene from *Rhodococcus erythropolis*, and its application to double chiral compound production, *Appl. Microbiol. Biotechnol.*, **80**, 597–604 (2008).
17. **Takeuchi M., Kishino S., Park S.B., Hirata A., Kitamura N., Saika A., and Ogawa J.:** Efficient enzymatic production of hydroxy fatty acids by linoleic acid Δ^9 hydratase from *Lactobacillus plantarum* AKU 1009a. *J Appl Microbiol.*, **120**, 1282–1288 (2016).
18. **Yamamura, E.-T.:** Bioconversion of pyridoxine to pyridoxamine through pyridoxal using a *Rhodococcus* expression system, *J. Biosci. Bioeng.*, **127**, 79–84 (2019).
19. **Bálint, J., Nagy, M.C., Dombrády, Z., Fogassy, E., Gajáry, A., and Suba, C., inventors; Sanofi-Aventis, assignee:** Resolution process for (*R*)-(-)-2-hydroxy-2-(2-chlorophenyl)acetic acid. United States patent US 7,381,835 B2. 2008 Jun 3.
20. **Kimoto, N., and Yamamoto, H., inventors; Daicel Chemical Industries, Ltd., assignee:** α -Keto acid reductase, method for producing the same, and method for producing optically active α -hydroxy acids using the same. United States patent US 7,250,278 B2. 2007 Jul 31.

SUMMARY

(*R*)-2-Chloromandelic acid (*R*-CM) is one of the chiral building blocks used in the pharmaceutical industry. As a result of screening for microorganisms that asymmetrically hydrolyze racemic 2-chloromandelic acid methyl ester (CMM), *Exophiala dermatitidis* NBRC6857 was found to produce *R*-CM at optical purity of 97% *ee*. The esterase that produces *R*-CM, EstE, was purified from *E. dermatitidis* NBRC6857, and the optimal temperature and pH of EstE were 30°C and 7.0, respectively. The *estE* gene that encodes EstE was isolated and overexpressed in *Escherichia coli* JM109. The activity of recombinant *E. coli* JM109 cells overexpressing *estE* was 553 times higher than that of *E. dermatitidis* NBRC6857. *R*-CM was produced at conversion rate of 49% and at optical purity of 97% *ee* from 10% CMM with 0.45 mg-dry-cell/L recombinant *E. coli* JM109 cells. Based on these findings, *R*-CM production by bioconversion of CMM may be of interest for future industrial applications.

SECTION 3

A novel method of producing the key intermediate ASI-2 of ranirestat using a porcine liver esterase (PLE) substitute enzyme

I aimed to produce ASI-2 [(*R*)-2-amino-2-ethoxycarbonylsuccinimide], which is a key intermediate used in the pharmaceutical industry. I constructed a scheme to synthesize the ASI-2 in a process in which bioconversion and chemical synthesis are combined. I sought to identify a novel esterase, EstBT, that substitutes for a porcine liver esterase (PLE) suitable for the scheme.

Materials and methods

Strains and plasmids *Bacillus thuringiensis* NBRC3951, NBRC101235, and NBRC13866 were obtained from the National Institute of Technology and Evaluation (Tokyo, Japan). *E. coli* JM109 was obtained from Toyobo Co., Ltd. (Osaka, Japan). The *E. coli* expression vector pQE-70 was obtained from Qiagen (Hilden, Germany).

Chemicals and enzymes All chemicals were purchased from FUJIFILM Wako Pure Chemical Corp. (Osaka, Japan) and Sigma-Aldrich (St. Louis, MO, USA). PLE was purchased from Sigma-Aldrich. All restriction enzymes and DNA modification enzymes were purchased from Toyobo Co., Ltd. (Osaka, Japan) and New England Biolabs, Inc. (Ipswich, MA, USA). The synthetic oligonucleotides used in this study were purchased from Hokkaido System Science Co., Ltd. (Hokkaido, Japan).

was performed by standard genetic manipulation techniques (1). *E. coli* transformations were performed using the *E. coli* Transformation Buffer Set (Zymo Research Corp., Irvine, CA, USA). Genomic DNA was isolated using the Genomic DNA Buffer set and the Genomic-tip 500/G (Qiagen, Hilden, Germany). PCR fragments were prepared with KOD -plus- (Toyobo Co., Ltd.). DNA sequences of the plasmid inserts were determined using the primer-walking method described by Yamamura (2). Sequence assembly and analysis were performed using GENETYX Ver.12 (GENETYX Corp., Tokyo, Japan) and DNASIS Pro Ver.2.0 (Hitachi Software Corp., Tokyo, Japan).

Synthesis of diethyl 2-benzyloxycarbonylamino-2-ethoxycarbonylsuccinate

(Z-MDE-AE)

A suspension of diethyl 2-benzyloxycarbonylaminomalonate (5.0 g), potassium carbonate (2.7 g), potassium iodide (0.27 g), and ethyl chloroacetate (2.6 g) in *N,N*-dimethylformamide (DMF, 50 mL) was stirred at 50°C for 1 h. The reaction mixture was cooled, and then poured into diluted hydrochloric acid, and the mixture was extracted with ethyl acetate. The extract was washed with saturated brine, and then dried over anhydrous magnesium sulfate. The solvent was evaporated under reduced pressure, and the residue was crystallized from ethyl acetate/*n*-hexane to obtain diethyl 2-benzyloxycarbonylamino-2-ethoxycarbonylsuccinate (Z-MDE-AE).

Screening of a bacterial library for asymmetric hydrolyzing activity of Z-

MDE-AE

I sought to identify an esterase, EstBT, that substitutes for PLE and constructed a scheme to synthesize the pharmaceutical intermediate ASI-2 in a process in which bioconversion and chemical synthesis are combined (Fig. 1). The actinomycetes and bacteria were inoculated into 5 mL of GPY broth (1% (w/v) glucose, 0.5% (w/v) Bacto peptone, and 0.3% (w/v) Bacto yeast extract) and incubated at 30°C with shaking for 3-7 days. The cells were harvested, freeze-dried, and suspended in 0.5

mL of 100 mM sodium phosphate buffer (pH 7.0) containing 0.1% (w/v) Z-MDE-AE and 10% (v/v) acetonitrile. The mixtures were incubated at 30°C with shaking for 72 h. The reactions were stopped by the addition of 1.5 mL of ethanol. Cell suspensions were centrifuged at $10,000 \times g$ for 10 min at 4°C, and the resulting supernatants were analyzed by high-performance liquid chromatography (HPLC) as described below.

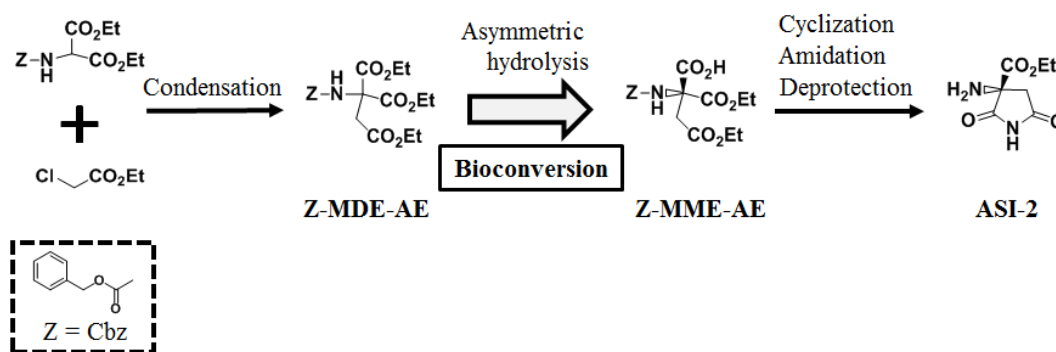


FIG. 1. Scheme for the synthesis of ASI-2 via the bioconversion of Z-MDE-AE to Z-MME-AE.

Z-MDE-AE is synthesized by condensation. Z-MME-AE is synthesized by bioconversion of Z-MDE-AE. ASI-2 is synthesized from Z-MME-AE by cyclization, amidation, and deprotection. Z, Z-MDE-AE, Z-MME-AE, and ASI-2 indicate benzyloxycarbonyl group (Cbz), diethyl 2-benzyloxycarbonylamino-2-ethoxycarbonylsuccinate, (R)-1-ethyl hydrogen 3-benzyloxycarbonylamino-3-ethoxycarbonylsuccinate, and (R)-2-amino-2-ethoxycarbonylsuccinimide, respectively.

Analysis of reaction mixtures by HPLC

The hydrolysis rate of Z-MDE-AE and optical purity of the product 1-ethyl hydrogen 3-benzyloxycarbonylamino-3-ethoxycarbonylsuccinate were determined by HPLC on a CHIRALCEL OJ-RH (ϕ 4.6 \times 150 mm; Daicel Corp., Tokyo, Japan). The mobile phase was acetonitrile/aqueous perchloric acid [pH 2.0, 30:70 (v/v)], the flow rate was 1.0 mL/min, the column

temperature was 20°C, and the detection wavelength was at 254 nm.

Purification of an esterase EstBT *B. thuringiensis* NBRC13866 cells were cultivated in GPY broth as described by Kozono et al. (3). An esterase EstBT was purified as described by Yamamura (4). *B. thuringiensis* NBRC 13866 was aerobically cultured in the GPY broth at 30°C for 16 h. Wet cells were collected from the culture broth by centrifugation (12,000 × g, 10 min) and suspended in 10 mM Tris buffer (pH 8.0). The suspension was disrupted by ultrasonication with an ultrasonic homogenizer US-300 (Nihonseiki Kaisha Ltd., Tokyo, Japan) on ice, and then centrifuged at 14,000 × g for 20 min. The resulting supernatant was used as the crude extract. The crude extracts were added with ammonium sulfate at 20% (w/v) saturated concentration on ice. The mixture was stirred and centrifuged (12,000 × g, 10 min), and the supernatant was removed. The precipitates were suspended in 10 mM Tris buffer (pH 8.0) containing 1 mM dithiothreitol (DTT), and dialyzed against the same buffer. This solution was added with DEAE Sepharose Fast Flow (GE Healthcare UK Ltd., Buckinghamshire, England), the samples were mixed, and the mixture was filtered to collect an active solution. The solution was added with 3-[(3-chloroamidopropyl)dimethylammonio]-propanesulfonate (CHAPS) at a final concentration of 1% (w/v) and mixed. The mixture was subjected to treatment with an ultrasonic homogenizer for 30 min on ice, and then applied to DEAE Sepharose equilibrated with 10 mM Tris buffer (pH 8.0) containing 1 mM DTT and 1% (w/v) CHAPS (henceforth referred to as buffer A). The proteins were eluted with a linear gradient of 0 to 0.3 M NaCl in buffer A. The active fraction was dialyzed to remove CHAPS, combined with polyoxyethylene lauryl ether (Brij 35) at a final concentration of 0.05% (w/v) and NaCl at a final concentration of 0.3 M. Samples were then applied to Phenyl Sepharose High Performance (GE Healthcare UK Ltd., Buckinghamshire, England) equilibrated with 10 mM Tris buffer (pH 8.0) containing 0.05% (w/v) Brij 35,

1 mM DTT, and 0.3 M NaCl. The proteins were eluted with a linear gradient of 0 to 0.3 M NaCl in 10 mM Tris buffer (pH 8.0) containing 0.05% (w/v) Brij 35 and 1 mM DTT. The active fraction was dialyzed against buffer A, concentrated by ultrafiltration, and applied to Mono Q (GE Healthcare UK Ltd., Buckinghamshire, England) equilibrated with buffer A. The proteins were eluted with a linear gradient of 0 to 0.5 M NaCl in buffer A. The active fraction was applied to Benzamidine Sepharose 4 Fast Flow (GE Healthcare UK Ltd., Buckinghamshire, England) equilibrated with buffer A and then proteins were eluted with a linear gradient of 0 to 0.5 M NaCl. Protein purity was analyzed on SDS-PAGE (5-20% gradient gel) by the method described by Laemmli (5) and was visualized by staining with Coomassie Brilliant Blue R-250 and Silver Stain 2 kit purchased from FUJIFILM Wako Pure Chemical Corp. (Osaka, Japan). The SDS-PAGE standards (Broad) purchased from Bio-Rad Laboratories, Inc. (Hercules, CA, USA) were used as molecular weight markers. The purified enzyme was designated as EstBT. The amino acid sequence of the purified EstBT was determined by automated Edman degradation and the analysis was carried out at APRO Science Inc. (Tokushima, Japan).

Enzyme and protein assays

The reaction mixture consisting of 1% (w/v) Z-MDE-AE, 100 mM phosphate buffer (pH 7.0), 10% (v/v) acetonitrile, and enzyme was incubated at 30°C for 2 h. The reactions were stopped by addition of three volumes of ethanol and were centrifuged at $12,000 \times g$ for 5 min at 4°C. The resulting supernatants were analyzed by high-performance liquid chromatography (HPLC) as described above. The activity for converting 1 μmol of Z-MDE-AE per 1 min was defined as 1 unit (U). Proteins were measured using a Bio-Rad Protein Assay (Bio-Rad Laboratories, Inc., Hercules, CA, USA) with bovine serum albumin as a standard.

Construction of *estBT* expression vectors

The *estBT* gene that encodes EstBT, which contains a deletion of 40 amino acids at the N-terminus, was

amplified using the following primers: P-F120: 5'-GTACAAAGCATGCAAAAAG AAACCAGTCTCTTTAACGGAGCG-3' (*SphI* site is underlined) and P-R1380: 5'-CTTTTGTTGTAGATCTTTTCTTTGTGTCGCATTGACCCA-3' (*BglIII* site is underlined), from the genomic DNA of *B. thuringiensis* NBRC13866 with a Mastercycler gradient thermal cycler (Eppendorf, Hamburg, Germany). The PCR fragment containing *estBT* was digested with *SphI* and *BglIII* and then ligated into the *SphI* and *BglIII* sites of pQE-70 to generate the plasmid pBTEST38, which produces recombinant EstBT (rEstBT) with deletion of 40 amino acids at the N-terminus. To produce the full-length rEstBT (rEstBT-full), the full-length *estBT* was amplified using the following primers: P-F1: 5'-AAACAGCATGCAAAAAAAGAAATTACAAAAATCAGCAC-3' (*SphI* site is underlined) and P-R1380: 5'-CTTTTGTTGTAGATCTTTTCTTTGTGTCGCATTGACCCA-3' (*BglIII* site is underlined) from the genomic DNA of *B. thuringiensis* NBRC13866. The PCR fragment was digested with *SphI* and *BglIII*, ligated into the *SphI* and *BglIII* sites of pQE-70, and designated as pBTEST12. The plasmids pBTEST38 and pBTEST12 produce rEstBT and rEstBT-full, respectively, with a His-tag attached to C-terminus.

Cultivation of recombinant *E. coli* expressed *estBT* and purification of

rEstBT Recombinant *E. coli* JM109 cells were inoculated into 5 mL of Luria-Bertani (LB) broth (1% Bacto tryptone, 0.5% Bacto yeast extract, and 1% NaCl) with ampicillin (100 µg/mL) and were incubated at 25°C with shaking for 16 h. Four milliliters of seed broth was transferred into 200 mL of LB broth with ampicillin (100 µg/mL) and isopropyl-β-D-thiogalactopyranoside (0.1 mM) and was incubated at 25°C with shaking for 24 h. With the Ni-NTA Fast Start Kit obtained from Qiagen (Hilden, Germany), the His-tagged rEstBT and the His-tagged rEstBT-full were purified from recombinant *E. coli* JM109 harboring the plasmids pBTEST38 and pBTEST12, respectively.

Activity measurements of recombinant *E. coli* JM109 cells The

reaction mixture consisting of 89 mM [3.5% (w/v) Z-MDE-AE, 100 mM buffer [standard buffer was phosphate buffer (pH 7.0)], and a portion of the cultured recombinant *E. coli* JM109 cells was incubated at 20-40°C (standard reaction condition was 25°C) for 2 h. The reaction was stopped by the addition of three volumes of ethanol and samples were centrifuged at $12,000 \times g$ for 5 min at 4°C. The resulting supernatant was analyzed by HPLC as described above. The activity for converting 1 μ mol of Z-MDE-AE per 1 min was defined as 1 U.

Producing (R)-1-ethyl hydrogen 3-benzyloxycarbonylamino-3-ethoxycarbonylsuccinate (Z-MME-AE) by bioconversion The

reaction mixture consisting of 89 mM [3.5% (w/v)] Z-MDE-AE, 100 mM phosphate buffer (pH 7.0), and 100 mU/mL enzyme (EstBT, rEstBT, PLE, or recombinant whole-cell) was incubated at 25°C. The pH of the reaction mixture was maintained at 7.0 with 28% NaOH automatically, since the pH decreases during the reaction. The reaction mixture was centrifuged at $12,000 \times g$ for 5 min at 4°C to obtain the supernatant containing Z-MME-AE.

Synthesis of ASI-2 from Z-MME-AE To cyclize Z-MME-AE, a

solution of Z-MME-AE (1.8 g) in tetrahydrofuran (THF, 20 mL) was combined with triethylamine (0.96 mL) and isobutyl chloroformate (0.87 g) in this order at -15°C with stirring, and the mixture was stirred for 5 min. A solution of 25% aqueous ammonia (0.47 mL) was dropped into the reaction mixture at the same temperature. The reaction mixture was stirred at the same temperature for 1 h, and then poured into diluted hydrochloric acid. The mixture was extracted with ethyl acetate, and the extract was dried over anhydrous magnesium sulfate. The solvent was evaporated under reduced pressure, and the residue was subjected to silica gel column chromatography, in which elution was

performed with n-hexane/ethyl acetate (1:1) for purification, and then crystallized from ethyl acetate/n-hexane. For amidation, a solution of the obtained crystals in dehydrated ethanol (75 mL) was added with sodium ethoxide (310 mg) on ice while stirring. The mixture was stirred at the same temperature for 2 h, then cold 1 mol/L hydrochloric acid was added, and the mixture was extracted with ethyl acetate. The extract was washed with saturated brine, and then dried over anhydrous magnesium sulfate. The solvent was evaporated under reduced pressure, and the residue was recrystallized from ethyl acetate/n-hexane. For deprotection, the obtained crystals were dissolved in ethanol (140 mL), the solution was added with 5% palladium/carbon (56 mg), and catalytic hydrogenation was performed at room temperature under a hydrogen atmosphere. After the catalyst was removed by filtration, the filtrate was concentrated under reduced pressure. The residue was recrystallized from ethanol to obtain ASI-2 as colorless crystals.

Nucleotide sequence accession number The sequence of the *estBT* gene has been submitted to the DDBJ/EMBL/GenBank databases under accession number LC434454.

Results

Screening for Z-MDE-AE-asymmetric hydrolyzing microorganisms

E. coli is the most useful host for the expression of various genes and has many advantages, including easy handling, short generation times, various genetic tools, and high transformation efficiency. To express a gene in recombinant *E. coli*, prokaryotes were screened. A total of 495 strains from our bacterial library were used, consisting of 151 strains of actinomycetes and 344 strains of bacteria. Among the microbial strains, only one strain, *B. thuringiensis* NBRC13866, exhibited Z-MDE-AE-asymmetric

hydrolyzing activity, and the optical purity of the product was 99.9% enantiomeric excess (ee) of the (*R*)-enantiomer.

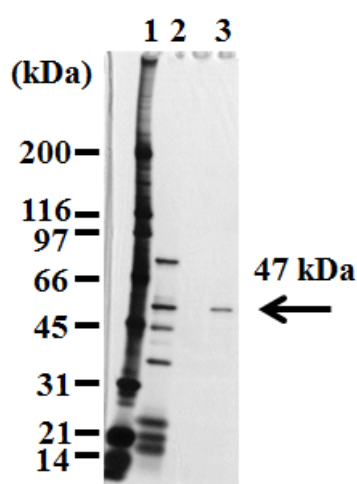
Identification of a Z-MDE-AE-asymmetric hydrolyzing enzyme from *B. thuringiensis* NBRC13866

In enzyme purifications, the target enzyme can be efficiently purified by the addition of a surfactant to the buffer. Therefore, 12 different types of surfactants were screened. With two surfactants, CHAPS and Brij 35, the enzyme showed high specific activities in the active fraction in the purification steps. Without surfactant, no activity of EstBT was detected in fractions. For these reasons, CHAPS or Brij 35 was added to the buffer in the purification steps. On the other hand, in the enzyme reaction, the activity of EstBT was detected with no surfactant. For this reason, the activity measurements were performed without adding surfactants to the reaction solution.

To identify the enzyme that hydrolyzes Z-MDE-AE to Z-MME-AE asymmetrically, the crude extracts of *B. thuringiensis* NBRC13866 were subjected to six purification steps (Table 1). In the first step, the ammonium sulfate precipitation step, the specific activity did not increase. However, when this step was omitted, EstBT could not be purified in next steps. For all purification steps, with the exception of the Phenyl Sepharose step, 1% (w/v) CHAPS was added to the buffer. In the Phenyl Sepharose step, 0.05% (w/v) Brij 35 was added to the buffer, since the specific activity of the active fraction increased. In this step, the addition of 1% (w/v) CHAPS hardly increased the specific activity. Fig. 2 shows that proteins in the Benzamidine Sepharose step displayed a single protein band with a molecular weight of 49 kDa via SDS-PAGE. The purified protein was designated as EstBT. The specific activity of the purified EstBT was 160 mU/mg, and the optical purity of the product was 99.9% ee of the (*R*)-enantiomer.

TABLE 1. Purification of esterase from *Bacillus thuringiensis* NBRC13866

Purification step	Total activity (mU)	Total protein (mg)	Specific activity (mU mg ⁻¹)	Yield (%)	Purification fold
Crude extracts	4740	7400	0.641	100	1.00
Ammonium sulfate precipitation (0–20%)	4700	7330	0.641	99.1	1.00
DEAE Sepharose Fast Flow (through)	4160	5240	0.794	87.7	1.24
DEAE Sepharose Fast Flow (0–0.3 M NaCl)	287	174	1.65	6.05	2.57
Phenyl Sepharose High Performance	98.1	12.3	7.97	2.07	12.4
Mono Q	52.9	1.81	29.3	1.12	45.7
Benzamidine Sepharose 4 Fast Flow	12.1	0.0756	160	0.255	250

**FIG. 2.** SDS-PAGE of EstBT from *Bacillus thuringiensis* NBRC13866.

Lane 1, size marker; lane 2, the active fraction of Mono Q; lane 3, the active fraction of Benzamidine Sepharose.

Amino acid and nucleotide sequence of EstBT

The amino acid sequence at the N-terminus of purified EstBT was determined by automated Edman degradation. Homology search for the obtained sequence (EKKPVSLTERTSLFF) was performed using the BLASTP 2.2.26 program (protein–protein Basic Local Alignment Search Tool, <https://www.ddbj.nig.ac.jp/index-e.html>) (6). The obtained sequence was homologous to α/β hydrolase (UniProt accession no. A0A243J741) derived from *B. thuringiensis* serovar pirenaica. Primers were prepared based on the sequence of the α/β hydrolase; the *estBT* gene that encodes EstBT was amplified by PCR from *B. thuringiensis* NBRC13866, and the sequence of the *estBT* gene was determined using the

primer walking method (2). The *estBT* gene is 1380 bp in length and encodes a protein of 460 amino acid residues (Fig. 3). According to the TBLASTN 2.2.26 program (protein–translated nucleotide Basic Local Alignment Search Tool) (6), EstBT is homologous to the α/β esterase (Table 2). EstBT contains a conserved serine protease motif (G-X-S-X-G) (9), and the serine protease belongs to the superfamily of proteins with α/β hydrolase fold. Analysis of the amino acid sequence presumed from the sequence of the obtained *estBT* gene revealed that the N-terminal sequence (EKKPVSLTERTSLFF) of EstBT that was purified from *B. thuringiensis* NBRC13866 was not at the N-terminal presumed from the obtained *estBT* gene sequence but rather at 41 amino acid residues (Fig. 3). The predicted molecular weight from the amino acid sequence EKKPVSLTERTSLFF to the C-terminus of EstBT was 47 kDa, which is agreement with the results of SDS-PAGE in Fig. 2.

TABLE 2. Features and identities between EstBT and known proteins

GenBank accession no.	Product	Organism	Identity	Ref.
AJA23081	hydrolase	<i>Bacillus thuringiensis</i> serovar galleriae	95%	-
ABY46486	putative hydrolase	<i>Bacillus mycooides</i> KBAB4	92%	(7)
AXR22762	α/β fold hydrolase	<i>Bacillus</i> sp. E25	92%	-
AXR17068	α/β fold hydrolase	<i>Bacillus</i> sp. CR71	92%	-
AJH17030	α/β hydrolase fold family protein	<i>Bacillus mycooides</i> strain ATCC 6462	91%	(8)

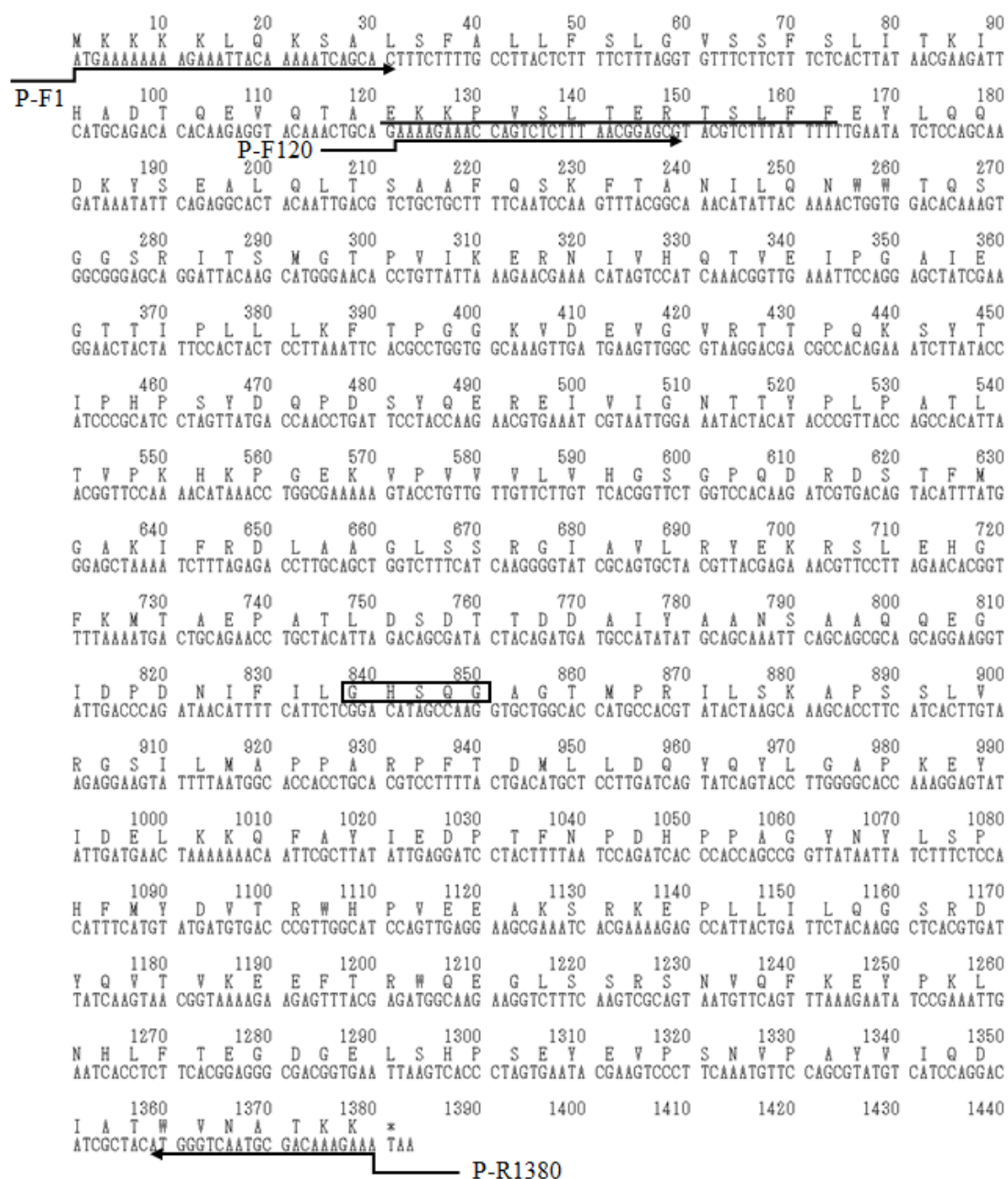


FIG. 3. Nucleotide sequence of *estBT* from *Bacillus thuringiensis* NBRC13866 and deduced amino acid sequence of full-length EstBT.

The conserved G-X-S-X-G motif of serine type proteases is boxed. The amino acid sequence at the N-terminus of EstBT purified from *Bacillus thuringiensis* NBRC13866 is underlined. Directing arrows indicate primers used to construct *estBT* expression vectors.

Expression of *estBT* in *E. coli* cells

For overexpression of the *estBT* gene in *E. coli*, two types of *estBT* expression vectors were constructed. The first is an expression vector that produces full-length EstBT with His-tag (rEstBT-full), designated as pBTEST12. The other is an expression vector that produces the His-tagged EstBT (rEstBT), which is truncated at 40 amino acid residues and resembles the EstBT purified from *B. thuringiensis* NBRC13866, designated as pBTEST38.

The plasmid pBTEST38 was transformed into *E. coli* JM109. rEstBT was overproduced in the recombinant *E. coli* JM109 and was detected in a soluble form with a molecular weight of 49 kDa on SDS-PAGE, which is in agreement with the predicted molecular weight (Fig. 4). The rEstBT was purified from the recombinant *E. coli* JM109 with the Ni-NTA Fast Start Kit (Fig. 4, lane 4). Analysis of the expression level of rEstBT by protein assay revealed $5.7 \pm 0.5\%$ rEstBT per dry cell weight (DCW). Moreover, the recombinant *E. coli* JM109 harboring the plasmid pBTEST12 also overproduced rEstBT-full. The rEstBT-full was detected in a soluble form with a molecular weight of 52 kDa on SDS-PAGE, which is in agreement with the predicted molecular weight. The production level of rEstBT-full was $5.5 \pm 0.7\%$ DCW.

The relative activities of native EstBT, rEstBT, rEstBT-full, and PLE were determined to be 168 ± 8 mU/mg, 164 ± 6 mU/mg, 161 ± 12 mU/mg, and 288 ± 18 mU/mg, respectively (Table 3). The relative activities between native EstBT, rEstBT, and rEstBT-full were nearly identical, while that of PLE being approximately 1.7 times higher than those of the other enzymes. Additionally, the optical purities of (*R*)-enantiomer of native EstBT, rEstBT, rEstBT-full, and PLE were 99.9% ee, 99.9% ee, 99.9% ee, and 93.6% ee, respectively (Table 3). The optical purities between native EstBT, rEstBT, and rEstBT-full were the same, while those of EstBT, rEstBT, and rEstBT-full were higher than that of PLE.

In the pH stability, incubation at pH 6, pH 7, and pH 8 for 2 h at 4 ° C did not reduce the enzyme activity of native EstBT, rEstBT, rEstBT-full, and PLE.

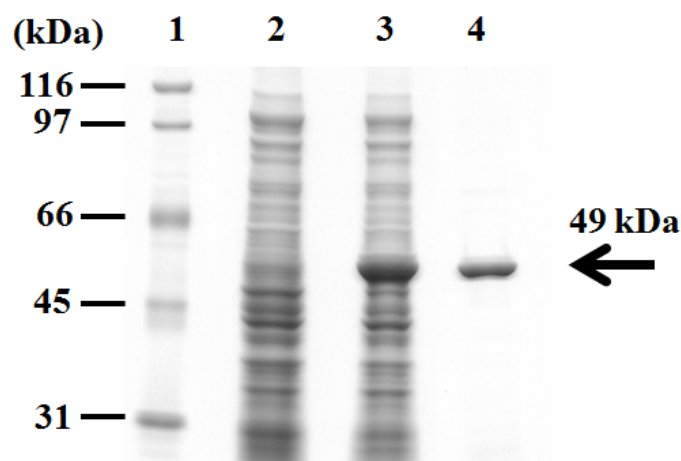


FIG 4. SDS-PAGE of crude extracts from recombinant *Escherichia coli* JM109 expressing the *estBT* gene and the purified rEstBT.

Lane 1, size marker; lane 2, the crude extracts from recombinant *E. coli* JM109 harboring pQE-70; lane 3, the crude extracts from recombinant *E. coli* JM109 harboring pBTEST38; lane 4, the rEstBT purified from the recombinant *E. coli* JM109 harboring pBTEST38.

TABLE 3. Comparison of the relative activity between EstBT, rEstBT, rEstBT-full, and PLE

Enzyme	Relative activity (mU/mg)	Optical purity (% ee)
EstBT	168 ± 8	99.9
rEstBT	164 ± 6	99.9
rEstBT- full	161 ± 12	99.9
PLE	288 ± 18	93.6

Characterization of recombinant *E. coli* JM109 producing rEstBT

The optimal reaction conditions of recombinant *E. coli* JM109 producing rEstBT, which harbors the plasmid pBTEST38, were investigated to efficiently produce Z-MME-AE from Z-MDE-AE. The optimal pH of the activity of the recombinant *E. coli* JM109 was examined from pH 4.0 to 10.0 and was found to be 7.0 (Fig. 5A). The effects of reaction temperature and stable temperature were also examined. The maximum activity was observed at 30°C (Fig. 5B) and the stable temperature was 30°C or lower (Fig. 5C). Therefore, the bioconversion described below was performed at 25°C.

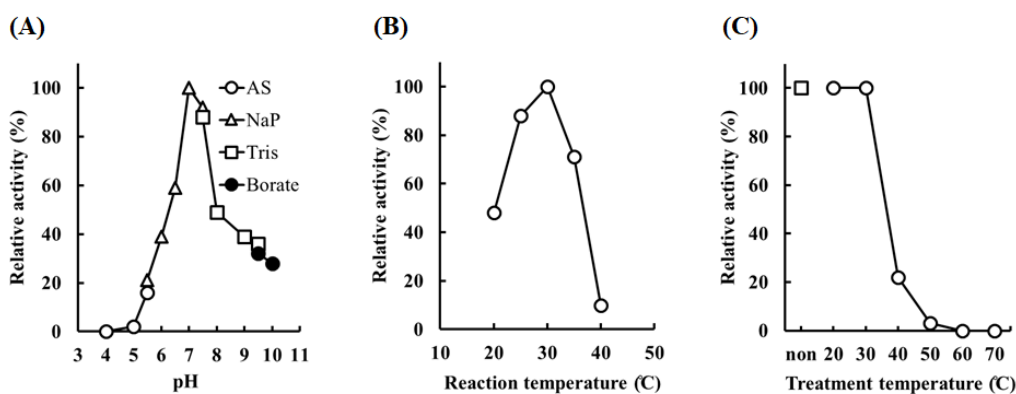


FIG. 5. Determination of optimal pH and temperature by recombinant *Escherichia coli* JM109 producing rEstBT.

(A) Effect of pH. Activity was assayed under standard reaction conditions, except for the buffer. Open circle, open triangle, open square, and closed circle indicate acetic acid-sodium acetate buffer (AS), sodium phosphate buffer (NaP), Tris buffer (Tris), and borate buffer (borate), respectively. (B) Effect of reaction temperature. Activity was assayed under standard reaction conditions, except for temperature. (C) Temperature stability of rEstBT. Activity was assayed under standard reaction conditions. Reaction mixture was incubated for 30 min at 20–70°C before adding substrate. Open square indicates no temperature treatment. Open circle indicates temperature treatment at 20–70°C.

Bioconversion of Z-MDE-AE to Z-MMD-AE

Figure 6A shows

bioconversion of Z-MDE-AE to Z-MMD-AE with 100 mU/mL of the enzymes EstBT, rEstBT, and PLE. The sequential changes in the production of Z-MME-AE with EstBT, rEstBT, and PLE were almost the same, and 89 mM [3.5% (w/v)] Z-MDE-AE was converted to approximately 61 mM Z-MME-AE (conversion rate 69%) in 33 h. On the other hand, Figure 6B shows bioconversion of Z-MDE-AE to Z-MMD-AE with 100 mU/mL recombinant whole-cell (wet-cell paste), which contains recombinant *E. coli* JM109 cells producing rEstBT. For 4 hours from the start of the reaction, the conversion rate with recombinant whole-cell was almost the same as those with enzymes of EstBT, rEstBT, and PLE. From the fourth hour onwards, the conversion rate with recombinant whole-cell was higher than those with EstBT, rEstBT, and PLE. In 33 h, 89 mM Z-MDE-AE was converted to approximately 81 mM Z-MME-AE (conversion rate 91%) with recombinant whole-cell.

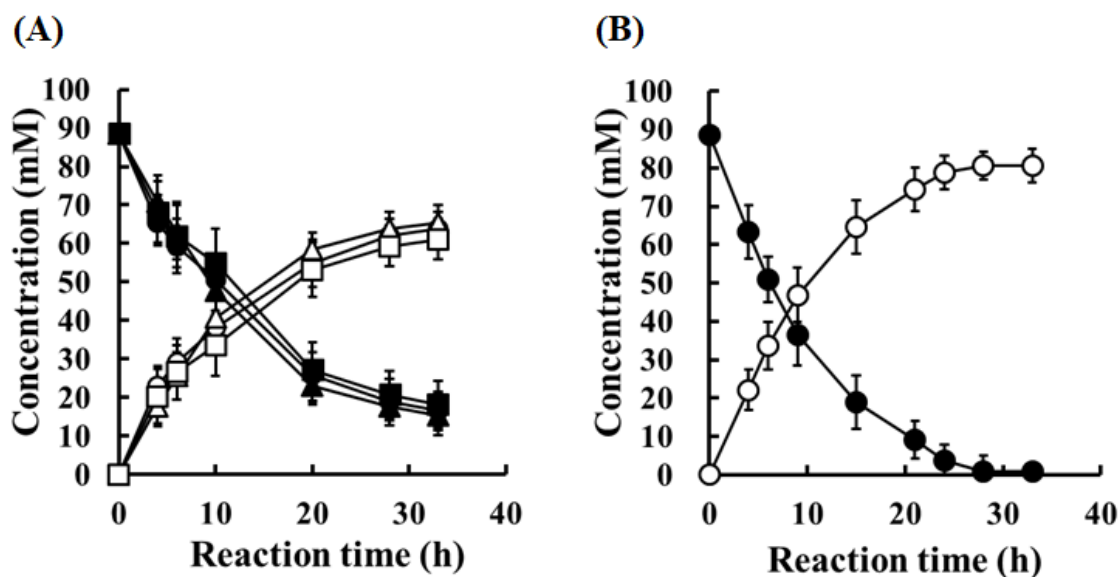


FIG 6. Bioconversion of Z-MDE-AE to Z-MME-AE with enzymes at a final activity concentration of 100 mU/mL.

(A) Bioconversion with purified enzymes. Substrate is 89 mM Z-MDE-AE. Closed circle, closed triangle, and closed square indicate Z-MDE-AE concentrations of native EstBT, recombinant EstBT, and commercial PLE, respectively. Open circle, open triangle, and open square indicate Z-MME-AE concentrations of native EstBT, recombinant EstBT, and commercial PLE, respectively. Vertical bars indicate SD from three independent experiments. (B) Bioconversion using recombinant *Escherichia coli* JM109 producing rEstBT. Substrate is 89 mM Z-MDE-AE. Closed circle and open circle indicate Z-MDE-AE and Z-MME-AE concentrations, respectively. Vertical bars indicate SD from three independent experiments.

Synthesis of ASI-2 by chemical synthesis and bioconversion

ASI-2 was synthesized from diethyl 2-benzyloxycarbonylamino malonate and ethyl chloroacetate (Fig. 1), which are readily and economically available starting materials.

Via bioconversion with recombinant whole-cell producing rEstBT, ASI-2 was synthesized with a total yield of 55%. On the other hand, ASI-2 was synthesized with a total yield of 38% via bioconversion with PLE. Using recombinant whole-cell rather than PLE, ASI-2 was synthesized with a 17% higher total yield. Through the novel method using the PLE substitute enzyme, which is recombinant whole-cell producing rEstBT, ASI-2 was synthesized.

Discussion

PLE is one of several valuable esterases (4,10–13) used in manufacturing industries, and the most useful esterase for process chemistry, including the synthesis of ASI-2 (14). However, commercial PLE has the drawback that the activity is different between various batches, since commercial PLE extracted from porcine liver tissue has different ratios of esterases (15) and contains a plurality of isoenzymes (α , β , and γ -PLE) (16). To address the problems associated with heterogeneous commercial PLE, many studies involving the production of recombinant γ -PLE have been reported. However, the activities of whole-cell are low for industrial applications.

I screened a PLE substitute enzyme that hydrolyzes Z-MDE-AE asymmetrically and is produced via recombinant techniques in *E. coli*. *B. thuringiensis* NBRC13866 hydrolyzed Z-MDE-AE asymmetrically and the optical purity of the product was 99.9% ee, while *B. thuringiensis* NBRC3951 and NBRC101235 from our bacterial library exhibited no hydrolysis activity of Z-MDE-AE. This might be due to differences in the membrane permeability of the substrate, expression levels of esterase gene, and substrate specificity of esterase among these strains. The freeze-dried cells and crude extracts of *B. thuringiensis* NBRC13866 hydrolyzed Z-MDE-AE, whereas wet cells of *B. thuringiensis*

NBRC13866 exhibited no hydrolysis activity of Z-MDE-AE. Z-MDE-AE might have poor membrane permeability in *B. thuringiensis* NBRC 13866 since it is a gram-positive bacterial species.

To identify the enzyme that hydrolyzes Z-MDE-AE to Z-MME-AE asymmetrically, an enzyme purification protocol was performed. Fig. 2 shows that proteins in the Benzamidine Sepharose step displayed the single protein band on the SDS-PAGE, suggesting that EstBT was purified from the crude extracts of *B. thuringiensis* NBRC13866 by six purification steps. In the first step of enzyme purification, which is the ammonium sulfate precipitation step, the specific activity did not increase, although this step was indispensable as biological substances other than proteins (e.g., lipids, sugars) might be removed at this time. The subsequent DEAE Sepharose step (through) was required. This is likely because many enzymes that interact strongly with DEAE were present in the active fraction of ammonium sulfate precipitation. In all purification steps, no activity of EstBT was detected without surfactant. Due to the absence of surfactant, it may be that the resin and EstBT directly interacted and the structure of EstBT was denatured (4). On the other hand, in the enzyme reaction, the activity of EstBT was detected with or without surfactant. This result suggests that EstBT is stable in aqueous solution with or without surfactant.

One of our research objectives is to obtain the gene of a PLE substitution enzyme that can be overexpressed in *E. coli*. To construct *estBT* expression vectors in *E. coli*, the nucleotide sequence of *estBT* was determined (Fig. 3). Homology search based on the determined sequence suggests that EstBT is a novel enzyme (Table 2) and contains a conserved serine protease motif (G-X-S-X-G) (9). During enzyme purification (Table 1), EstBT was purified with Benzamidine Sepharose, which is a carrier for the purification of serine proteases, suggesting that EstBT is a serine protease.

Two kinds of the recombinant *E. coli* JM109 cells were constructed. The recombinant *E. coli* JM109 cells expressed the *estBT* gene in a soluble form, which is consistent with the predicted molecular weight. The production levels of rEstBT and rEstBT-full, which were produced in recombinant *E. coli* JM109 harboring pBTEST38 and pBTEST12, were $5.9\pm 0.5\%$ DCW and $5.5\pm 0.8\%$ DCW, respectively. These results suggest that the *estBT* gene was overexpressed in *E. coli* JM109.

The relative activities and the optical purities between native EstBT, rEstBT, rEstBT-full, and PLE were compared. The relative activities and the optical purities between native EstBT, rEstBT, and rEstBT-full were nearly identical, suggesting that native EstBT, rPLE (truncated recombinant EstBT), and rEstBT-full (full-length recombinant EstBT) have the same activity. The relative activity of PLE was only 1.7 times higher than those of the other enzymes and the optical purity of PLE was lower than those of the other enzymes. These results suggest that rEstBT is the PLE substitute enzyme. However, I cannot explain the effect due to the difference of 40 amino acid residues between rEstBT and rEstBT-full. Due to the low solubility of Z-MDE-AE [$<0.05\%$ (w / v)], parameters (e.g., k_{cat} , K_m , or k_{cat}/K_m) of enzyme reaction could not be determined. In addition, substrate inhibition was not observed in 4% (w/v) Z-MDE-AE. This may be due to the low concentration of Z-MDE-AE dissolved in the reaction solution.

Bioconversion of the prochiral ester Z-MDE-AE to the optically active carboxylic acid Z-MME-AE is the key reaction in this process, since Z-MME-AE is synthesized at a theoretical yield of 100% (Fig. 1). For bioconversion of Z-MDE-AE to Z-MME-AE, the optimal reaction conditions of EstBT using recombinant *E. coli* JM109 producing rEstBT were investigated. The optimal pH, maximum reaction temperature, and stable temperature were 7.0, 30°C, and 30°C or less, respectively, which represent neutral pH and ambient temperature. These results suggest that EstBT is suitable for

bioconversion.

Using enzymes (EstBT, rEstBT, PLE, and recombinant whole-cell producing rEstBT) at a final activity concentration of 100 mU/mL, bioconversion of Z-MDE-AE to Z-MME-AE was performed. For 4 hours from the start of the reaction, the Z-MME-AE concentrations among these enzymes in recombinant whole-cell were almost the same. These results suggest that there is almost no issue of membrane permeability of Z-MDE-AE and Z-MME-AE when recombinant whole-cell is used. From the fourth hour onwards, the Z-MME-AE concentration with recombinant whole-cell producing rEstBT was higher than that with the purified rEstBT. This result suggests that rEstBT is more stable in the cell than the purified rEstBT, and there is nearly no issue of compound stability of Z-MDE-AE and Z-MME-AE when the recombinant whole-cell is used. In addition, since cultured cells can be directly used for bioconversion, rather than purified enzyme, the synthesis process of Z-MME-AE is simplified. Moreover, the sequential changes in the production of Z-MME-AE with EstBT, rEstBT, and PLE were nearly identical. This result suggests that enzyme stabilities of EstBT and rEstBT are nearly identical to that of PLE. At 30 hours from the start of the reaction using enzymes, compounds presumed to be decomposition products of Z-MME-AE were detected, although the structures could not be determined. If the cause of this decomposition is clarified, it may be possible to synthesize Z-MME-AE via bioconversion at a conversion rate of 100%.

Numerous reports (17–23) have shown efficient methods to produce a wide range of optically active molecules using commercial PLE. In this study, we used recombinant whole-cell produced rEstBT, rather than PLE, to synthesize ASI-2 with a 17% higher total yield. This may be due to the fact that the yield was 20% higher in the bioconversion of Z-MDE-AE to Z-MME-AE (Fig. 6). In addition, Z-MME-AE may have been lost in the separation of Z-MME-AE from the reaction solution containing

recombinant cells after bioconversion. Future studies to investigate the range of substrate specificity of rEstBT compared to PLE will be conducted using a wide range of molecules.

By making only effective optical isomers for pharmaceutical products, the effect is often enhanced and side effects are often reduced. As with PLE, EstBT is one of the useful enzymes in the pharmaceutical industry, since EstBT hydrolyzed Z-MDE-AE asymmetrically and the optical purity of the product was 99.9% ee.

In conclusion, a novel esterase EstBT, which is the PLE substitute enzyme, was identified and produced stably in *E. coli*. Using a novel method that combines chemical synthesis and bioconversion using recombinant whole-cell produced rEstBT, the pharmaceutical intermediate ASI-2 was synthesized efficiently.

REFERENCES

1. **Sambrook, J., Fritsch, E.F., and Maniatis, T.:** Molecular cloning: a laboratory manual, 2nd ed. Cold Spring Laboratory, Cold Spring Harbor, NY (1989).
2. **Yamamura, E.-T.:** Construction of *Rhodococcus* expression vectors and expression of the aminoalcohol dehydrogenase gene in *Rhodococcus erythropolis*, *Biosci. Biotechnol. Biochem.*, **82**, 1396–1403 (2018).
3. **Kozono, I., Mihara, K., Minagawa, K., Hibi, M., and Ogawa, J.:** Engineering of the cytochrome P450 monooxygenase system for benzyl maltol hydroxylation, *Appl. Microbiol. Biotechnol.*, **101**, 6651–6658 (2017).
4. **Yamamura, E.-T. and Kita, S.:** A novel method of producing the pharmaceutical intermediate (*R*)-2-chloromandelic acid by bioconversion, *Biosci. Biotechnol. Biochem.*, **83**, 309–317 (2019).
5. **Laemmli, U.K.:** Cleavage of structural proteins during the assembly of the head of bacteriophage T4, *Nature*, **227**, 680–685 (1970).
6. **Altschul, S.F., Madden, T.L., Schäffer, A.A., Zhang, J., Zhang, Z., Miller, W., and Lipman, D.J.:** Gapped BLAST and PSI-BLAST: a new generation of protein database search programs, *Nucleic Acids Res.*, **25**, 3389-3402 (1997).
7. **Lapidus, A., Goltsman, E., Auger, S., Galleron, N., Ségurens, B., Dossat, C., Land, M.L., Broussolle, V., Brillard, J., Guinebretiere, M.H., Sanchis, V., Nguen-The, C., Lereclus, D., Richardson, P., Wincker, P., Weissenbach, J., Ehrlich, S.D., and Sorokin, A.:** Extending the *Bacillus cereus* group genomics to putative food-borne pathogens of different toxicity, *Chem. Biol. Interact.*, **171**, 236–249 (2008).
8. **Johnson, S.L., Daligault, H.E., Davenport, K.W., Jaissle, J., Frey, K.G., Ladner, J.T., Broomall, S.M., Bishop-Lilly, K.A., Bruce, D.C., Gibbons, H.S., Coyne,**

- S.R., Lo, C.C., Meincke, L., Munk, A.C., Koroleva, G.I., Rosenzweig, C.N., Palacios, G.F., Redden, C.L., Minogue, T.D., Chain, P.S.:** Complete genome sequences for 35 biothreat assay-relevant *Bacillus* species. *Genome Announc.* **3**, e00151–15 (2015). DOI:10.1128/genomeA.00151-15
9. **Obst, M., Oppermann-Sanio, F.B., Luftmann, H., and Steinbüchel, A.:** Isolation of cyanophycin-degrading bacteria, cloning and characterization of an extracellular cyanophycinase gene (*cphE*) from *Pseudomonas anguilliseptica* strain BI. The *cphE* gene from *P. anguilliseptica* BI encodes a cyanophycinhydrolyzing enzyme, *J. Biol. Chem.*, **277**, 25096–25105 (2002).
10. **Hayashi, Y., Onaka, H., Itoh, N., Seto, H., and Dairi, T.:** Cloning of the gene cluster responsible for biosynthesis of KS-505a (longestin), a unique tetraterpenoid, *Biosci. Biotechnol. Biochem.*, **71**, 3072–3081 (2007).
11. **Okazaki, R., Kiyota, H., and Oritani, T.:** Enzymatic resolution of (±)-epoxy-β-cyclogeraniol, a synthetic precursor for abscisic acid analogs, *Biosci. Biotechnol. Biochem.*, **64**, 1444–1447 (2000).
12. **Kanjanavas, P., Khuchareontaworn, S., Khawsak, P., Pakpitcharoen, A., Pothivejkul, K., Santiwatanakul, S., Matsui, K., Kajiwara, T., and Chansiri, K.:** Purification and characterization of organic solvent and detergent tolerant lipase from thermotolerant *Bacillus* sp. RN2, *Int. J. Mol. Sci.*, **11**, 3783–3792 (2010).
13. **Park, E.Y., Sato, M., and Kojima, S.:** Lipase-catalyzed biodiesel production from waste activated bleaching earth as raw material in a pilot plant, *Bioresour. Technol.*, **99**, 3130–3135 (2008).
14. **Kasai, M., Kita, S., Ogawa, T., Tokai, H., inventors; Dainippon Sumitomo Pharma Co., Ltd., and Kyowa Hakko Bio Co., Ltd., assignees:** Process for producing optically active succinimide derivatives and intermediates thereof, United

- States patent US 8,633,001 B2. 2014 Jan 21.
15. **Seebach, D. and Eberle, M.:** Enantioselective cleavage of meso-nitrodiol diacetates by an esterase concentrate from fresh pig liver: Preparation of useful nitroaliphatic building blocks for EPC syntheses, *Chimia.*, **40**, 315–318 (1986).
 16. **Faber, D. and Jencks, W.P.:** Different forms of pig liver esterase, *Arch. Biochem. Biophys.*, **203**, 214–226 (1980).
 17. **Kudo, Y., Yamada, O., inventors; Nissan Chemical Industries, Ltd., Dainippon Sumitomo Pharma Co., Ltd., assignees:** Method for producing optically active succinimide compound, United States patent US 7,994,342 B2. 2011 Aug 9.
 18. **Inagaki, T. and Yamakawa, Y., inventors; Dainippon Sumitomo Pharma Co., Ltd., and Katayama Seiyakusyo Co., Ltd., assignees:** Succinic acid diester derivative, process for production thereof, and use of the derivative in the production of pharmaceutical preparation, United States patent US 8,030,486 B2. 2011 Oct 4.
 19. **Bornscheuer, U.T. and Kazlauskas, R.J.:** *Hydrolases in organic synthesis -regio- and stereoselective biotransformations*, 2nd edn. Weinheim: Wiley-VCH; 2006.
 20. **Faber, K.:** *Biotransformations in organic chemistry*, 5th edn. Berlin, Heidelberg, New York: Springer; 2004.
 21. **de Maria, P.D., Kossmann, B., Potgrave, N., Buchholzc, S., Trauthweinc, H., Maya, O., and Gröger, H.:** Improved process for the enantioselective hydrolysis of prochiral diethyl malonates catalyzed by pig liver esterase, *Synlett.*, **11**, 1746–1748 (2005).
 22. **Lam, L.K.P., Hui, R.A.H.F., and Jones, J.B.:** *Enzymes in organic synthesis*. 35. Stereoselective pig liver esterase catalyzed hydrolyses of 3-substituted glutarate diesters. Optimization of enantiomeric excess via reaction conditions control, *J. Org. Chem.*, **51**, 2047–2050 (1986).

23. **Bornscheuer U, Hummel A, Böttcher D, Brisehaber, E., Doderer, K., and Trauthwein, H., inventors; Enzymicals AG, assignee:** Isoforms of pig liveresterase. United States patent US 8,304,223 B2. 2012 Nov 6.

SUMMARY

(*R*)-2-amino-2-ethoxycarbonylsuccinimide (ASI-2) is a key intermediate used in the pharmaceutical industry and is valuable for the industrial synthesis of ranirestat, which is a potent aldose reductase inhibitor. ASI-2 was synthesized in a process combining chemical synthesis and bioconversion. Bioconversion in this study is a key reaction, since optically active carboxylic acid derivative ((*R*)-1-ethyl hydrogen 3-benzyloxycarbonylamino-3-ethoxycarbonylsuccinate, Z-MME-AE) is synthesized from a prochiral ester, diethyl 2-benzyloxycarbonylamino-2-ethoxycarbonylsuccinate, Z-MDE-AE, at a theoretical yield of 100%. Upon screening for microorganisms that asymmetrically hydrolyze Z-MDE-AE, *Bacillus thuringiensis* NBRC13866 was found. A novel esterase EstBT that produces Z-MME-AE was purified from *Bacillus thuringiensis* NBRC13866 and was stably produced in *Escherichia coli* JM109 cells. Using EstBT rather than porcine liver esterase (PLE), ASI-2 was synthesized with a 17% higher total yield by a novel method, suggesting that the esterase EstBT is a PLE substitute enzyme and therefore, may be of interest for future industrial applications.

CONCLUSIONS

As described in the GENERAL INTRODUCTION, environmental aspects are emphasized in addition to production costs in the manufacturing industries. Many production processes using bioconversion reactions occur at ambient temperature and pressure, and are good for environmental conservation. Therefore, I developed processes producing the pharmaceutical intermediates using bioconversion.

Many *Rhodococcus* strains contain diverse enzymes that are beneficial for manufacturing industries. In particular, *Rhodococcus erythropolis* tolerates organic solvents and is utilized in the industrial production of chiral building blocks, pharmaceuticals, and chemicals. Since genetic tools are needed to further analyze and utilize *Rhodococcus* in manufacturing industries, the novel *Rhodococcus* expression system was constructed as described in CHAPTER I.

In CHAPTER I, two plasmids, pRET1100 and pRET1200, were isolated from *R. erythropolis* IAM1400. pRET1100 carries the *repT* gene, which code for a cryptic replication protein. On the other hand, pRET1200 carries the *repA* and *repB* genes, which are highly homologous to pN30 from *R. erythropolis*. Since the new cryptic pRET1100 plasmid is the compatible and stable plasmid, pRET1100 is useful for co-expressing multiple genes.

Using the pRET1100 plasmid, the pRET1172 plasmid carrying *repT* gene, *aadh* gene, and the strong promoter *TRR* was constructed for expressing *aadh* gene in many actinomycete strains. The pRET1172 plasmid was transformed into 22 types of the actinomycete strains. The AADH activities of all strains transformed with the plasmid pRET1172 were higher than those strains transformed with the pRET1102 plasmid. Deleted the *aadh* gene from pRET1172, the *Rhodococcus* expression vector pRET11100,

which expresses gene in many actinomycete strains, was constructed.

In CHAPTER II, bioconversion processes producing the pharmaceutical intermediates were developed. In SECTION 1 of CHAPTER II, process producing PM from PN was developed using the *Rhodococcus* expression vector pRET11100. Approximately 145 mM PM was produced from 200 mM PN through PL demonstrating a bioconversion rate of 75%. Moreover, recombinant *R. erythropolis* overexpressing *pno* produced approximately 450 mM PL from 500 mM PN without chaperonins.

In SECTION 2 of CHAPTER II, the novel method of producing the pharmaceutical intermediate *R*-CM from CMM by the bioconversion was developed using the novel esterase EstE. *R*-CM was produced at conversion rate of 49% and at optical purity of 97% *ee* from 10% CMM in 24 h with 0.45 mg-dry-cell/L recombinant *E. coli* JM109 cells. Since (*S*)-2-chloromandelic acid is racemized in the presence of sodium methoxide easily, unreacted (*S*)-2-chloromandelic acid is able to be reused for a bioconversion, and the method is efficient.

In SECTION 3 of CHAPTER II, the novel method of producing the key intermediate ASI-2 in the process in which bioconversion and chemical synthesis are combined was developed using the novel esterase EstBT that substitutes for PLE. Using EstBT rather than porcine liver esterase (PLE), ASI-2 was synthesized with a 17% higher total yield

In conclusion, the novel *Rhodococcus* expression system that is useful for bioconversion was constructed and processes producing the pharmaceutical intermediates, PM, *R*-CM, and ASI-2, using bioconversion were developed.

ACKNOWLEDGMENTS

I sincerely acknowledge Prof. Jun Ogawa of Kyoto University for his kind instruction.

I am grateful to Prof. Michihiko Kataoka of Osaka Prefecture University and Prof. Emer. Sakayu Shimizu of Kyoto University for the information on the *aadh* gene.

I would like to thank to Prof. Emer. Hideaki Yamada of Kyoto University and Prof. Emer. Toshiharu Yagi of Kochi University for their information regarding the bioconversion of pyridoxine to pyrioxamine.

I gratefully acknowledge Assoc. Prof. Makoto Hibi of Toyama Prefectural University and Program-Specific Assist. Prof. Michiki Takeuchi of Kyoto University for their valuable discussion and critical review.

I would like to express my deepest gratitude to my co-workers for their support throughout this study.

I sincerely appreciate Ms. Yasuko Yamamura for her zeal for science.

Ei-Tora Yamamura

LIST OF PUBLICATIONS

Yamamura, E.-T.: Isolation of two plasmids, pRET1100 and pRET1200, from *Rhodococcus erythropolis* IAM1400 and construction of a *Rhodococcus–Escherichia coli* shuttle vector, J. Biosci. Bioeng., **125**, 625–631 (2018).

Yamamura, E.-T.: Construction of *Rhodococcus* expression vectors and expression of the aminoalcohol dehydrogenase gene in *Rhodococcus erythropolis*, Biosci. Biotechnol. Biochem., **82**, 1396–1403 (2018).

Yamamura, E.-T.: Bioconversion of pyridoxine to pyridoxamine through pyridoxal using a *Rhodococcus* expression system, J. Biosci. Bioeng., **127**, 79–84 (2019).

Yamamura, E.-T. and Kita, S.: A novel method of producing the pharmaceutical intermediate (*R*)-2-chloromandelic acid by bioconversion, Biosci. Biotechnol. Biochem., **83**, 309–317 (2019).

Yamamura, E.-T., Tsuzaki, K., and Kita, S.: A novel method of producing the key intermediate ASI-2 of ranirestat using a porcine liver esterase (PLE) substitute enzyme, Biosci. Biotechnol. Biochem., **83**, 1124–1135 (2019).

